Lecture Notes
Satellitengeodäsie (BSc)

Dynamic Satellite Geodesy

Nico Sneeuw
Institute of Geodesy
University of Stuttgart

October 10, 2022

These are lecture notes in progress. Please contact me (`sneeuw@gis.uni-stuttgart.de`) for remarks, errors, suggestions, etc.

Contents

1. Introduction **7**

2. The two-body problem **9**

2.1. Kepler's laws . . . 9
2.1.1. First law: elliptical motion . . . 10
2.1.2. Second law: area law . . . 12
2.1.3. Third law: harmony . . . 14
2.2. Further geometry . . . 15
2.2.1. Three-dimensional orbit description . . . 15
2.2.2. Back to the orbital plane: anomalies . . . 17
2.3. Newton equations and conservation laws . . . 22
2.3.1. Conservation of energy . . . 22
2.3.2. Conservation of angular momentum . . . 23
2.3.3. Conservation of orbit vector . . . 24
2.3.4. Vis viva – living force . . . 25
2.3.5. Transfer orbit . . . 27
2.4. Further useful relations . . . 31
2.4.1. Understanding Kepler . . . 31
2.4.2. Partial derivatives $\nu \leftrightarrow E \leftrightarrow M$ . . . 32
2.5. Transformations Kepler $\longleftrightarrow$ Cartesian . . . 33
2.5.1. Kepler $\longrightarrow$ Cartesian . . . 33
2.5.2. Cartesian $\longrightarrow$ Kepler . . . 34

3. Introduction to perturbation theory – Lagrange Planetary Equations **39**

3.1. Representation of orbit perturbations . . . 39
3.2. Osculating Kepler elements . . . 42
3.2.1. Effect on Kepler elements . . . 42
3.2.2. Investigation of orbit perturbations . . . 42
3.3. Canonical Equations . . . 43
3.4. Crash course LPE . . . 44

3.5. Gauss form of LPE 48

4. Orbit perturbation due to Earth flattening **53**
4.1. Qualitative assessment 53
4.2. Quantitative assessment 54
4.3. Repeat orbit 58

5. Non gravitational orbit perturbations **61**
5.1. Atmospheric drag 61
5.2. Solar radiation pressure 63
5.3. Relativistic corrections 67

6. The gravitational potential and its representation **69**
6.1. Representation on the sphere 69
6.2. Representation in Kepler elements 71
6.3. Lumped coefficient representation 76
6.4. Pocket guide of dynamic satellite geodesy 77
6.5. Derivatives of the geopotential 78
6.5.1. First derivatives: gravitational attraction 78
6.5.2. Second derivatives: the gravity gradient tensor 81

7. Gravitational orbit perturbations **85**
7.1. The J_2 secular reference orbit 85
7.2. Periodic gravity perturbations in linear approach 88
7.3. The orbit perturbation spectrum 91

8. A viable alternative: Hill Equations **95**
8.1. Acceleration in a rotating reference frame 95
8.2. Hill equations 98
8.3. Solutions of the Hill equations 101
8.3.1. The homogeneous solution 102
8.3.2. The particular solution 103
8.3.3. The complete solution 105
8.3.4. The resonant solution 106

A. Modeling CHAMP, GRACE and GOCE observables **109**
A.1. The Jacobi integral 109
A.2. Range, range rate and range acceleration 110
A.3. Spaceborne gravimetry 112

A.4. GRACE-type gradiometry 113
A.5. GOCE gradiometry 113

B. Coordinate Systems in Satellite Geodesy 115
B.1. Coordinate systems 115
B.2. Transformation between systems 117
B.3. Gradient 119

C. Numerical integration 121
C.1. Methods of Euler 122
C.1.1. Explicit Euler method (Euler polygon) 122
C.1.2. Backward Euler method 123
C.2. Accuracy, convergence and stability 123
C.3. Explicit Runge-Kutta method 125

D. Clairaut's differential equation 129
D.1. Radial symmetric force fields 129
D.2. Clairaut's differential equation 131
D.3. Clairaut's differential equation and the Kepler problem 132
D.3.1. Derive the orbit from the potential 132
D.3.2. Derive the potential from the orbit 134

E. Theory of epicycles und Equant 137
E.1. Aristotele 137
E.2. Theory of epicycles 138
E.3. Equant 140
E.3.1. Focus with central mass 141
E.3.2. Focus without mass 142

1. Introduction

Dynamic satellite geodesy is the application of celestial mechanics to geodesy. It aims in particular at describing satellite orbits under the influence of gravitational and non-gravitational forces. Conversely, if we know how orbit perturbations arise from gravity field disturbances, we have a tool for gravity field recovery from orbit analysis.

The first part of the course aims at the understanding of the ideal Kepler orbit. These orbits are completely determined by six initial values, i.e. a position vector $\boldsymbol{r}(t_0)$ and a velocity vector $\boldsymbol{v}(t_0)$ with 3 components at a given time point t_0. Further orbit locations can be found by numerical integration of Newton's *equation of motion*. If the orbit is transformed into so-called *Kepler elements*, five out of six values will remain constant, while the angular anomaly M turns out to be linear in time. An inverse transformation of Kepler elements into Cartesian coordinates will generate the ideal Kepler orbit as well.

Bewegungsgleichung

Keplerelmente

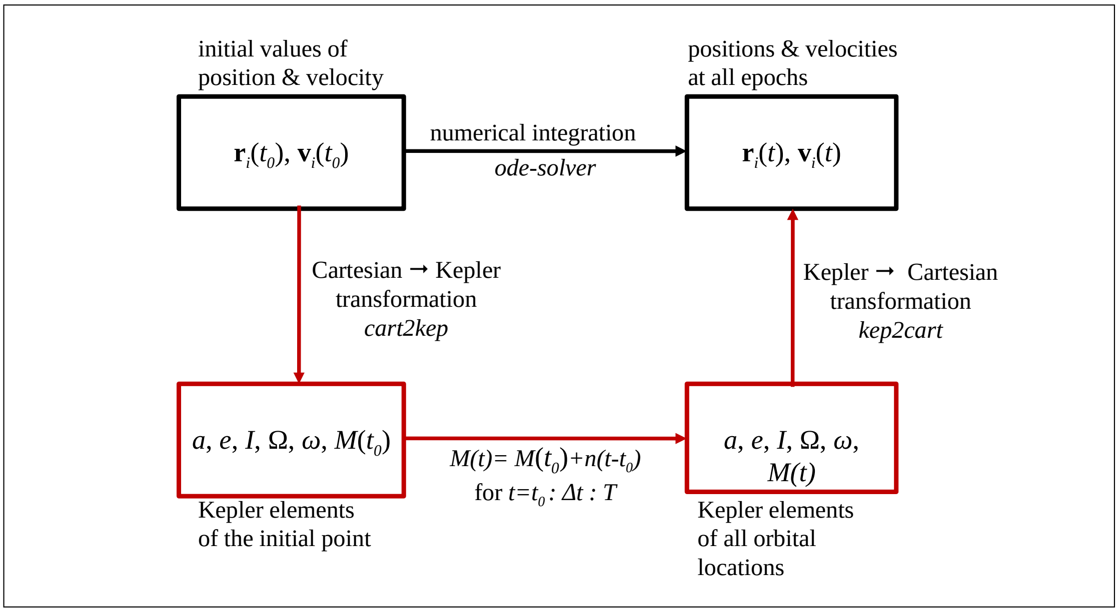

Figure 1.1.: Orbit propagation of a Kepler orbit based on initial position and velocity.

Bahnstörungen

The second part of the course investigates *orbit perturbations*, i.e. all effects which causes deviations in positions and velocities in comparison to the Kepler orbit. We analyze gravitational and non-gravitational perturbations via analytical formulas and numerical methods. The dominant orbit perturbation is the flattening of the Earth, i.e. the difference between reference ellipsoid and reference sphere, which causes long term trends in the orientation of the orbit but not in the shape.

2. The two-body problem

The two-body problem is concerned with the motion of two gravitating masses, M and m, for instance planets around the Sun or satellites around the Earth. For convenience we consider M as the main attracting mass, and the orbiting mass $m \ll M$. This is not a mathematical necessity, though.

2.1. Kepler's laws

Kepler[1] was the first to give a proper mathematical description of (planetary) orbits. Dissatisfied with the mathematical trickery of the geocentric cosmology, necessary to explain astronomical observations of planetary motion, he was an early adopter of the Copernican heliocentric model. Although a mental breaktrough at the time, Kepler even went further.

Based on observations, most notably from the Danish astronomer Brahe[2], Kepler empirically formulated three laws, providing a geometric-kinematical description of planetary motion. The first two laws were presented 1609 in his *Astronomia Nova* (The New Astronomy), the third one 1619 in *Harmonice Mundi* (Harmony of the World). They are:

i) Planets move on an elliptical path around the sun, which occupies one of the focal points.

ii) The line between sun and planet sweeps out equal areas in equal periods of time.

iii) For a given central body, the cube of the semi-major axes a of satellite is

[1] Johannes Kepler (1571–1630). Born in Weil der Stadt, lived in Leonberg, studied at Tübingen University. Being unable to obtain a faculty position at Tübingen University, he became mathematics teacher in Graz. He later became research associate with Tycho Brahe in Prague and — after Brahe died — succeeded him as imperial mathematician.

[2] Tycho Brahe (1546–1601). He attended the universities of Copenhagen and Leipzig, and then traveled through the German region, studying further at the universities of Wittenberg, Rostock, and Basel. During this period his interest in alchemy and astronomy was aroused, and he bought several astronomical instruments.

proportional to the square of the satellite's period of revolution T:

$$a^3 \propto T^2 \tag{2.1}$$

For two satellites—or celestial bodies—this can be expressed by the ratio

$$\left(\frac{a_1}{a_2}\right)^3 = \left(\frac{T_1}{T_2}\right)^3 \tag{2.2}$$

which is constant per celestial body. The law also holds in good approximation, if we use the Sun as central body, although there are several planets and moons involved:

Table 2.1.: Revolution period T in sidereal years and semi-major axis a in astronomical units in the solar system

planet	–	T in year	a in AU	T^2/a^3
Mercury	–	0.241	0.387	1.002
Venus	–	0.615	0.723	1.000
Earth	–	1	1	1
Mars	–	1.881	1.524	0.999
Jupiter	–	11.863	5.203	0.991
Saturn	–	11.863	5.203	0.991

mittlerer Radius

In his formulation of the third law Kepler equated the cube of the *mean radius* to T^2. Later we will learn that the current radius r is a function of the semi-major axis, the eccentricity e and an the eccentric anomaly E

$$r(a, e, E) = a(1 - e\cos E). \tag{2.3}$$

The average of the radius within one revolution

$$\frac{1}{2\pi}\int_0^{2\pi} r(a, e, E)\,\mathrm{d}E = \frac{1}{2\pi}\Big[aE - ae\sin E\Big]_0^{2\pi} = a \tag{2.4}$$

is in fact the semi-major axis.

2.1.1. First law: elliptical motion

According to Kepler, planets move in ellipses around the sun. Although that was a daring statement already at a time when church dogma still prevailed over scientific thought, Kepler even put the Sun outside the geometric centre of these ellipses. Instead he asserted that the Sun is at one of the foci.

Geometry

An ellipse is defined as the set of points whose sum of distances to both foci is constant. Inspection of fig. 2.1, in which we choose a point on the major axis (left panel), tells us that this sum must be $(a + x) + (a - x) = 2a$, the length of the major axis. The quantity a is called the *semi-major axis*. lange Halbachse

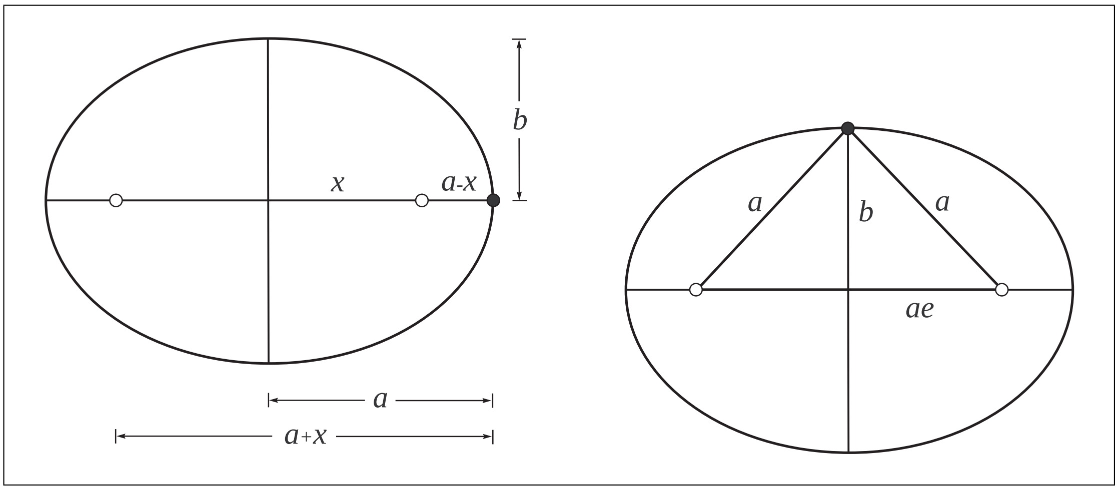

Figure 2.1.: Geometry of the Kepler ellipse in the orbital plane.

But then, for a point on the minor axis, see right panel, we have a symmetrical configuration. The distance from this point to each of the foci is a. The length b is called the *semi-minor axis*. Knowing both axes, we can express the distance to focus and centre of the ellipse. It is $\sqrt{a^2 - b^2}$. Usually it is expressed as a proportion e of the semi-major axis a: kurze Halbachse

$$(ae)^2 + b^2 = a^2 \Longrightarrow e^2 = \frac{a^2 - b^2}{a^2}\ , \text{ or } b = \sqrt{1 - e^2}\ a\,.$$

The proportionality factor e is called the *eccentricity*; the out-of-centre distance ae is known as the *linear eccentricity*. Exzentrizität

From mathematics we know the polar equation of an ellipse:

$$r(\nu) = \frac{p}{1 + e\cos\nu}\,, \tag{2.5}$$

in which r is the radius, ν the *true anomaly* and p the *parameter of the ellipse* (semi latus rectum). From the left panel of fig. 2.2 we are able to express p in terms of a and e. We can write down two equations: wahre Anomalie Ellipsenparameter

1. sum of sides: $p + x = 2a$ or $x^2 = 4a^2 - 4ap + p^2$

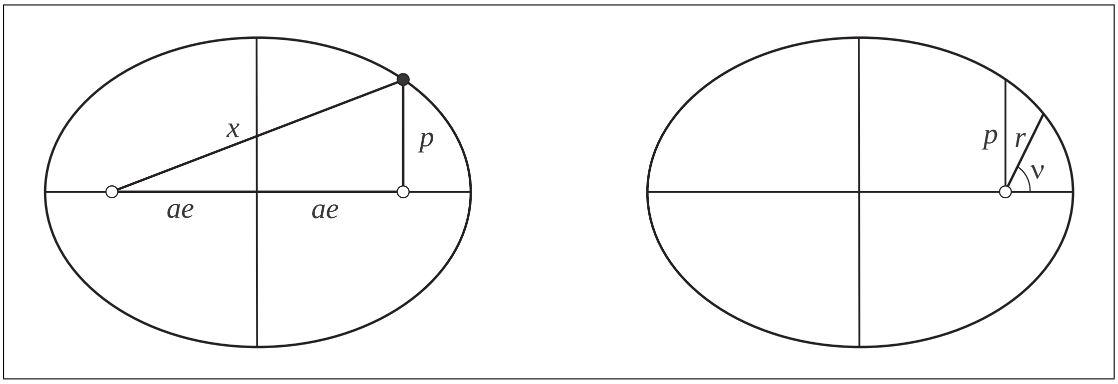

Figure 2.2.: Parameters of the polar equation for the ellipse.

$$
\begin{aligned}
\text{2. Pythagoras:} \quad x^2 &= p^2 + 4a^2e^2 \\
\text{eliminate } x\text{:} \quad p^2 + 4a^2e^2 &= 4a^2 - 4ap + p^2 \\
\text{delete } p^2\text{:} \quad ae^2 &= a - p \\
\text{rewrite:} \quad p &= a(1-e^2) \\
&= \frac{b^2}{a}\,.
\end{aligned}
$$

Knowing p, we recast the polar equation (2.5) into:

$$r(\nu) = \frac{a(1-e^2)}{1+e\cos\nu} \overset{\text{or}}{=} \frac{a(1+e)(1-e)}{1+e\cos\nu} \tag{2.6}$$

Exercise 2.1 *Insert $\nu = 0$ or $180°$ and check whether the outcome of (2.6) makes sense.*

Perihel
Perigäum
Aphel, Apogäum

The orbital point closest to the mass-bearing focus is called *perihelion* in case of planetary motion around the Sun (Helios) or *perigee* for satellite motion around the Earth (Gaia). More generally one can speak of *perifocus*. The farthest point at $\nu = 180°$ is called, respectively, *aphelion*, *apogee* or *apofocus*. Since we are mostly discussing satellite motion, we will predominantly use perigee and apogee.

Remark 2.1 (circular orbit) *In case of zero eccentricity ($e = 0$) the ellipse becomes a circle and $a = b = p = r$.*

2.1.2. Second law: area law

Flächensatz

The line through focus and satellite (or planet) sweeps out equal areas A during equal intervals of time Δt. This is also known as Kepler's area law. From the left panel of fig. 2.3 it is seen that this effect is most extreme if a time interval around perigee is compared to one at apogee.

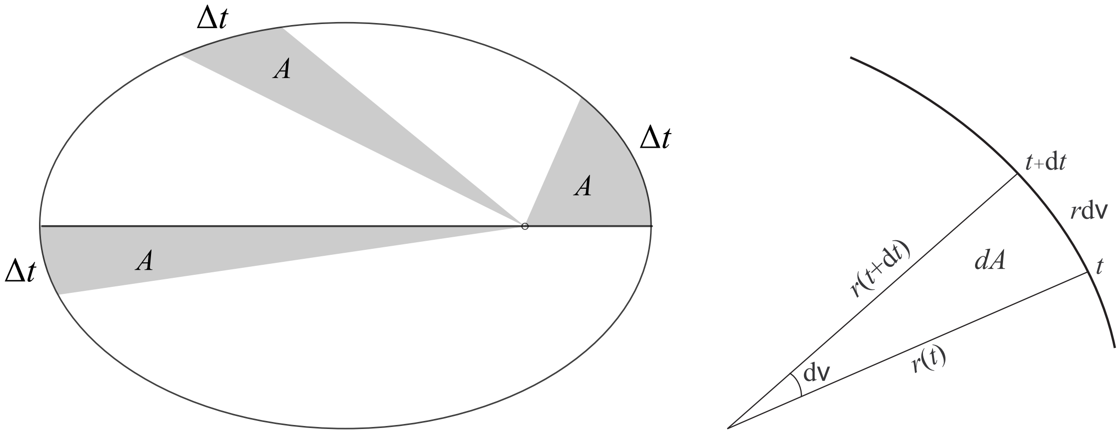

Figure 2.3.: Kepler's area law (left) and infinitesimal area (right).

As a consequence of Kepler's second law, the angular velocity $\dot{\nu}$ must be variable during an orbital revolution: fast around perigee and slow around apogee. Bahnumlauf

The infinitesimal picture of this law looks as follows. In an infinitesimal amount of time $\mathrm{d}t$ the satellite travels an arc segment $r\,\mathrm{d}\nu$. The infinitesimal, nearly triangular area, reads $\mathrm{d}A = \frac{1}{2}r^2\,\mathrm{d}\nu$. Therefore:

$$\begin{aligned} \mathrm{d}A = \frac{1}{2}r^2\,\mathrm{d}\nu \;&\sim\; \mathrm{d}t \\ \Longrightarrow r^2\,\mathrm{d}\nu &= c\;\mathrm{d}t \\ \Longrightarrow r^2\dot{\nu} \;&=\; c \end{aligned}$$

This sheds a different light on the area of Kepler's law. It is the quantity $r^2\dot{\nu}$ that is conserved. In a later section we will bring this in connection to the conservation of *angular momentum*. Here we can see already that, if we write $v = r\dot{\nu}$ for linear velocity, rv is constant. Drehimpuls

Angular Momentum

Consider the epifocal coordinate system in fig. 2.4. In this frame the position and velocity vector read:

$$\boldsymbol{r}_f = \begin{pmatrix} r\cos\nu \\ r\sin\nu \\ 0 \end{pmatrix} \quad \text{and} \quad \boldsymbol{v}_f = \begin{pmatrix} \dot{r}\cos\nu - r\dot{\nu}\sin\nu \\ \dot{r}\sin\nu + r\dot{\nu}\cos\nu \\ 0 \end{pmatrix}.$$

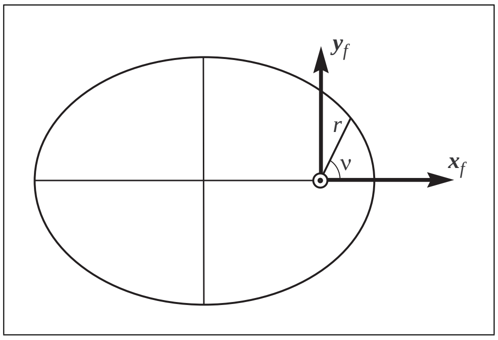

Figure 2.4: Epifocal frame: x_f towards perigee, z_f perpendicular to orbital plane towards angular momentum, and y_f complementary in right-hand sense.

The angular momentum vector, by its very definition, will be perpendicular to both and thus perpendicular to the orbital plane:

$$\boldsymbol{L_f} = \boldsymbol{r}_f \times \boldsymbol{v}_f = \begin{pmatrix} 0 \\ 0 \\ r\dot{r}\cos\nu\sin\nu + r^2\cos^2\nu\dot{\nu} - r\dot{r}\sin\nu\cos\nu + r^2\sin^2\nu\dot{\nu} \end{pmatrix} = \begin{pmatrix} 0 \\ 0 \\ r^2\dot{\nu} \end{pmatrix}$$

2.1.3. Third law: harmony

Kepler's third law can be rephrased as

> *The cubes of the semi-major axes*[3] *of the orbits are proportional to the squares of the revolution periods.*

If we cast this law into mathematics, we obtain with proportionality factor c:

$$a^3 \sim T^2 \iff a^3 = cT^2 \,.$$

The orbital period T is inversely related to the mean orbital angular velocity n:

$$T = \frac{2\pi}{n} \,.$$

mittlere Bewegung

The angular velocity n is conventionally referred to as *mean motion*. We now obtain:

$$a^3 = c\frac{(2\pi)^2}{n^2} \quad \Longrightarrow \quad n^2a^3 = c(2\pi)^2 \,.$$

After Newton had developed his universal law of gravitation the seemingly arbitrary constant right hand side turned out to be more fundamental: the gravitational constant G times the mass M of the attracting body[4].

[3] Kepler: mean radius in the sense of (2.4)

[4] $GM_{\mathrm{E}} = 3.986\,004\,415 \cdot 10^{14}\ \frac{\mathrm{m}^3}{\mathrm{s}^2}$
$GM_{\odot} = 1.327\,122\,440\,018 \cdot 10^{20}\ \frac{\mathrm{m}^3}{\mathrm{s}^2}$

$$\boxed{n^2 a^3 = GM} \tag{2.7}$$

Although Kepler's third law is intriguing, the particular combination of powers—a square and a cube—should not come as a surprise. Compare the situation of a circular orbit with angular velocity[5] ω. The centripetal force (per mass unit) is balanced by the gravitational attraction:

$$\omega^2 r = \frac{GM}{r^2} \quad \Longrightarrow \quad \omega^2 r^3 = GM\,,$$

which is of the same form as Kepler's third law.

Exercise 2.2 *Many orbits and orbital features can be calculated using (2.7).*

geostationary orbit:	$n = \dfrac{2\pi}{1\ day} = \omega_E$	$\Longrightarrow \quad a \approx 40\,000\,\mathrm{km}$
GPS:	$n = 2\omega_E$	$\Longrightarrow \quad a = \ldots$
LEO:	$n \approx 15\omega_E$	
satellite at zero height:	$n \approx 16\omega_E$	$\Longrightarrow$ *Schuler frequency*

2.2. Further geometry

2.2.1. Three-dimensional orbit description

The Kepler ellipse was defined in size by its semimajor axis a and in shape by its eccentricity e. The location of the satellite within the orbit was indicated by the true anomaly ν. In three-dimensional space, though, we need two more parameters to indicate the orientation of the orbital plane, and again one more to orient the ellipse within this plane. In total we thus have 6 orbital elements or Kepler elements. The number 6 is equal to the the sum of 3 Cartesian position coordinates and 3 velocity components. Please refer to fig. 2.6.

The orbital plane is inclined with respect to the equator. The corresponding angle I is obviously called *inclination*. The intersection line between orbital plane and equator is the *nodal line*. The node, in which the satellite crosses the equator from South to North is the *ascending node*. The angle Ω in inertial space between the *vernal equinox* (or x_i-axis) and ascending node is the *right ascension* of the ascending node. The *angle of*

Bahnneigung
Knotenlinie
steigender Knoten
Frühlingspunkt
Rektaszension

[5] Unfortunately, the symbol ω is used for the argument of perigee, one of the Kepler elements, and the angular velocity.

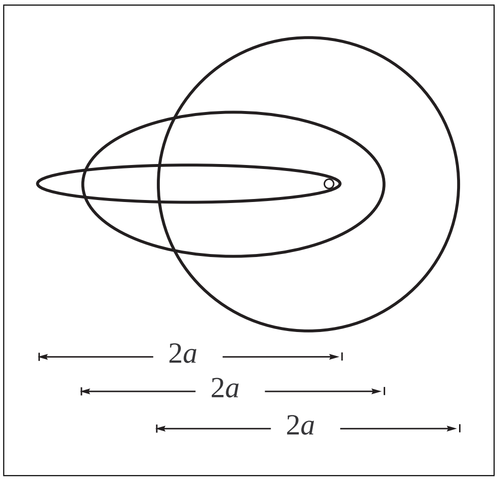

Figure 2.5: The eccentricity e is not involved in Kepler's third law. A circular orbit of radius a apparently has the same orbital revolution period as a highly eccentric (cigar-shaped) orbit of semi-major axis a as in fig. 2.5. Nevertheless, at $e = 0$ one orbit has a length of $2\pi a$ (the circumference of a sphere), whereas if the eccentricity approaches 1, one revolution approaches $4a$ ($2a$ forth plus $2a$ back).

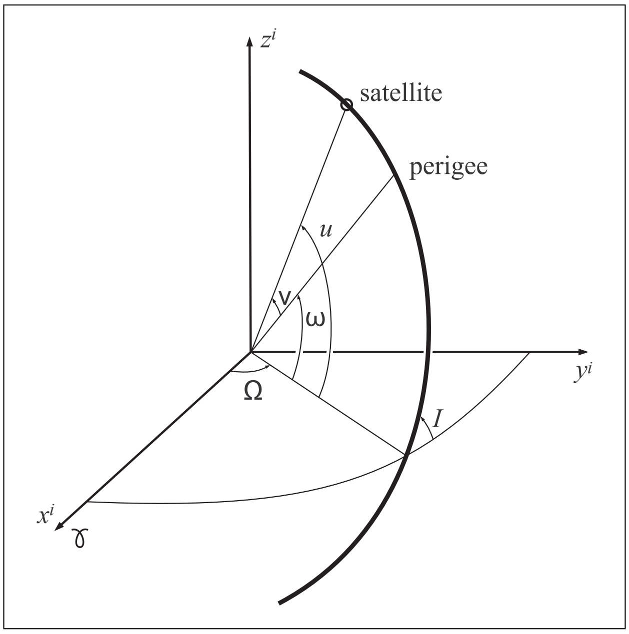

Figure 2.6: Three-dimensional geometry of the Kepler orbit.

perigee ω is counted from ascending node to perigee. The sum of angle of perigee and true anomaly is referred to as *argument of latitude*: $u = \omega + \nu$. This is a useful angle for circular and near-circular orbits for which the perigee is not or weakly defined. Perigäumswinkel

We can classify the 6 Kepler elements as follows:

a, e – size and shape of ellipse
Ω, I – orientation of orbital plane in space
ω, ν – position within orbital plane

Another classification is the following:

a, e, I – metric Kepler elements
Ω ω, ν – angular Kepler elements

The three angular Kepler elements are required for the transformation between the orbit vector $\boldsymbol{r}_f$ in the epifocal frame and the vector $\boldsymbol{r}_i$ in the inertial frame:

$$\boldsymbol{r}_f = \mathbf{R}_3(\omega)\mathbf{R}_1(I)\mathbf{R}_3(\Omega)\boldsymbol{r}_i \quad \Leftrightarrow \quad \boldsymbol{r}_i = \mathbf{R}_3(-\Omega)\mathbf{R}_1(-I)\mathbf{R}_3(-\omega)\boldsymbol{r}_f \,. \tag{2.8}$$

For the inclination we have in general $I \in [0°; 180°]$. Depending on the specific inclination (range) the orbits are known as:

$I = 0°$	– equatorial, prograde
$I < 90°$	– prograde
$I = 90°$	– polar
$I > 90°$	– retrograde
$I = 180°$	– equatorial, retrograde

Remark 2.2 *A radial projection of the satellite orbit onto the spherical surface of the Earth provides the* ground track, *which illustrates the spatial coverage of the mission. In this mapping, the maximum latitude of the groundtrack is direct related to the inclination:* Bodenspur

$$\phi_{\max} = \begin{cases} I, & \text{prograde} \\ 180° - I, & \text{retrograde} \end{cases} \tag{2.9}$$

2.2.2. Back to the orbital plane: anomalies

From Kepler's area law it was clear that ν is not uniform in time. In order to describe the time evolution more explicitly Kepler introduces two more angles: eccentric anomaly E

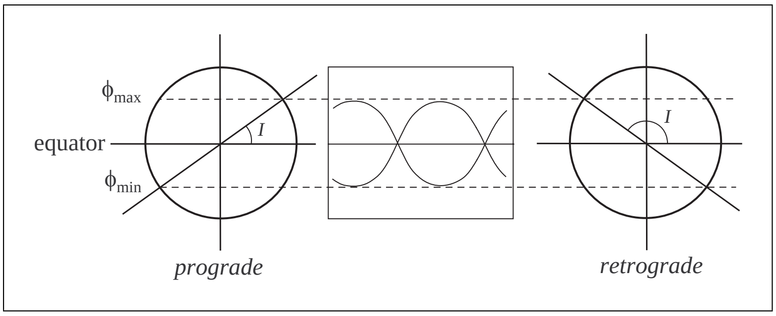

Figure 2.7.: The inclination determines the maximum and minimum latitude that ground-tracks can attain: ϕ_{min}, ϕ_{max}.

and mean anomaly M. The latter will be uniform in time, in the sense that we will be able to write $M = n(t - t_0)$ later on.

eccentric anomaly Consider fig. 2.8 with the epifocal f-frame and the eccentric x-frame. In the epifocal frame the position vector reads:

$$\boldsymbol{r}_f(r,\nu) = \begin{pmatrix} r\cos\nu \\ r\sin\nu \\ 0 \end{pmatrix}, \qquad r(\nu) = \frac{a(1-e^2)}{1+e\cos\nu} \tag{2.10}$$

Using the position vector in the eccentric frame we derive:

$$\boldsymbol{r}_x(a,E) = \begin{pmatrix} a\cos E \\ b\sin E \\ 0 \end{pmatrix} \quad \Longrightarrow \quad \boldsymbol{r}_f(a,E) = \begin{pmatrix} a\cos E - ae \\ a\sqrt{1-e^2}\sin E \\ 0 \end{pmatrix}. \tag{2.11}$$

The ratio of second and first component provides

$$\frac{r\sin\nu}{r\cos\nu} = \frac{a\sqrt{1-e^2}\sin E}{a\cos E - ae} \Leftrightarrow \tan\nu = \frac{\sqrt{1-e^2}\sin E}{\cos E - e}. \tag{2.12}$$

After some manipulation we determine the current radius:

$$\begin{aligned} r &= \|\boldsymbol{r}_f(a,E)\| \\ &= \sqrt{a^2\cos^2 E - 2a^2 e\cos E + a^2e^2 + a^2\sin^2 E - a^2e^2\sin^2 E} \\ &= \sqrt{a^2(\cos^2 E + \sin^2 E) - 2a^2e\cos E + a^2e^2(1-\sin^2 E)} \\ &= \sqrt{a^2 - 2a^2\cos E + a^2e^2\cos^2 E} \\ &= a - ae\cos E\,. \end{aligned} \tag{2.13}$$

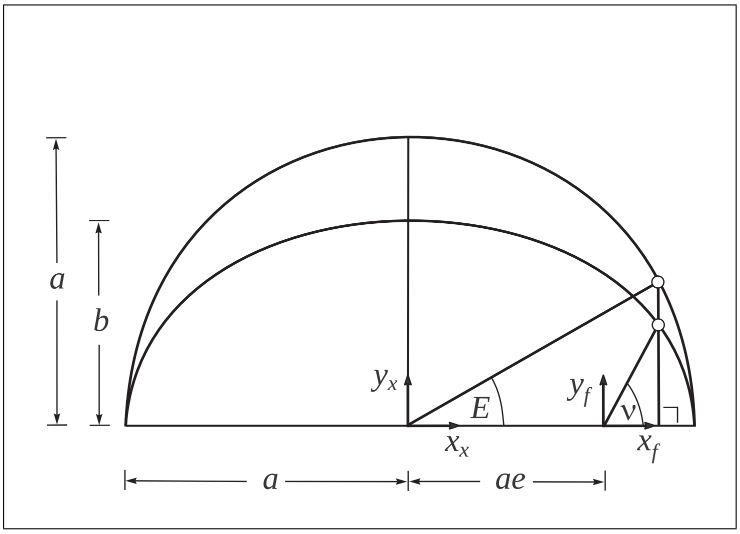

Figure 2.8.: Definition of eccentric anomaly E from true anomaly ν. The geometric construction is similar to the definition of a reduced latitude from a geodetic latitude.

mean anomaly Neither ν nor E is uniform (linear in time). Kepler therefore defined the mean anomaly M. The following equation is usually referred to as the *Kepler equation*:

$$\boxed{M = E - e \sin E} \,. \tag{2.14}$$

The mean anomaly is a fictitious angle. It cannot be drawn in fig. 2.8. It can only be calculated from E. But it evolves linearly in time. Thus one can write:

$$M = n(t - t_0)\,,$$

in which t_0 stands for the time of perigee passage, where $\nu = E = M = 0$. This allows us to calculate the orbit evolution over time, say from t_0 to t_1 by the following scheme:

$$\boxed{\boldsymbol{r},\, \boldsymbol{v} \text{ @ } t_0} \longrightarrow \boxed{a, e, I, \omega, \Omega, M_0} \xrightarrow{\Delta t} \boxed{a, e, I, \omega, \Omega, M_1} \longrightarrow \boxed{\boldsymbol{r},\, \boldsymbol{v} \text{ @ } t_1}\,,$$

in which the time step Δt stands more explicitly for $M_1 = M_0 + n(t_1 - t_0)$. The (Cartesian) position and velocity vectors at t_0 are known as the *initial state*. In summary, if one wants to know the orbital position and velocity as a function of time, one should transform the initial state into Kepler elements. In the Kepler element domain, only the mean anomaly M changes over time. To be precise, it changes linearly with time. After the time step, the Kepler elements need to be transformed back to position and velocity again (cf. fig. 2.9).

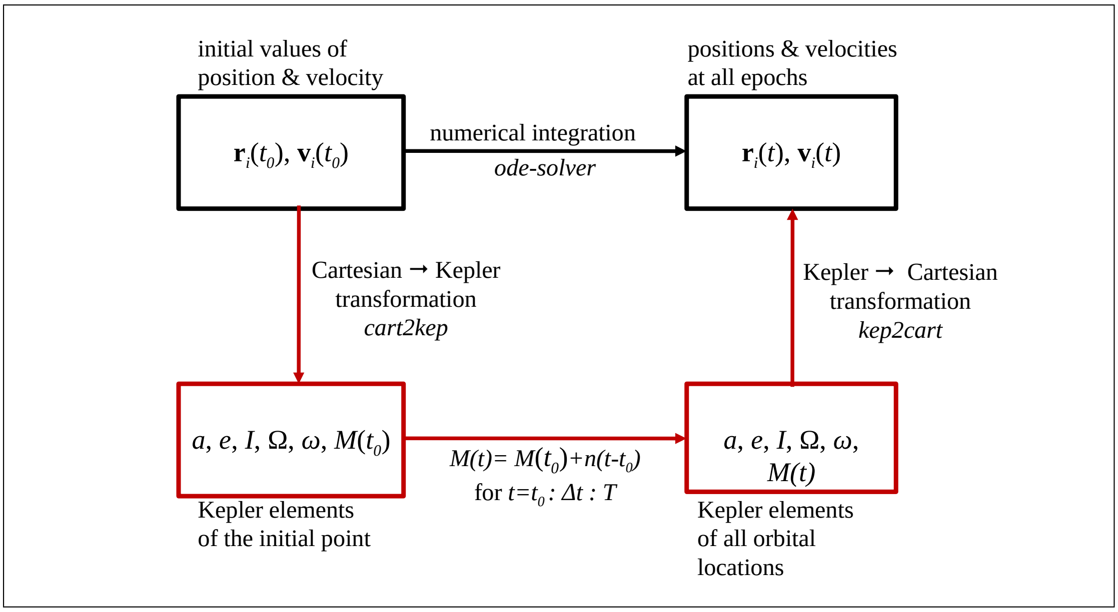

Figure 2.9.: Determination of a Kepler orbit based on initial positions and velocity.

Reverse Kepler equation For the reverse transformation of the Kepler equation (2.14) an iteration is required. We first recast it into $E = M + e \sin E$, which on the first sight is not helpful to calculate E from M. However, since e is usually small, we can approximate the true anomaly by the iteration $E_{i+1} = M + e \sin E_i$:

$$\begin{aligned} E_0 &= 0 \\ E_1 &= M \\ E_2 &= M + e \sin E_1 \\ E_3 &= M + e \sin E_2 \\ &\text{etc.} \end{aligned}$$

Exercise 2.3 *Determine the eccentric anomaly E and the true anomaly ν, when the mean anomaly $M = 70\overset{\circ}{.}4500$ and the eccentricity $e = 0.345$ are given:*

$$\begin{aligned} M = E_0 &= \frac{70.45\pi}{180} = \underline{1}.229\,584 \\ E_1 = M + e \sin E_0 &= \underline{1.5}54\,695 \\ E_2 = M + e \sin E_1 &= \underline{1.574}\,539 \\ E_3 = M + e \sin E_2 &= \underline{1.574\,58}2 \end{aligned}$$

$$E_4 = M + e \sin E_3 = \underline{1.574\,581}$$
$$E_4 = 1.574581 \hat{=} 90\overset{\circ}{.}2168$$

For the true anomaly

$$\tan \nu = \frac{\sqrt{1-e^2} \sin E}{\cos E - e} = \frac{0.938\,595}{-0.348\,785}$$
$$\nu = \arctan \frac{0.938\,595}{-0.348\,785} = -1.215\,006 + \pi = 1.926\,586 \hat{=} 110\overset{\circ}{.}3852$$

the quadrant of the angle must be considered. In several programming languages, this can be realized by the function `atan2(.,.)` *with two arguments.*

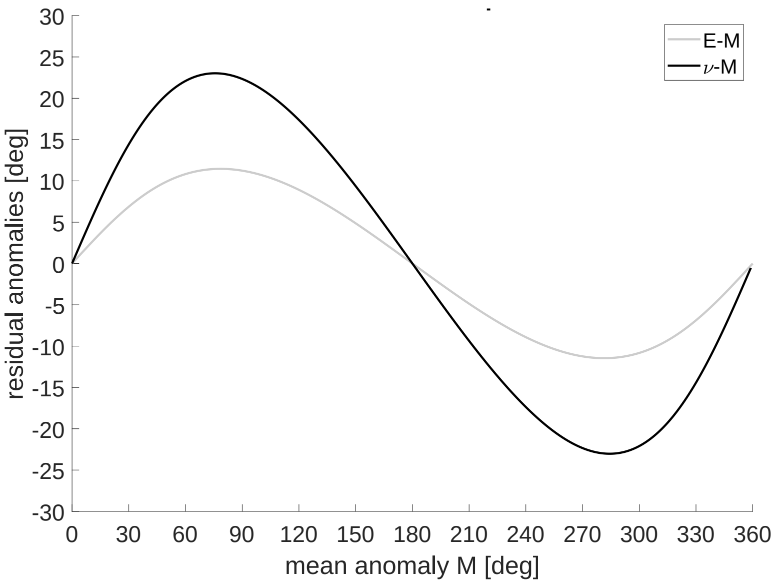

Figure 2.10.: Differences of the anomalies $E - M$ and $\nu - M$ for an ellipse with the eccentricity $e = 0.2$. The three anomalies coincides only in perigee and apogee, and the values differ up to 20°.

Remark 2.3 *In satellite geodesy, it is very common to note down angles like inclination, anomalies or latitude and longitude in degrees. However, the solution of the Kepler equation is only meaningful if the angles E and M are considered in radians.*

Remark 2.4 *For non-circular orbits, the numerical values of the three anomalies coincides only in perigee and apogee (cf. fig. 2.10).*

2.3. Newton equations and conservation laws

Kepler's laws provide a geometric and kinematic picture of orbital motion. Although the area law hints at angular momentum conservation already and the third law at gravitation, the concept of forces was unknown to Kepler. A dynamic description of the Kepler orbit had to wait for Newton. Moreover, Kepler derived his laws empirically.

In this section we will take Newton's equations of motion — in the inertial frame — for the two-body problem:

$$\ddot{\boldsymbol{r}} = \nabla \frac{GM}{r} = -\frac{GM}{r^3}\boldsymbol{r} \ , \text{ or } \boxed{\ddot{\boldsymbol{r}} + \frac{GM}{r^3}\boldsymbol{r} = 0} \ , \tag{2.15}$$

and apply three tricks to it:

i) scalar multiplication with velocity: $\dot{\boldsymbol{r}} \cdot \ldots$,

ii) vectorial multiplication with position: $\boldsymbol{r} \times \ldots$,

iii) vectorial multiplication with angular momentum: $\boldsymbol{L} \times \ldots$.

After a subsequent time integration we will end up with fundamental conservation laws and, eventually, with the Kepler orbit. Thus, at the end of this section we will have achieved a dynamical description of the Kepler orbit, based on a physical principle.

2.3.1. Conservation of energy

Trick 1: "$\dot{\boldsymbol{r}} \cdot \boxed{\text{Newton}}$".

Remark 2.5 *If $\dot{\boldsymbol{r}} = \boldsymbol{v}$ and r and v are respectively the length of $\boldsymbol{r}$ and $\boldsymbol{v}$, then $\dot{r} \neq v$! Instead, the scalar radial velocity is only the projection of the velocity vector on the radial direction: $\dot{r} = \dot{\boldsymbol{r}} \cdot \boldsymbol{r}/r = \dot{\boldsymbol{r}}\boldsymbol{e}_r$.*

$$\begin{aligned}
\dot{\boldsymbol{r}} \cdot \ddot{\boldsymbol{r}} + \dot{\boldsymbol{r}} \cdot \frac{GM}{r^3}\boldsymbol{r} &= 0 \\
\Longleftrightarrow \boldsymbol{v} \cdot \dot{\boldsymbol{v}} + \frac{GM}{r^3}\dot{\boldsymbol{r}} \cdot \boldsymbol{r} &= 0 \\
\Longleftrightarrow \boldsymbol{v} \cdot \dot{\boldsymbol{v}} + \frac{GM}{r^2}\dot{r} &= 0 \ , \text{ (because } \dot{r}r = \dot{\boldsymbol{r}} \cdot \boldsymbol{r}) \\
\Longleftrightarrow \frac{1}{2}\frac{\mathrm{d}}{\mathrm{d}t}(\boldsymbol{v} \cdot \boldsymbol{v}) - \frac{\mathrm{d}}{\mathrm{d}t}\left(\frac{GM}{r}\right) &= 0 \qquad \text{(lucky guess)}
\end{aligned}$$

$$\begin{aligned} &\iff \frac{\mathrm{d}}{\mathrm{d}t}\left(\frac{1}{2}v^2 - \frac{GM}{r}\right) = 0 \\ &\implies \frac{1}{2}v^2 - \frac{GM}{r} = c\,. \end{aligned}$$

This demonstrates that the sum of kinetic and potential energy is constant: $c = E$. Later we will evaluate the exact amount of energy using the vis-viva equation.

Figure 2.11.: Interpretation of $\dot{r}$ as projection of $\dot{\boldsymbol{r}}$ in the direction $\boldsymbol{r}$

Remark 2.6 *Please be aware that in satellite geodesy the (gravitational) acceleration is defined by $\ddot{\boldsymbol{r}} = \nabla V$, while textbooks in physics prefer $\ddot{\boldsymbol{r}} = -\nabla V$ with $V = \frac{GM}{r}$. We also call the energy equation a sum of the kinetic energy and the potential energy, which is somehow inconsistent.*

2.3.2. Conservation of angular momentum

Trick 2: "$\boldsymbol{r}\times$ $\boxed{\text{Newton}}$".

$$\begin{aligned} \boldsymbol{r} \times \ddot{\boldsymbol{r}} + \frac{GM}{r^3}\underbrace{\boldsymbol{r} \times \boldsymbol{r}}_{=\boldsymbol{0}} &= \boldsymbol{0} \\ \iff \boldsymbol{r} \times \ddot{\boldsymbol{r}} &= \boldsymbol{0} \\ \iff \frac{\mathrm{d}}{\mathrm{d}t}(\boldsymbol{r} \times \dot{\boldsymbol{r}}) &= \underbrace{\dot{\boldsymbol{r}} \times \dot{\boldsymbol{r}}}_{=\boldsymbol{0}} + \boldsymbol{r} \times \ddot{\boldsymbol{r}} = \boldsymbol{0} \\ \implies \boldsymbol{r} \times \dot{\boldsymbol{r}} &= \boldsymbol{c} \end{aligned}$$

This demonstrates that the angular momentum $\boldsymbol{L} = \boldsymbol{r} \times \dot{\boldsymbol{r}}$ is constant: $\boldsymbol{c} = \boldsymbol{L}$. We have more or less reproduced Kepler's area law from Newton's equation. Note, however, that we have achieved here conservation of the 3D angular momentum vector. Not only are the areas equal over equal times (one dimension), but also is the orbital plane constant in inertial space (two dimensions). The latter will lead to Ω and I.

Remark 2.7 *The angular momentum is conserved not only in the Kepler problem but for all radial symmetric force fields of the form $\boldsymbol{F} = f(r)\boldsymbol{r}$ (see appendix D).*

2.3.3. Conservation of orbit vector

Trick 3: "$\boxed{\text{Newton}} \times \boldsymbol{L}$".

$$
\begin{aligned}
\ddot{\boldsymbol{r}} \times \boldsymbol{L} + \frac{GM}{r^3}\boldsymbol{r} \times \boldsymbol{L} &= \boldsymbol{0} \\
\Longleftrightarrow \underbrace{\ddot{\boldsymbol{r}} \times \boldsymbol{L}}_{\text{LHS}} &= \underbrace{\frac{GM}{r^3}\boldsymbol{L} \times \boldsymbol{r}}_{\text{RHS}} \\
\text{LHS}: \qquad \frac{\mathrm{d}}{\mathrm{d}t}(\dot{\boldsymbol{r}} \times \boldsymbol{L}) &= \ddot{\boldsymbol{r}} \times \boldsymbol{L} + \boldsymbol{r} \times \underbrace{\dot{\boldsymbol{L}}}_{=\boldsymbol{0}} \\
\text{RHS}: \qquad \frac{GM}{r^3}\boldsymbol{L} \times \boldsymbol{r} &= \frac{GM}{r^3}(\boldsymbol{r} \times \dot{\boldsymbol{r}}) \times \boldsymbol{r} \\
&= \frac{GM}{r^3}[(\boldsymbol{r} \cdot \boldsymbol{r})\dot{\boldsymbol{r}} - (\boldsymbol{r} \cdot \dot{\boldsymbol{r}})\boldsymbol{r}] \\
&= \frac{GM}{r}\dot{\boldsymbol{r}} - \frac{GM}{r^2}\dot{r}\boldsymbol{r} \\
GM\frac{\mathrm{d}}{\mathrm{d}t}\frac{\boldsymbol{r}}{r} &= \frac{GM}{r}\dot{\boldsymbol{r}} - \frac{GM}{r^2}\dot{r}\boldsymbol{r} \text{ , (lucky guess)} \\
\text{LHS} = \text{RHS}: \qquad \frac{\mathrm{d}}{\mathrm{d}t}(\dot{\boldsymbol{r}} \times \boldsymbol{L}) &= GM\frac{\mathrm{d}}{\mathrm{d}t}\frac{\boldsymbol{r}}{r} \\
\Longrightarrow \dot{\boldsymbol{r}} \times \boldsymbol{L} &= \frac{GM}{r}\boldsymbol{r} + \boldsymbol{B}
\end{aligned}
$$

Laplace Vektor

The vector $\boldsymbol{B}$ is a constant of the integration. It is a quantity that is conserved in the two-body problem. It is known as Runge-Lenz vector or *Laplace vector*. The above derivation shows that $\boldsymbol{B}$ is a linear combination of $\dot{\boldsymbol{r}} \times \boldsymbol{L}$ and $\boldsymbol{r}$. Therefore $\boldsymbol{B}$ must lie in the orbital plane.

At this point we have conserved 7 quantities or parameters, E(1D), $\boldsymbol{L}$(3D) and $\boldsymbol{B}$(3D). Given the fact that only 5 Kepler elements are constant, the 7 conserved quantities cannot be independent.

The last equation can be written in a different form if we perform scalar multiplication with the position vector: $\boldsymbol{r} \cdot \ldots$, which reduces 2 dimensions.

$$\boldsymbol{r} \cdot (\dot{\boldsymbol{r}} \times \boldsymbol{L}) = \frac{GM}{r} \boldsymbol{r} \cdot \boldsymbol{r} + \boldsymbol{r} \cdot \boldsymbol{B} \tag{2.16}$$

Under cyclic permutation[6] the left-hand side is equal to $\boldsymbol{L} \cdot (\boldsymbol{r} \times \dot{\boldsymbol{r}}) = \boldsymbol{L} \cdot \boldsymbol{L} = L^2$, leading to

$$\begin{aligned} L^2 &= GMr + r\|\boldsymbol{B}\| \cos\alpha \\ \Longrightarrow r &= \frac{\frac{L^2}{GM}}{1 + \frac{\|\boldsymbol{B}\|}{GM} \cos\alpha} \,. \end{aligned}$$

If we now identify the following quantities:

$$\alpha := \nu \quad , \quad \frac{L^2}{GM} := p \quad , \quad \frac{\|\boldsymbol{B}\|}{GM} := e \,, \tag{2.17}$$

then we obtain the polar equation of the ellipse (2.5) again:

$$r(\nu) = \frac{p}{1 + e\cos\nu} \,.$$

At the same time we have learnt that the Laplace vector $\boldsymbol{B}$ points towards perigee.

Remark 2.8 *Effectively we have now solved the Kepler problem using Newton's equation of motion. We have implicitly obtained Kepler's laws.*

2.3.4. Vis viva – living force

It was demonstrated that the total energy[7] E is conserved:

$$\begin{aligned} \frac{1}{2}v^2 - \frac{GM}{r} &= E \\ T + V &= E \,. \end{aligned}$$

[6] In the scalar triple product $\boldsymbol{a} \cdot (\boldsymbol{b} \times \boldsymbol{c}) = \boldsymbol{c} \cdot (\boldsymbol{a} \times \boldsymbol{b}) = \boldsymbol{b} \cdot (\boldsymbol{c} \times \boldsymbol{a})$ the vectors can be cyclically permuted.

[7] Please note, that the variable E can refer to the total energy or to eccentric anomaly. The meaning shall be clear by the content.

We will settle now the question: How much is the constant energy?

Since the energy is constant along the orbit, we can evaluate it at a convenient location, e.g. in the perigee:

$$L = \|\boldsymbol{L}\| = rv\sin\alpha = r_{\text{apo}}v_{\text{apo}} = r_{\text{per}}v_{\text{per}}$$
$$\Longrightarrow E = \frac{1}{2}\frac{L^2}{r^2\sin^2\alpha} - \frac{GM}{r} \overset{\text{e.g.}}{=} \frac{L^2}{2r_{\text{per}}^2} - \frac{GM}{r_{\text{per}}}.$$

Making use of

$$p = a(1-e^2) = \frac{L^2}{GM} \Rightarrow L^2 = GMa(1-e^2)$$

we obtain

$$\begin{aligned} E &= \frac{GMa(1-e^2)}{2a^2(1-e)^2} - \frac{GM}{a(1-e)} \\ &= \frac{1}{2}GM\frac{1+e}{a(1-e)} - \frac{GM}{a(1-e)} \\ &= \frac{GM}{a(1-e)}\left[\frac{1}{2}(1+e) - 1\right] \\ &= -\frac{GM}{2a}. \end{aligned}$$

This energy level is historically known as the vis-viva equation:

$$\boxed{E = \frac{1}{2}v^2 - \frac{GM}{r} = -\frac{GM}{2a}} \tag{2.18}$$

Remark 2.9 *The energy level only depends on the semi-major axis a but not on the eccentricity e (cf. revolution time). This can be used for estimating the energy or impulse of a transfer orbit (e.g. Hohmann transfer in Section 2.3.5)*

The scalar velocity $v = \|\boldsymbol{v}\|$ can be derived, when the current radius r is known:

$$\frac{1}{2}v^2 - \frac{GM}{r} = -\frac{GM}{2a} \qquad (= E)$$
$$v^2 = 2\frac{GM}{r} - \frac{GM}{a}$$
$$\boxed{v = \sqrt{GM\left(\tfrac{2}{r} - \tfrac{1}{a}\right)}}$$

Remark 2.10 (Cosmic velocities) *A satellite which falls on a circular orbit very close to the surface of the central body —and without orbit perturbations—will show the* first cosmic velocity *with $r = a$ and $v_I = \sqrt{GM/a}$. If a space probe should leave the gravity field of the central body, the semi-major axis must increase beyond limits ($a \to \infty$). This leads to the* second cosmic velocity *with $v_{II} = \sqrt{2GM/r} = v_I\sqrt{2}$, when starting from the ground. In case of the Earth, the cosmic velocities are $v_I = \sqrt{GM/R_\mathrm{E}} \approx 7.91\,\mathrm{km\,s^{-1}}$ and $v_{II} = v_I\sqrt{2} \approx 11.18\,\mathrm{km\,s^{-1}}$.*

Erste kosmische Geschwindigkeit

zweite kosmische Geschwindigkeit

2.3.5. Transfer orbit

Every satellite will remain in its Kepler orbit forever, when orbit disturbances and orbit maneuvers are ignored. However, there are several reasons for moving a satellite intentionally into another orbit:

- lifting onto operational altitude after rocket launch
- elongating life time of the mission
- lifting onto graveyard orbit
- adapting ground track sampling
- collision avoidance

For changing the orbit, a satellite must generate an impulse via propulsion. The propulsion is limited in magnitude of impulse and onboard fuel. Hence, the epochs of the impulses and the transfer orbit must be chosen carefully.

Hohmann transfer orbit

A Hohmann transfer brings a satellite from one circular orbit into another co-planar circular orbit by two so-called Δv-thrusts. The first thrust—a short engine burn at perigee of the transfer passage—brings the satellite into an elliptical transfer orbit. A second boost at apogee circularizes the orbit again. It is assumed herein, that the impulse is acting instantaneously on the satellite's orbit, and that a boost occurs in negligible time.

The circular initial orbit in fig. 2.12 is a low-Earth-orbit (LEO) with radius R_1 and the satellite should be transferred to a geostationary orbit (GEO). The energy is found via the semi-major axis and the vis-viva equation:

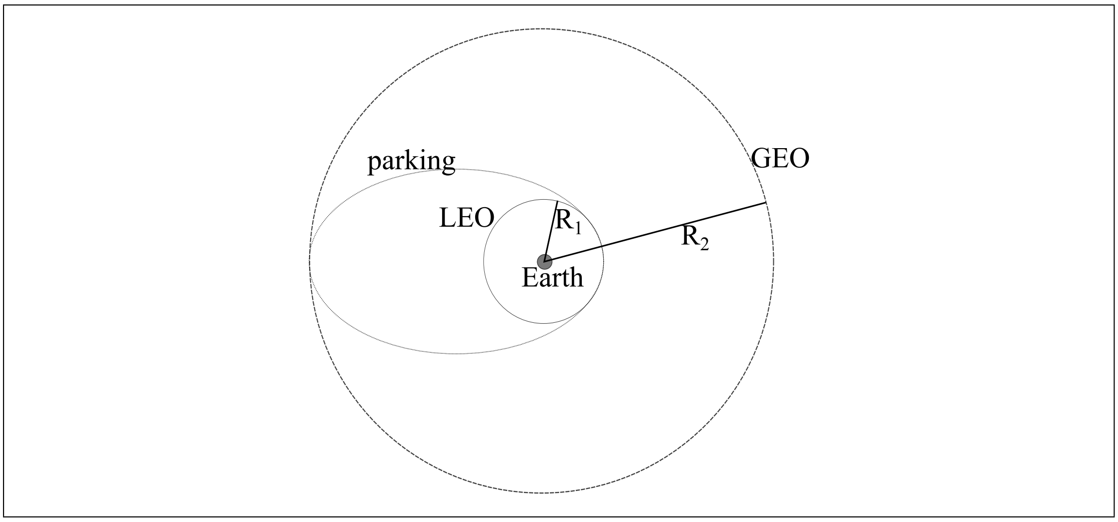

Figure 2.12.: Hohmann transfer between two circular orbits.

$$
\begin{aligned}
&\text{Orbit 1 (circular LEO):} && a_1 = R_1 && E_1 = -\frac{GM}{2R_1} \\
&\text{Orbit 2 (transfer ellipse):} && a_2 = \frac{R_1 + R_2}{2} && E_2 = -\frac{GM}{(R_1 + R_2)} \\
&\text{Orbit 3 (circular GEO):} && a_3 = R_2 && E_3 = -\frac{GM}{2R_2}
\end{aligned}
$$

The quantity Δv also known as "Delta-v" is used as scalar measure of impulse per unit of spacecraft mass in flight dynamics. In a Hohmann transfer we have 4 phases:

1. $v_1 = \sqrt{GM\left(\frac{2}{R_1} - \frac{1}{R_1}\right)} = \sqrt{\frac{GM}{R_1}}$ on the circular low-Earth-orbit with $r = a = R_1$ before the perigee boost.
2. $v_2 = \sqrt{GM\left(\frac{2}{R_1} - \frac{1}{(R_1+R_2)/2}\right)}$ in the perigee of the transfer ellipse with $a = \frac{R_2+R_1}{2}$ after perigee boost.
3. $v_3 = \sqrt{GM\left(\frac{2}{R_2} - \frac{1}{(R_1+R_2)/2}\right)}$ in the apogee of the transfer ellipse with $a = \frac{R_2+R_1}{2}$ before apogee boost.
4. $v_4 = \sqrt{\frac{GM}{R_2}}$ on the final circular orbit after apogee boost.

The necessary impulse per unit mass is now given by

$$\Delta v = (v_2 - v_1) + (v_4 - v_3)\,.$$

Exercise 2.4 *The Hohmann transfer of a satellite between circular LEO with* $r_1 = 6800\,\text{km}$ *and a circular GEO with* $r_2 = 42000\,\text{km}$ *requires the following changes in velocity:*

$$
\begin{aligned}
v_1 &= \sqrt{\frac{GM}{r_1}} = 7656.2\,\text{m/s} \\
v_2 &= \sqrt{GM\left(\frac{2}{r_1} - \frac{1}{(r_1+r_2)/2}\right)} = 10044.8\,\text{m/s} \\
v_3 &= \sqrt{GM\left(\frac{2}{r_2} - \frac{1}{(r_1+r_2)/2}\right)} = 1626.3\,\text{m/s} \\
v_4 &= \sqrt{\frac{GM}{r_2}} = 3080.6\,\text{m/s}
\end{aligned}
$$

and in total $\Delta v = (v_2 - v_1) + (v_4 - v_3) = 3842.9\,\text{m/s}$.

Remark 2.11 *The Hohmann transfer is optimal for co-planar and circular orbits if the ratio* $r_2 : r_1 < 11.94$ *holds. If the ratio is larger a so-called bi-elliptic transfer might perform better.*

Remark 2.12 *Thrusters can only deliver a limited amount of* Δv*. The Hohmann transfer can be applied in successive steps, leading to phase of apogee raising with small perigee boosts at every perigee passage. In the second phase, when the right altitude has been achieved, the orbit is circulated by a sequence of apogee boosts.*

Remark 2.13 *The concept is reversible, i.e. the calculation can be used for moving to a lower orbit, but the propulsion must fire in opposite directions then.*

Bi-elliptic transfer orbit

A bi-elliptic transfer brings a satellite from one circular orbit into another co-planar circular orbit by three Δv-thrusts and via two subsequent elliptic transfer orbits. In opposite to intuition, the first ellipse has a semi-major axis which is larger than the final circular orbit.

We can reformulate the calculation:

1. $\Delta v_{p1} = \sqrt{GM\left(\frac{2}{R_1} - \frac{1}{a_1}\right)} - \sqrt{\frac{GM}{R_1}}$ is the impulse for moving the satellite from the initial circular orbit with radius $r = R_1$ to an elliptic orbit with semi-major axis $a_1 = \frac{R_1 + r_b}{2}$ by a boost in the perigee.

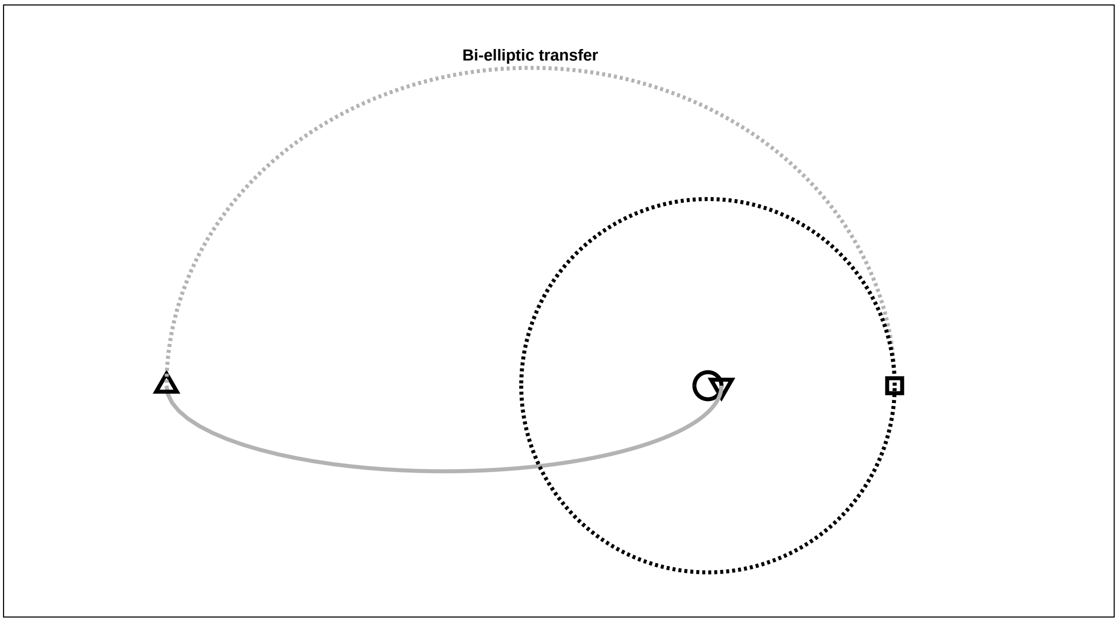

Figure 2.13.: Bi-elliptic transfer (in gray) between two circular orbits (in black).

2. $\Delta v_a = \sqrt{GM\left(\frac{2}{r_b} - \frac{1}{a_2}\right)} - \sqrt{GM\left(\frac{2}{r_b} - \frac{1}{a_1}\right)}$ is the impulse for moving the satellite from the first ellipse onto another with semi-major axis $a_2 = \frac{R_2+r_b}{2}$ by a boost in the apogee

3. $\Delta v_{p2} = \sqrt{GM\left(\frac{2}{R_2} - \frac{1}{a_2}\right)} - \sqrt{\frac{GM}{R_2}}$ is the impulse for moving a satellite from the second ellipse onto a circular orbit with radius $r = R_2$ with a boost in the perigee.

The "radius" r_b is the maximum distance between the central mass and the satellite. This value is a degree of freedom in the calculation.

Exercise 2.5 *Verify that a bi-elliptic transfer with* $R_1 = 6800\,\text{km}$, $R_2 = 93800\,\text{km}$ *and* $r_b = 40R_1$ *requires a smaller total impulse than the corresponding Hohmann transfer.*

2.4. Further useful relations

2.4.1. Understanding Kepler

Epifocal; $\boldsymbol{r, \nu}$

$$\boldsymbol{r}_f = \begin{pmatrix} r\cos\nu \\ r\sin\nu \\ 0 \end{pmatrix} \qquad \dot{\boldsymbol{r}}_f = \begin{pmatrix} \dot{r}\cos\nu - r\dot{\nu}\sin\nu \\ \dot{r}\sin\nu + r\dot{\nu}\cos\nu \\ 0 \end{pmatrix}$$

$$\boldsymbol{L}_f = \boldsymbol{r}_f \times \dot{\boldsymbol{r}}_f = \begin{pmatrix} 0 \\ 0 \\ r^2\dot{\nu} \end{pmatrix} \qquad \boldsymbol{r}_f \cdot \dot{\boldsymbol{r}}_f = r\dot{r}$$

Eccentric; $\boldsymbol{a, E}$

$$\boldsymbol{r}_x = \begin{pmatrix} a\cos E \\ b\sin E \\ 0 \end{pmatrix} \qquad \dot{\boldsymbol{r}}_x = \begin{pmatrix} -a\dot{E}\sin E \\ b\dot{E}\cos E \\ 0 \end{pmatrix} \qquad \dot{E} = \frac{n}{1 - e\cos E}$$

Epifocal; $\boldsymbol{a, E}$

$$\boldsymbol{r}_f = \begin{pmatrix} a\cos E - ae \\ a\sqrt{1-e^2}\sin E \\ 0 \end{pmatrix} \qquad \dot{\boldsymbol{r}}_f = \begin{pmatrix} -a\dot{E}\sin E \\ a\sqrt{1-e^2}\dot{E}\cos E \\ 0 \end{pmatrix}$$

$$\begin{aligned}
L &= \|\boldsymbol{r} \times \dot{\boldsymbol{r}}\| = \|\boldsymbol{L}_{f=3}\| \\
&= a^2\cos^2 E\sqrt{1-e^2}\dot{E} - a^2 e\sqrt{1-e^2}\dot{E}\cos E + a^2\sqrt{1-e^2}\dot{E}\sin^2 E \\
&= a^2\sqrt{1-e^2}\dot{E} - a^2 e\sqrt{1-e^2}\dot{E}\cos E \\
&= a^2\sqrt{1-e^2}\dot{E}(1 - e\cos E) \\
\text{from (2.18) we have: } \frac{L^2}{GM} &= p = a(1-e^2) \\
L &= \sqrt{GMa(1-e^2)} \\
&\Longrightarrow \sqrt{GMa(1-e^2)} = a^2\sqrt{1-e^2}\dot{E}(1 - e\cos E) \\
&\Longleftrightarrow \sqrt{\frac{GM}{a^3}} = \dot{E}(1 - e\cos E) = n
\end{aligned}$$

If we integrate the last line w.r.t. time, we obtain the Kepler equation $M = E - e\sin E$. Hence, the equation, which popped up in page 19, is a consequence of Kepler's laws!

$$\begin{aligned}
\text{Now: } \boldsymbol{r}\cdot\dot{\boldsymbol{r}} &= -a^2\cos E\sin E\dot{E} + a^2 e\dot{E}\sin E + a^2(1-e^2)\dot{E}\sin E\cos E \\
&= a^2 e\dot{E}\sin E - a^2e^2\dot{E}\sin E\cos E \\
&= a^2 e\dot{E}\sin E(1-e\cos E) \\
&= a^2 en\sin E
\end{aligned}$$

Together with $\boldsymbol{r}\cdot\dot{\boldsymbol{r}} = r\dot{r}$ we obtain

$$r\dot{r} = a^2 en\sin E = \sqrt{GMa}e\sin E \tag{2.19}$$

2.4.2. Partial derivatives $\nu \leftrightarrow E \leftrightarrow M$

Goal:

$$\frac{\partial\nu}{\partial M} = \frac{\partial\nu}{\partial E}\frac{\partial E}{\partial M}$$

The first part at the right side is difficult. We need to get back to the expression of the radial distance, both in terms of true anomaly ν and of eccentric anomaly E.

$$\begin{aligned}
r(\nu) = \frac{a(1-e^2)}{1+e\cos\nu} &\Rightarrow \frac{\partial r}{\partial\nu} = \frac{a(1-e^2)}{(1+e\cos\nu)^2}e\sin\nu = \frac{r^2e\sin\nu}{a(1-e^2)} \\
r(E) = a(1-e\cos E) &\Rightarrow \frac{\partial r}{\partial E} = ae\sin E
\end{aligned}$$

Thus, we get:

$$\frac{\partial\nu}{\partial E} = \frac{\partial\nu}{\partial r}\frac{\partial r}{\partial E} = \frac{a(1-e^2)}{r^2\sin\nu}a\sin E$$

Remember that the y-coordinate in the epifocal frame can either be expressed as $y_f = r\sin\nu$ or as $y_f = b\sin E$. Therefore, we end up with

$$\frac{\partial\nu}{\partial E} = \frac{a^2(1-e^2)}{rb} = \frac{b^2}{rb} = \frac{b}{r}$$

The second part at the right side of the equation above is easily obtained from Kepler's equation:

$$M = E - e\sin E \Rightarrow \frac{\partial M}{\partial E} = 1 - e\cos E = \frac{r}{a}$$

Combining all information, we get:

$$\frac{\partial\nu}{\partial M} = \frac{\partial\nu}{\partial E}\frac{\partial E}{\partial M} = \frac{ab}{r^2}$$

2.5. Transformations Kepler ⟷ Cartesian

2.5.1. Kepler ⟶ Cartesian

Problem: Given 6 Kepler elements $(a, e, I, \omega, \Omega, M)$, find the corresponding inertial position $\boldsymbol{r}_i$ and velocity $\dot{\boldsymbol{r}}_i$.

Solution: First get the eccentric anomaly E from the mean anomaly M by iteratively solving Kepler's equation:

$$E - e\sin E = M \;\Rightarrow\; E_{i+1} = e\sin E_i + M \text{ , with starting value } E_0 = M \tag{2.20}$$

Next, get the position and the velocity in the epifocal f-frame, which has its z-axis perpendicular to the orbital plane and its x-axis pointing to the perigee:

$$\boldsymbol{r}_f = \begin{pmatrix} a(\cos E - e) \\ a\sqrt{1-e^2}\sin E \\ 0 \end{pmatrix} \;,\; \dot{\boldsymbol{r}}_f = \frac{na}{1 - e\cos E}\begin{pmatrix} -\sin E \\ \sqrt{1-e^2}\cos E \\ 0 \end{pmatrix} \tag{2.21}$$

In case the true anomaly ν is given in the original problem instead of the mean anomaly M, the vectors $\boldsymbol{r}_f$ and $\dot{\boldsymbol{r}}_f$ are obtained by:

$$\boldsymbol{r}_f = \begin{pmatrix} r\cos\nu \\ r\sin\nu \\ 0 \end{pmatrix} \;,\; \dot{\boldsymbol{r}}_f = \frac{na}{\sqrt{1-e^2}}\begin{pmatrix} -\sin\nu \\ e + \cos\nu \\ 0 \end{pmatrix} \tag{2.22}$$

with

$$r = \frac{a(1-e^2)}{1 + e\cos\nu} \tag{2.23}$$

The transformation from inertial i-frame to the epifocal f-frame is performed by the rotation sequence $R_3(\omega)R_1(I)R_3(\Omega)$. So, vice versa, the inertial position and velocity are obtained by the inverse transformations:

$$\boldsymbol{r}_i = \mathbf{R}_3(-\Omega)\mathbf{R}_1(-I)\mathbf{R}_3(-\omega)\boldsymbol{r}_f \tag{2.24}$$

$$\dot{\boldsymbol{r}}_i = \mathbf{R}_3(-\Omega)\mathbf{R}_1(-I)\mathbf{R}_3(-\omega)\dot{\boldsymbol{r}}_f \,. \tag{2.25}$$

In particular, we find by multiplication of the rotation matrices

$$\mathbf{R}_3(-\Omega)\mathbf{R}_1(-I)\mathbf{R}_3(-\omega) = \tag{2.26}$$

$$\begin{pmatrix} \cos\omega\cos\Omega - \sin\omega\sin\Omega\cos I & -\sin\omega\cos\Omega - \cos\omega\sin\Omega\cos I & \sin I\sin\Omega \\ \cos\omega\sin\Omega + \sin\omega\cos\Omega\cos I & -\sin\omega\sin\Omega + \cos\omega\cos\Omega\cos I & -\sin I\cos\Omega \\ \sin I\sin\omega & \sin I\cos\omega & \cos I \end{pmatrix}$$

and for the position

$$\boldsymbol{r}_i = \mathbf{R}_3(-\Omega)\mathbf{R}_1(-I)\mathbf{R}_3(-\omega)\boldsymbol{r}_f = r\begin{pmatrix}\cos u\cos\Omega - \sin u\sin\Omega\cos I\\ \cos u\sin\Omega + \sin u\cos\Omega\cos I\\ \sin I\sin u\end{pmatrix}. \tag{2.27}$$

Gaußvektoren

Remark 2.14 *Please not that the direction towards the satellite in equation (2.27) is also the first column of the rotation matrix (2.26) for $\nu = 0°$. The second column of the matrix can be found from the first one by differentiation w.r.t. ω, or by inserting $\nu = 90°$. The third column of the rotation matrix is orthogonal to the orbital plane. Hence, these three vectors form an orthogonal triad related to the Kepler orbit, which is also labeled as* Gaussian vectors *(Montenbruck and Gill, 2001, p.27)*

2.5.2. Cartesian ⟶ Kepler

Problem: Given a satellite's inertial position $\boldsymbol{r}_i$ and velocity $\dot{\boldsymbol{r}}_i$, find the corresponding Kepler elements $(a, e, I, \omega, \Omega, M)$.

Solution: The angular momentum vector per unit mass is normal to the orbital plane. It defines the inclination I and right ascension of the ascending node Ω:

$$\boldsymbol{L}_i = \boldsymbol{r}_i \times \dot{\boldsymbol{r}}_i \tag{2.28}$$

$$\tan\Omega = \frac{L_{i=1}}{-L_{i=2}} \tag{2.29}$$

$$\tan I = \frac{\sqrt{L_{i=1}^2 + L_{i=2}^2}}{L_{i=3}} \tag{2.30}$$

Rotate $\boldsymbol{r}_i$ into the orbital plane now and derive the argument of latitude u:

$$\boldsymbol{r}_n = \mathbf{R}_1(I)\mathbf{R}_3(\Omega)\boldsymbol{r}_i \tag{2.31}$$

$$\tan u = \tan(\omega + \nu) = \frac{r_{n=2}}{r_{n=1}} \tag{2.32}$$

The semi-major axis a comes from the vis-viva equation and requires the scalar velocity $v = \|\dot{\boldsymbol{r}}\|$. The eccentricity e comes from the description of the Laplace-vector and needs the scalar angular momentum $L = \|\boldsymbol{L}\|$:

$$T - V = \frac{v^2}{2} - \frac{GM}{r} = -\frac{GM}{2a} \tag{2.33}$$

Figure 2.14.: n-frame

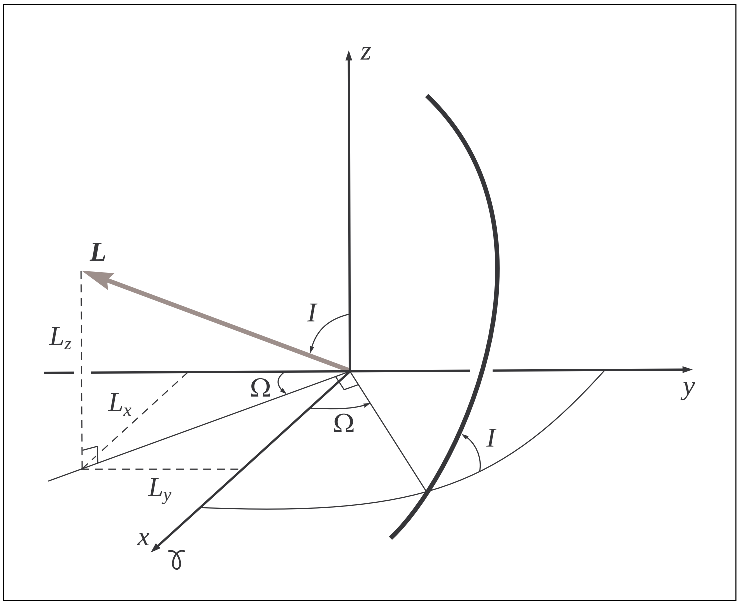

Figure 2.15.: The angular momentum vector $\boldsymbol{L}$ defines the orientation of the orbital plane in terms of Ω and I.

$$\text{(vis-viva equation)} \qquad a = \frac{GM\, r}{2GM - rv^2} \tag{2.34}$$

$$\text{(Laplace vector)} \qquad e = \sqrt{1 - \frac{L^2}{GM\, a}} \tag{2.35}$$

In order to extract the eccentric anomaly E, we need to know the radial velocity first:

$$\dot{r} = \frac{\boldsymbol{r} \cdot \dot{\boldsymbol{r}}}{r} \tag{2.36}$$

$$\cos E = \frac{a - r}{ae} \tag{2.37}$$

$$\sin E = \frac{r\dot{r}}{e\sqrt{GM\,a}} \tag{2.38}$$

The true anomaly is obtained from the eccentric one:

$$\tan \nu = \frac{\sqrt{1-e^2}\sin E}{\cos E - e} \tag{2.39}$$

$$\tan E = \frac{\sqrt{1-e^2}\sin \nu}{\cos \nu + e} \tag{2.40}$$

Subtracting ν from the argument of latitude u yields the argument of perigee ω. Finally, Kepler's equation provides the mean anomaly:

$$E - e\sin E = M \tag{2.41}$$

Exercise 2.6 *The initial values of a satellite orbit are given by*

$$\boldsymbol{r}_0 = \begin{pmatrix} -11\,092\,826.57 \\ 2\,174\,279.13 \end{pmatrix} \text{m} \qquad \dot{\boldsymbol{r}}_0 = \begin{pmatrix} -1\,883.7915 \\ -5\,207.2702 \end{pmatrix} \frac{\text{m}}{\text{s}}$$

in its orbital plane. Determine all possible Kepler elements.

1. *complement the vectors to 3D form (for the latter cross product)*

$$\boldsymbol{r}_0 = \begin{pmatrix} -11\,092\,826.57 \\ 2\,174\,279.13 \\ 0.00 \end{pmatrix} \text{m} \qquad \dot{\boldsymbol{r}}_0 = \begin{pmatrix} -1\,883.7915 \\ -5\,207.2702 \\ 0.0000 \end{pmatrix} \frac{\text{m}}{\text{s}}$$

2. *norm of vectors:*

$$r = \|\boldsymbol{r}_0\| = 11\,303\,906.01\,\text{m} \qquad v = \|\dot{\boldsymbol{r}}_0\| = 5\,537.5385\,\frac{\text{m}}{\text{s}}$$

3. *specific energy:* $E = \frac{1}{2}v^2 - \frac{GM}{r} = -19\,930\,025\,\frac{\text{J}}{\text{kg}}$
   (negative energy implies an elliptic orbit)

4. *angular momentum:* $\boldsymbol{L} = \boldsymbol{r} \times \dot{\boldsymbol{r}} = \begin{pmatrix} 0, & 0, & 61\,859\,233\,775 \end{pmatrix}\,\frac{\text{m}^2}{\text{s}}$

5. *semi-major axis:* $a = -\frac{GM}{2E} = 10\,000\,000\,\mathrm{m}$
6. *parameter of the ellipse:* $p = \frac{\|\boldsymbol{L}\|^2}{GM} = 9\,600\,000\,\mathrm{m}$
7. *eccentricity:* $e = \sqrt{1 - \frac{p}{a}} = \sqrt{1 - \frac{96}{100}} = 0.2$
8. *radial velocity:* $\dot{r} = \frac{\boldsymbol{r} \cdot \dot{\boldsymbol{r}}}{r} = 847.009\,\frac{\mathrm{m}}{\mathrm{s}}$
9. *eccentric anomaly:*

$$
\begin{aligned}
\cos E &= \frac{a - r}{ae} = -0.651953 \\
\sin E &= \frac{r\dot{r}}{e\sqrt{GMa}} = 0.758259 \\
E &= \operatorname{atan2}(\sin E, \cos E) = 2.280953 \widehat{=} 130.^\circ 68901
\end{aligned}
$$

10. *true anomaly:* $\tan\nu = \frac{\sqrt{1-e^2}\sin E}{\cos E - e} \Rightarrow \nu = 2.424440 \widehat{=} 138.^\circ 91018$
11. *If we assume, that the vectors are given in the n-frame, we can calculate also the argument of latitude and the angle of perigee:*

$$
\begin{aligned}
u &= \operatorname{atan2}(2\,174\,279.13, -11\,092\,826.57) = 2.94803 \widehat{=} 168.^\circ 91018 \\
\omega &= u - \nu = 30.^\circ 00000
\end{aligned}
$$

The angle I and Ω cannot be determined as the vectors are in the orbital plane.

3. Introduction to perturbation theory – Lagrange Planetary Equations

-

3.1. Representation of orbit perturbations

In the Kepler problem, a satellite falls around a central body on a conic section. Both objects are considered as point masses (or spheres with radial symmetric density) with gravitational attraction between them. All other forces are ignored. The potential $V = \frac{GM}{r}$ leads to Newton's equation of motion $\ddot{\boldsymbol{r}} = \nabla V = -\frac{GM}{r^3}\boldsymbol{r}$ in the inertial frame and the solution is called a Kepler orbit.

If any force influences the satellite motion, we will observe *orbit perturbations*. Orbit perturbations can be investigated in two forms: Bahnstörungen

1. *disturbing force* Störkraft

$$\ddot{\boldsymbol{r}} = -\frac{GM}{r^3}\boldsymbol{r} + \sum_i \boldsymbol{f}_i \tag{3.1}$$

Disturbing forces $\boldsymbol{f}_i$ can depend on position and velocity of the satellite, but also on time or other parameter like the density of the atmosphere. (Any effect can be written in this form)

2. *disturbing potential* Störpotential

$$V = \frac{GM}{r} + R(\boldsymbol{r}, t) \tag{3.2}$$

$$\Rightarrow \ddot{\boldsymbol{r}} = \nabla V = -\frac{GM}{r^3}\boldsymbol{r} + \nabla R(\boldsymbol{r}, t) \tag{3.3}$$

Disturbing potentials $R(\boldsymbol{r}, t)$ can depend on position or time, but not on velocity[1].

[1] Unfortunately, the symbol R is used by convention for the disturbing potential and the radius of the central body (and also for rotation matrices) in satellite geodesy.

Version 1 is possible for all forces, while version 2 requires a conservative force field with a corresponding potential. Hence, we distinguish between:

Volumenkräfte, konservative Kräfte

- *conservative forces*, acting on volume or center of mass
  ⇒ (in-)homogeneous gravity field represented by K_{lm}-coefficients (in Chapter 4, 6 and 7), gravity of other celestial bodies, and relativistic effects
  (The magnetic field is also a conservative vector field with a potential, but its impact on orbits is usually neglected.)

Oberflächenkräfte, Reibungskräfte

- *non-conservative or dissipative forces*, acting on surfaces (of the satellite)
  ⇒ atmospheric drag, solar radiation pressure, albedo (in Chapter 5)

Order of Magnitudes

The order of magnitude of all orbit perturbations in different orbital heights is presented in fig. 3.1. Details will be discussed in the following sections and chapters.

Let us collect some first information from the figure:

- The axes are in a log-log style, which leads to straight lines for all functions of the form $y = ax^k$. In a strict sense, only the central term is exactly radial dependent, for the other accelerations averaged values are presented.
- The main acceleration of a satellite motion is the $-\frac{GM}{r^3}$-term of the central mass, which is labeled by GM in the figure.
- The non-homogeneous gravity field of the Earth is modeled by a (generalized) Fourier series (see Chapter 6). A few components are labeled here by their coefficients $\{J_{2,0}, J_{2,2}, J_{6,6}, J_{18,18}\}$. The dominant orbit perturbation is the flattening of the Earth corresponding to the disturbing potential

$$R_{2,0}(r,\lambda,\theta) = -\frac{GM}{R} J_2 \left(\frac{R}{r}\right)^3 J_2 P_{2,0}(\cos\theta)$$

- The forces of other celestial bodies (Moon, Sun, Venus and Jupiter) depend on their distance to the satellite. The acceleration of the Moon is larger than the corresponding value of the Sun. For the planets, these forces differ significantly during a year, which is not shown here.
- The drag describes the acceleration due to the atmosphere, up to a distance of $r = 780\,\text{km}$. As the atmosphere is very variable, maximal and minimal acceleration are visualized.
- ...

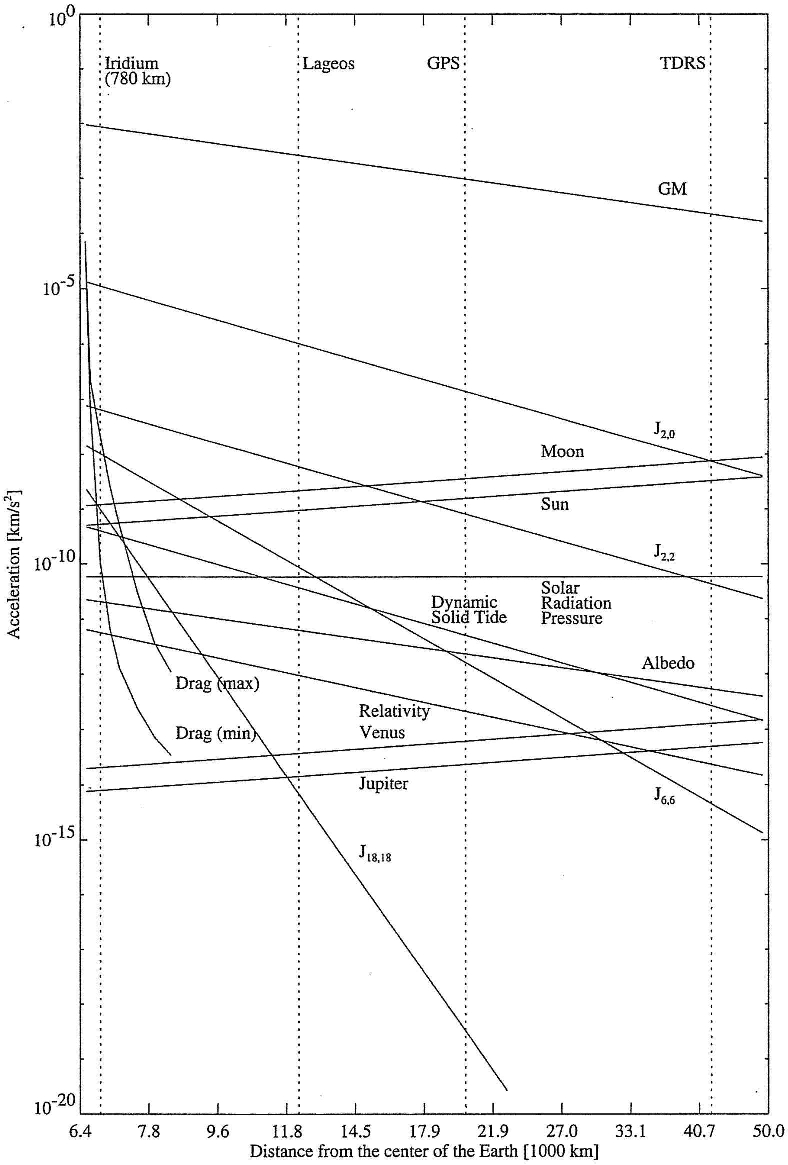

Figure 3.1.: Order of magnitude per orbit perturbation type in different orbital heights (*Montenbruck and Gill*, 2001, p. 55).

3.2. Osculating Kepler elements

3.2.1. Effect on Kepler elements

All orbit perturbations are small compared to the acceleration of the central body. Hence, the orbit differs only slightly from a Kepler orbit. At each epoch, we can calculate 6 Kepler elements based on current position and velocity. Any (subsequent) location will produce another set of Kepler elements. All elements are now time-dependent:

$$\{\boldsymbol{r}(t), \dot{\boldsymbol{r}}(t)\} \Leftrightarrow \{a(t), e(t), I(t), \Omega(t), \omega(t), M(t)\}$$

Oskulierende Keplerelemente

For a given epoch, we can draw the orbit and the Kepler ellipse, and the curves coincide in most cases only in one location and adapt to each other in the close surrounding, which is rephrased as osculating ellipse or *osculating Kepler elements*[2]. A time series of resulting Kepler elements may consist of

- short-time periodic perturbations, often with frequencies like once per revolution or twice per revolution,
- long-time periodic perturbation with periods ranging from sub-daily to months,
- secular effects, often in the form of a linear trend.

3.2.2. Investigation of orbit perturbations

Orbit perturbations can be investigated in two ways:

- Numerical integration of the force model 3.1 provides a time series of Cartesian positions and velocities. The method can be applied for several orbit perturbations in one “run” and can consider very complex models. For a better understanding, the solution should be converted to Kepler elements.
- Analytical solutions, i.e. closed formulas for the variable Kepler elements dependent on the disturbing forces, are only possible for certain orbit perturbations and require the Lagrange planetary equations (cf. section 3.4) or their Gaussian counter part. In particular, the long term effects caused by the inhomogeneous gravity field of the Earth are described and analyzed in this way.

Exercise 3.1 *Use the vis-viva equation to investigate how an extra impulse in flight direction influences the semi-major axis a.*

[2] os, oris (lat): mouth; osculum: small mouth, kiss

The vis-viva equation (2.18) provides a relation between scalar velocity and the semi-major axis:

$$v^2 = GM\left(\frac{2}{r} - \frac{1}{a}\right)$$

An impulse in flight direction will not effect the current radius r. The total derivative provides then

$$2v\,\mathrm{d}v = GM\left(\frac{\partial 2r^{-1}}{\partial r}\,\mathrm{d}r - \frac{\partial a^{-1}}{\partial a}\,\mathrm{d}a\right) = GM\left(-(-a^{-2}\,\mathrm{d}a)\right) = \frac{GM}{a^2}\,\mathrm{d}a$$

$$\Rightarrow\ \mathrm{d}a = \frac{2a^2}{GM}v\,\mathrm{d}v$$

- *A positive impulse in the flight direction ($\mathrm{d}v > 0$) will increase the semi-major axis, and the effect depends on the current size of the ellipse.*
- *The change $\mathrm{d}a$ in the semi-major axis will be maximal, when the velocity is maximal, i.e. in the perigee.*

3.3. Canonical Equations

Newton's equations of motion $\ddot{\boldsymbol{r}} = \nabla V$ are a set of three coupled differential equations of 2^{nd} order. Using the components of position and velocity as variables, the equations are rewritten as ODEs of 1^{st} order.

$$\begin{cases} \dot{\boldsymbol{r}} = \boldsymbol{v} \\ \dot{\boldsymbol{v}} = \nabla V \end{cases} \tag{3.4}$$

The sum of potential and kinetic energy

$$F := T - V = \frac{1}{2}\boldsymbol{v}\cdot\boldsymbol{v} - V(\boldsymbol{r}) \tag{3.5}$$

is also known as *force function* F or *Hamiltonian* (often written as H), although it is not a force in a physical sense. Kraftfunktion, Hamiltonfunktion

We can combine the differential equation and the derivatives of the force function F to obtain the system

$$\begin{cases} \dot{\boldsymbol{r}} = \dfrac{\partial F}{\partial \boldsymbol{v}} = \dfrac{\partial T}{\partial \boldsymbol{v}} \\[2ex] \dot{\boldsymbol{v}} = -\dfrac{\partial F}{\partial \boldsymbol{r}} = -\dfrac{\partial V}{\partial \boldsymbol{r}} \end{cases} \tag{3.6}$$

Written out in 6 dimensions one obtaines the matrix-vector form

$$\begin{pmatrix} \dot{r_1} \\ \dot{r_2} \\ \dot{r_3} \\ \dot{v_1} \\ \dot{v_2} \\ \dot{v_3} \end{pmatrix} = \left(\begin{array}{ccc|ccc} 0 & 0 & 0 & 1 & 0 & 0 \\ 0 & 0 & 0 & 0 & 1 & 0 \\ 0 & 0 & 0 & 0 & 0 & 1 \\ \hline -1 & 0 & 0 & 0 & 0 & 0 \\ 0 & -1 & 0 & 0 & 0 & 0 \\ 0 & 0 & -1 & 0 & 0 & 0 \end{array}\right) \begin{pmatrix} \partial F/\partial r_1 \\ \partial F/\partial r_2 \\ \partial F/\partial r_3 \\ \partial F/\partial v_1 \\ \partial F/\partial v_2 \\ \partial F/\partial v_3 \end{pmatrix} \tag{3.7}$$

$$\Longrightarrow \begin{pmatrix} \dot{\boldsymbol{r}} \\ \dot{\boldsymbol{v}} \end{pmatrix} = \begin{pmatrix} \mathbf{0} & \mathbf{I} \\ -\mathbf{I} & \mathbf{0} \end{pmatrix} \begin{pmatrix} \nabla_{\boldsymbol{r}} F \\ \nabla_{\boldsymbol{v}} F \end{pmatrix} \Longrightarrow \dot{\boldsymbol{s}} = \mathbf{J} \nabla_{\boldsymbol{s}} F \,. \tag{3.8}$$

kanonische Gleichung
kanonische Variable

Any equation of motion that can be brought into this form is called a *canonical equation*. The variables $\boldsymbol{r}$ and $\boldsymbol{v}$ are correspondingly called *canonical variables*. The skew-symmetric structure, represented by the matrix $\mathbf{J}$, is called *symplectic*. In its most general form, in which the canonical variables are not the Cartesian position and velocity anymore, the canonical equation read:

$$\begin{cases} \dot{q}_i = \dfrac{\partial H}{\partial p_i}, & \text{generalized coordinates} \\[2ex] \dot{p}_i = -\dfrac{\partial H}{\partial q_i} & \text{generalized moments} \end{cases}$$

3.4. Crash course LPE

Starting from the Newton equations in the form of eqn. (3.6) we now want to address the question: Can we find a set of 1^{st} order differential equations for the Kepler elements, which relates their variations to a force function F?

$$\left.\begin{aligned} \dot{\boldsymbol{r}} &= \frac{\partial F}{\partial \boldsymbol{v}} \\ \dot{\boldsymbol{v}} &= -\frac{\partial F}{\partial \boldsymbol{r}} \end{aligned}\right\} \Longrightarrow \dot{\boldsymbol{s}} = ?$$

$$\boldsymbol{s} = \begin{pmatrix} a & e & I & \Omega & \omega & M \end{pmatrix}^{\mathsf{T}}$$

The differential equations are found by using the Hamiltonian $F = T - V$:

$$\begin{cases} \dfrac{\mathrm{d}\boldsymbol{r}}{\mathrm{d}t} = \dfrac{\partial \boldsymbol{r}}{\partial \boldsymbol{s}}\dfrac{\mathrm{d}\boldsymbol{s}}{\mathrm{d}t} \implies \dot{\boldsymbol{r}} = \mathbf{A}\dot{\boldsymbol{s}} = \dfrac{\partial F}{\partial \boldsymbol{v}} \\ \\ \dfrac{\mathrm{d}\boldsymbol{v}}{\mathrm{d}t} = \dfrac{\partial \boldsymbol{v}}{\partial \boldsymbol{s}}\dfrac{\mathrm{d}\boldsymbol{s}}{\mathrm{d}t} \implies \dot{\boldsymbol{v}} = \dot{\mathbf{A}}\dot{\boldsymbol{s}} = -\dfrac{\partial F}{\partial \boldsymbol{r}} \end{cases}$$

We want to solve for the vector $\dot{\boldsymbol{s}}$, but the matrices $\mathbf{A}, \dot{\mathbf{A}} \in \mathbb{R}^{3\times 6}$ cannot be inverted. Therefore we apply the following trick:

$$\begin{cases} \dot{\mathbf{A}}^\mathsf{T}\dot{\boldsymbol{r}} = \dot{\mathbf{A}}^\mathsf{T}\mathbf{A}\dot{\boldsymbol{s}} = \dot{\mathbf{A}}^\mathsf{T}\dfrac{\partial F}{\partial \boldsymbol{v}} \\ \\ \mathbf{A}^\mathsf{T}\dot{\boldsymbol{v}} = \mathbf{A}^\mathsf{T}\dot{\mathbf{A}}\dot{\boldsymbol{s}} = \mathbf{A}^\mathsf{T}\dfrac{\partial F}{\partial \boldsymbol{r}} \end{cases}$$

Note that $\mathbf{A}^\mathsf{T}\dot{\mathbf{A}}$ and $\dot{\mathbf{A}}^\mathsf{T}\mathbf{A}$ are 6×6 matrices of rank 3 each. We combine them into

$$\begin{aligned} \left(\mathbf{A}^\mathsf{T}\dot{\mathbf{A}} - \dot{\mathbf{A}}^\mathsf{T}\mathbf{A}\right)\dot{\boldsymbol{s}} &= \mathbf{A}^\mathsf{T}\frac{\partial V}{\partial \boldsymbol{r}} - \dot{\mathbf{A}}^\mathsf{T}\frac{\partial T}{\partial \boldsymbol{v}} \\ &= -\left(\dot{\mathbf{A}}^\mathsf{T}\frac{\partial F}{\partial \boldsymbol{v}} + \mathbf{A}^\mathsf{T}\frac{\partial F}{\partial \boldsymbol{r}}\right) \end{aligned}$$

The composite matrix at the left is abbreviated as $\mathbf{L}$, yielding

$$\begin{aligned} \mathbf{L}\dot{\boldsymbol{s}} &= -\frac{\partial F}{\partial \boldsymbol{s}} \qquad \mathbf{L} = \text{matrix of Lagrange brackets } \{s_k, s_l\} \\ \{s_k, s_l\} &= \sum_{i=1}^{3} \frac{\partial r_i}{\partial s_l}\frac{\partial v_i}{\partial s_k} - \frac{\partial r_i}{\partial s_k}\frac{\partial v_i}{\partial s_l} \end{aligned}$$

with $\boldsymbol{s} = \begin{pmatrix} a & e & I & \Omega & \omega & M \end{pmatrix}^\mathsf{T}$. After inversion of $\mathbf{L}$ we obtain the desired result

$$\dot{\boldsymbol{s}} = -\mathbf{L}^{-1}\frac{\partial F}{\partial \boldsymbol{s}}$$

which is called *Lagrange Planetary Equation*.

Properties L

- antisymmetric:

$$\mathbf{L}^\mathsf{T} = -\mathbf{L} \implies 15 \text{ independents elements}$$

- time invariant:

$$\begin{aligned}
\dot{\mathbf{L}} &= \mathbf{A}^\top \ddot{\mathbf{A}} - \ddot{\mathbf{A}}^\top \mathbf{A} = 0 \\
\ddot{\mathbf{A}}_{ik} &= \frac{\partial \dot{\boldsymbol{v}}_i}{\partial \boldsymbol{s}_k} = \frac{\partial^2 V}{\partial r_i \partial s_k} \\
\left(\mathbf{A}^\top \ddot{\mathbf{A}}\right)_{lk} &= \sum_{i=1}^{3} \frac{\partial r_i}{\partial s_l} \frac{\partial^2 V}{\partial r_i \partial s_k} = \frac{\partial^2 V}{\partial s_l \partial s_k} = \text{ symmetric} \\
&\Longrightarrow \text{evaluate e.g. in perigee}
\end{aligned}$$

Exercise 3.2 *Determine the Lagrange bracket* $\{a, e\}$*.*

For the Lagrange brackets, the position and velocity are represented in the epifocal frame with a subsequent rotation $\boldsymbol{r}_i = \mathbf{R}(\omega, I, \Omega)\boldsymbol{r}_f$ *and* $\dot{\boldsymbol{r}}_i = \mathbf{R}(\omega, I, \Omega)\dot{\boldsymbol{r}}_f$ *into the inertial frame.*

$$\begin{aligned}
\left\{a, e\right\} &= \sum_{\ell=1}^{3} \tfrac{\partial r_{i=\ell}}{\partial a} \tfrac{\partial v_{i=\ell}}{\partial e} - \tfrac{\partial r_{i=\ell}}{\partial a} \tfrac{\partial v_{i=\ell}}{\partial e} = \\
&= \left(\tfrac{\partial \boldsymbol{r}}{\partial a}\right)^\top \left(\tfrac{\partial \boldsymbol{v}}{\partial e}\right) - \left(\tfrac{\partial \boldsymbol{r}}{\partial e}\right)^\top \left(\tfrac{\partial \boldsymbol{v}}{\partial a}\right) = \\
&= \left(\mathbf{R}\tfrac{\partial \boldsymbol{r}_f}{\partial a}\right)^\top \left(\mathbf{R}\tfrac{\partial \boldsymbol{v}_f}{\partial e}\right) - \left(\mathbf{R}\tfrac{\partial \boldsymbol{r}}{\partial e}\right)^\top \left(\mathbf{R}\tfrac{\partial \boldsymbol{v}_f}{\partial a}\right) = \\
&= \left(\tfrac{\partial \boldsymbol{r}}{\partial a}\right)^\top \mathbf{R}^\top \mathbf{R} \left(\tfrac{\partial \boldsymbol{v}_f}{\partial e}\right) - \left(\tfrac{\partial \boldsymbol{r}}{\partial e}\right)^\top \mathbf{R}^\top \mathbf{R} \left(\tfrac{\partial \boldsymbol{v}_f}{\partial a}\right) = \\
&= \left(\tfrac{\partial \boldsymbol{r}}{\partial a}\right)^\top \left(\tfrac{\partial \boldsymbol{v}_f}{\partial e}\right) - \left(\tfrac{\partial \boldsymbol{r}}{\partial e}\right)^\top \left(\tfrac{\partial \boldsymbol{v}_f}{\partial a}\right)
\end{aligned}$$

An evaluation in the perigee simplifies the calculation, as the vectors (2.22)

$$\begin{aligned}
\boldsymbol{r}_f &= \tfrac{a(1-e^2)}{1+e\cos\nu} \begin{pmatrix} \cos\nu \\ \sin\nu \\ 0 \end{pmatrix}\Bigg|_{\nu=0} = \tfrac{a(1-e^2)}{1+e} \begin{pmatrix} 1 \\ 0 \\ 0 \end{pmatrix} \\
\dot{\boldsymbol{r}}_f &= \tfrac{na}{\sqrt{1-e^2}} \begin{pmatrix} -\sin\nu \\ e+\cos\nu \\ 0 \end{pmatrix}\Bigg|_{\nu=0} = \tfrac{na}{\sqrt{1-e^2}}(1+e) \begin{pmatrix} 0 \\ 1 \\ 0 \end{pmatrix}
\end{aligned}$$

are orthogonal. A differentiation w.r.t. semi-major axis or eccentricity will not change the orthogonality. Hence, we find the Lagrange-bracket $\{a, e\} = 0$*.*

LPE

$$\dot{\boldsymbol{s}} = -\mathbf{L}^{-1}\frac{\partial F}{\partial \boldsymbol{s}} \qquad \mathbf{L}^{-1} = \text{matrix of Poisson brackets } [s_k, s_l]$$

- equations of motion in $\boldsymbol{s}$ e.g. in Kepler elements
- 6 ODE of 1^{st} order
- non-linear
- coupled

The equations of motion with disturbing potential[3] R in Cartesian coordinates are:

$$\ddot{\boldsymbol{r}} = \nabla \frac{GM}{r} + \nabla R \tag{3.9}$$

After transforming position $\boldsymbol{r}$ and velocity $\dot{\boldsymbol{r}}$ into Kepler elements, the equations of motion are called the *Lagrange Planetary Equations* (LPE):

Lagrange'sche Störungsgleichungen

$$\dot{a} = \frac{2}{na}\frac{\partial R}{\partial M} \tag{3.10a}$$

$$\dot{e} = \frac{1-e^2}{na^2 e}\frac{\partial R}{\partial M} - \frac{\sqrt{1-e^2}}{na^2 e}\frac{\partial R}{\partial \omega} \tag{3.10b}$$

$$\dot{I} = \frac{\cos I}{na^2\sqrt{1-e^2}\sin I}\frac{\partial R}{\partial \omega} - \frac{1}{na^2\sqrt{1-e^2}\sin I}\frac{\partial R}{\partial \Omega} \tag{3.10c}$$

$$\dot{\Omega} = \frac{1}{na^2\sqrt{1-e^2}\sin I}\frac{\partial R}{\partial I} \tag{3.10d}$$

$$\dot{\omega} = -\frac{\cos I}{na^2\sqrt{1-e^2}\sin I}\frac{\partial R}{\partial I} + \frac{\sqrt{1-e^2}}{na^2 e}\frac{\partial R}{\partial e} \tag{3.10e}$$

$$\dot{M} = n - \frac{1-e^2}{na^2 e}\frac{\partial R}{\partial e} - \frac{2}{na}\frac{\partial R}{\partial a} \tag{3.10f}$$

The differential equation can be re-written into a matrix vector form:

$$\frac{d}{dt}\begin{pmatrix} a \\ e \\ I \\ \Omega \\ \omega \\ M \end{pmatrix} = \left(\begin{array}{c|ccc} & 0 & 0 & \frac{2}{na} \\ 0 & 0 & -\frac{\sqrt{1-e^2}}{na^2 e} & \frac{1-e^2}{na^2 e} \\ & -\frac{1}{nab\sin I} & \frac{\cot I}{nab} & 0 \\ \hline \text{anti-symm} & & 0 & \end{array}\right)\begin{pmatrix} \partial F/\partial a \\ \partial F/\partial e \\ \partial F/\partial I \\ \partial F/\partial \Omega \\ \partial F/\partial \omega \\ \partial F/\partial M \end{pmatrix} \tag{3.11a}$$

Please note, that we switch the representation from the disturbing potential R to the complete Hamiltonian

$$F = T - V = T - \frac{GM}{r} - R = -\frac{GM}{2a} - R$$

[3] This implies that only gravitational forces can be treated in the following. For dissipative forces, the Gauss form of the equations of motion should be used. To reduce confusion with the Earth radius, we note down the later one by R_{E} in the following.

with

$$\frac{2}{na}\frac{\partial F}{\partial a} = \frac{2}{na}\frac{\partial\left\{-\frac{GM}{2a} - R\right\}}{\partial a} = \frac{2}{na}\frac{\partial\left\{-\frac{GM}{2a}\right\}}{\partial a} - \frac{2}{na}\frac{\partial R}{\partial a} = n - \frac{2}{na}\frac{\partial R}{\partial a} \tag{3.12}$$

Remark 3.1 *Kepler elements are not canonical variables, but the matrix is still anti-symmetric and relative sparse.*

The LPE will be used in sections 4.2 and 7.2 for analyzing the orbit perturbation due to the inhomogeneous gravity field of the Earth. For non-gravitational orbit perturbations, the Gauss representation of LPE is introduced.

3.5. Gauss form of LPE

The LPE describe perturbed motion as long as the force can be written as the gradient of a potential and with the Kepler elements as variables. For non-gravitational forces, e.g. solar pressure or air drag, Gauss found an alternative form. To simplify the modelling, we introduce two rotating coordinate systems with the origin in the center of the satellite:

- Hill-frame $(x^{\mathrm{H}}, y^{\mathrm{H}}, z^{\mathrm{H}})$ (H-frame):
  - z^{H}: radial component is parallel to $\boldsymbol{r}$
  - y^{H}: cross-track component is parallel to $\boldsymbol{L}$
  - x^{H}: complements the RHS and points quasi-along track
- tangential frame $(x^{\mathrm{t}}, y^{\mathrm{t}}, z^{\mathrm{t}})$ (t-frame)
  - x^{t}: along-track component is parallel to $\boldsymbol{v}$
  - y^{t}: cross-track component si parallel to $\boldsymbol{L}$
  - z^{t}: complements the RHS and is quasi-radial component

For non-circular orbits the two systems differ by a rotation around the common y-axis.

LPE in Gauss form in Hill frame

When the (specific) force $\boldsymbol{f} = \begin{pmatrix} f_1, & f_2, & f_3 \end{pmatrix}^{\mathsf{T}}$ is expressed in the Hill-frame, the Gauss-form of LPE are the following equations

$$\dot{a} = \frac{2}{n\sqrt{1-e^2}}\left(e\sin\nu f_3 + \frac{p}{r}f_1\right) \tag{3.13a}$$

$$\dot{e} = \frac{\sqrt{1-e^2}}{na}\left(\sin\nu f_3 + (\cos E + \cos\nu)\, f_1\right) \tag{3.13b}$$

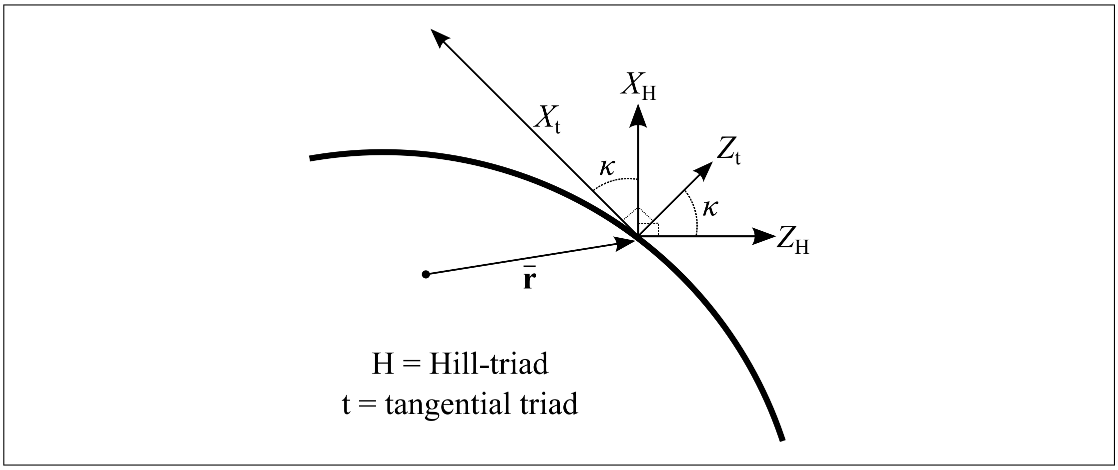

Figure 3.2.: Hill-triad H, tangential triad t.

$$\dot{I} = \frac{r}{nab}\cos(\omega+\nu) f_2 \tag{3.13c}$$

$$\dot{\Omega} = \frac{r}{nab\sin I}\sin(\omega+\nu) f_2 \tag{3.13d}$$

$$\dot{\omega} = \frac{\sqrt{1-e^2}}{nae}\left(-\cos\nu\, f_3 + \left(\frac{r}{p}+1\right)\sin\nu\, f_1\right) - \cos I\,\dot{\Omega} \tag{3.13e}$$

$$\dot{M} = n - \frac{1}{na}\left(\frac{2r}{a} - \frac{1-e^2}{e}\cos\nu\right) f_3 - \frac{1-e^2}{nae}\left(1+\frac{r}{p}\right)\sin\nu f_1 \tag{3.13f}$$

In the formula we have considered:

$$\begin{aligned} r &= \frac{p}{1+e\cos\nu} \Longrightarrow \frac{p}{r} = 1+e\cos\nu \\ p &= a(1-e^2) \text{ and } p = \frac{L^2}{GM} \\ &\Longrightarrow L = \sqrt{pGM} = \sqrt{a(1-e^2)n^2a^3} = nab \\ a^2 - a^2e^2 &= b^2 \Longrightarrow a\sqrt{1-e^2} = b \end{aligned}$$

Exercise 3.3 *Assume a constant or a periodic ("once per revolution") component in the force* $\boldsymbol{f}$ *given in the Hill-frame. How will the Kepler elements* a, I, *or* Ω *change due to this force?*

For near-circular orbits ($e \approx 0$) the Gauss LPE reduce to:

$$\dot{a} = \frac{2}{n} f_1 \tag{3.14a}$$

$$\dot{e} = \frac{1}{na} \left(\sin\nu f_3 + 2\cos\nu f_1 \right) \tag{3.14b}$$

$$\dot{I} = \frac{1}{na} \cos u f_2 \tag{3.14c}$$

$$\dot{\Omega} = \frac{1}{na\sin I} \sin u f_2 \tag{3.14d}$$

$$\dot{\omega} + \dot{M} = n - \frac{e}{na} f_3 - \cos I \dot{\Omega} \tag{3.14e}$$

Attention: The atmospheric drag is an orbit perturbation, which acts in flight direction, i.e. in tangential direction. In the tangential frame the force vector has only a first non-zero component:

$$\boldsymbol{f}_t^{\text{drag}} = \begin{pmatrix} f_1 \\ 0 \\ 0 \end{pmatrix}_t$$

To use the previous formulas, we must rotate the system from the tangential frame to the Hill-frame via a rotation matrix:

$$\boldsymbol{f}_H^{\text{drag}} = \mathbf{R}_2(-\kappa) \boldsymbol{f}_t^{\text{drag}} \,.$$

The matrix itself is expressed in Kepler elements

$$\boldsymbol{f}_t = \mathbf{R}_2(\kappa) \boldsymbol{f}_H \quad \text{with} \qquad \tan\kappa = \frac{e\sin\nu}{1 + e\cos\nu}$$

$$\mathbf{R}_2(\kappa(\nu)) = \begin{pmatrix} \frac{1+e\cos\nu}{\sqrt{1+e^2+2e\cos\nu}} & 0 & \frac{-e\sin\nu}{\sqrt{1+e^2+2e\cos\nu}} \\ 0 & 1 & 0 \\ \frac{e\sin\nu}{\sqrt{1+e^2+2e\cos\nu}} & 0 & \frac{1+e\cos\nu}{\sqrt{1+e^2+2e\cos\nu}} \end{pmatrix} \Leftrightarrow \mathbf{R}_2(\kappa) = \begin{pmatrix} \cos\kappa & 0 & -\sin\kappa \\ 0 & 1 & 0 \\ \sin\kappa & 0 & \cos\kappa \end{pmatrix} .$$

Exercise 3.4 *Verify, that the matrix $\mathbf{R}_2(\kappa(\nu))$ is a rotation matrix. Check its determinant and the orthogonality.*

LPE in Gauss form in tangential frame

The previous rotation can be avoided by using the representation of the Gauss' LPE directly in the tangential frame:

$$\dot{a} = \frac{2a^2 v}{GM} f_1 \tag{3.15a}$$

$$\dot{e} = \frac{1}{v}\left(\frac{r}{a}\sin\nu\, f_3 + 2(e+\cos\nu) f_1\right) \tag{3.15b}$$

$$\dot{I} = \frac{r}{L}\cos u\, f_2 \tag{3.15c}$$

$$\dot{\Omega} = \frac{r}{L\sin I}\sin u\, f_2 \tag{3.15d}$$

$$\dot{\omega} = \frac{1}{ev}\left(-\left(2e+\frac{r}{a}\right)\cos\nu\, f_3 + 2\sin\nu\, f_1\right) - \frac{r\cos I}{L\sin I}\sin u\, f_2 \tag{3.15e}$$

$$\dot{M} = n + \frac{b}{a}\frac{1}{ev}\left(\frac{r}{a}\cos\nu\, f_3 - 2\left(1+e^2\frac{r}{p}\right)\sin\nu\, f_1\right) \tag{3.15f}$$

In the formula we have considered:

$$\begin{aligned} L &= na^2\sqrt{1-e^2} \; = \; nab \\ \frac{p}{r} &= 1 + e\cos\nu \\ v &= \frac{L}{p}\sqrt{1+e^2+2e\cos\nu} \\ u &= \omega + \nu \end{aligned}$$

Exercise 3.5 *Most geosynchronous satellite are injected by a rocket into the "standard geostationary transfer orbit" (GTO) and continue their journey with subsequent Hohmann transfers. Due to malfunction of Arianne 5, the telecommunication satellite Artemis was injected into an elliptic low-energy orbit ($h_{\mathrm{per}} = 592\,\mathrm{km}$,$h_{\mathrm{apo}} = 17528\,\mathrm{km}$[4]) below GTO in July 2001. The onboard chemical propellant was not enough to reach the geostationary orbit, but the satellite could be lifted into an orbit 5000 km below the GEO via 5 perigee boosts and 3 apogee boost and a series of engine burns. Luckily, the satellite also carried experimental ion thrusters, which were now used to alter the semi-major axis by permanent thrusts ($\approx 10\,\frac{\mu\mathrm{m}}{\mathrm{s}^2}$) (Oppenhäuser and Bird, 2003). Which time is necessary to lift the satellite into its geosynchronous orbit? Which changing rate could be observed for the semi-major axis?*

[4] `spaceflightnow.com/arianne/v142/01073followup.html`

- *geostationary – one revolution per (sidereal) day:*

$$a_{\text{GEO}} = \sqrt[3]{GM\left(\frac{T}{2\pi}\right)^2} = \sqrt[3]{3.986005\cdot 10^{14}\,\frac{\text{m}^3}{\text{s}}\,\frac{(86164\,\text{s})^2}{4\pi^2}} = 42\,164\,\text{km}$$
$$E_{\text{GEO}} = \frac{GM}{2a_{\text{GEO}}} = -4.726\,\frac{\text{km}^2}{\text{s}^2}$$

- *starting ion thrusters*

$$a_{\text{ion}} = a_{\text{GEO}} - 5000\,\text{km} = 37164\,\text{km}$$
$$E_{\text{ion}} = \frac{GM}{2a_{\text{GEO}}} = -5.362\,\frac{\text{km}^2}{\text{s}^2}$$

- *differences in velocities are relative small*

$$v_{\text{GEO}} = \sqrt{\frac{GM}{a_{\text{GEO}}}} = 3074\,\frac{\text{m}}{\text{s}}$$
$$v_{\text{ion}} = \sqrt{\frac{GM}{a_{\text{ion}}}} = 3274\,\frac{\text{m}}{\text{s}}$$

  and can be replace by the average $v = 3174\,\frac{\text{m}}{\text{s}}$

- *permanent firing of ion thrusters*

$$\Delta E = \int_s \boldsymbol{f}\cdot \mathrm{d}\boldsymbol{s} = \int \underbrace{f_1}_{\text{along-track}} \mathrm{d}s = \int fv\,\mathrm{d}t \approx fv\Delta t$$

  (The acceleration is considered to act only and always in flight direction.)

- *transfer time*

$$\Delta t \approx \frac{|\Delta E|}{fv} = \frac{5.362\,\frac{\text{km}^2}{\text{s}^2} - 4.726\,\frac{\text{km}^2}{\text{s}^2}}{10\cdot 10^{-6}\,\frac{\text{m}}{\text{s}^2}3174\,\frac{\text{m}}{\text{s}}} \approx 20030518\,\text{s} \approx 231\,\text{days} \tag{3.16}$$

- LPE *in Gauss-form*

$$\dot{a} = \frac{2}{n}f_1 = 2\sqrt{\frac{a_{\text{ion}}^3}{GM}} = 0.22\,\frac{\text{m}}{\text{s}} \approx 19\,\frac{\text{km}}{\text{day}} \tag{3.17}$$

According to Oppenhäuser and Bird (2003) the "lifting rate" might reach 20 $\frac{\text{km}}{\text{day}}$ *in best scenarios with an average value of 15* $\frac{\text{km}}{\text{day}}$*. The ion thruster started in 19 February 2002 and finished their firing in 31 January 2003. This is longer then our estimation, but three out of four thruster units failed during the journey.*

Changing the satellite's maneuvers in space required "largest" software patch of onboard systems so far with more than 15 000 words of code!

4. Orbit perturbation due to Earth flattening

-

The main deviation from a central gravitational field $V = \frac{GM}{r}$ is caused by the dynamic flattening of the Earth. In the GRS80 normal field the flattening is represented by the dimensionless constant $J_2 = 1.082\,63 \cdot 10^{-3}$, while the central term has the numerical value $C_{0,0} = 1$. For actual gravity fields, the flattening is represented by the spherical harmonic coefficient $C_{2,0} = -J_2$.

4.1. Qualitative assessment

In a thought experiment, we want to understand the J_2-effect on the ascending node without calculations.

The gravity of a reference ellipsoid can be replaced by a mass in the center and an additional ring in the equatorial plane representing the difference between sphere and ellipsoid, i.e. the *equatorial bulge*. Äquatorwulst

A satellite is now attracted by the point mass and the ring. Considering the differences in magnitudes and the directions, the satellite gets an extra force $\boldsymbol{F}$ pulling towards the equatorial plane in almost all locations of the orbit.

A force acting with a distance $\boldsymbol{r}$ on a rotating object leads to a *torque* $\boldsymbol{T} = \boldsymbol{F} \times \boldsymbol{r} = \frac{\mathrm{d}\boldsymbol{L}}{\mathrm{d}t}$, which changes then the *angular momentum* $\boldsymbol{L}$, i.e. the orbital plane. Drehmoment Drehimpuls

Now we imagine the figure of the modulus of the torque $\|\boldsymbol{T}\|$ for one revolution:

- The figure will show a maximum, when the argument of latitude is $u = \pi/2$ and the satellite has the largest distance to the equatorial plane at its northernmost point.
- In the opposite location $u = 3\pi/2$, both the force $\boldsymbol{F}$ and the radius $\boldsymbol{r}$ change their sign and the term $\|\boldsymbol{T}\|$ has another maximum.
- The minimum is obtained, when the satellite is in the equatorial plane with $u = 0$

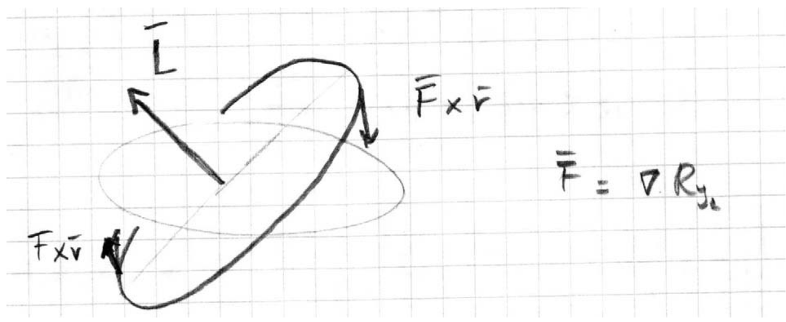

Figure 4.1.: Torque on a satellite orbit.

(ascending node) or $u = \pi$ (descending node) as force and radius are parallel here.

- The average value T_a will be a positive.

If we assume a circular orbit, the sum

$$T = \|\boldsymbol{T}\| = T_a + T_a \sin(2nt)$$

with two maxima and two minima per revolution (and with $t = 0$ in the ascending node) fits to the previous facts.

Exercise 4.1 *Which torque will occur, when the satellite orbit remains in the equatorial plane with inclination $I = 0$?*

4.2. Quantitative assessment

To analyze the effect, the gravitational potential must be complemented by the so-called $C_{2,0}$-term[1]:

$$\begin{aligned} F &= T - V \\ &= \frac{1}{2}v^2 - \frac{GM}{r} - R_{2,0}(r, \phi, \lambda) \end{aligned}$$

[1]The modeling of the gravitational potential will be part of Chapter 6. For the moment, we have to accept, that a complicated gravity field can be represented in a kind of Fourier series in 3 variables, i.e. (r, λ, ϕ). In East-West direction the basis functions are trigonometric functions $\{\cos m\lambda, \sin m\lambda\}$, as the field must be continuous after one revolution. In radial direction the inhomogenous structure must get damped for large distances, but the exact form $\{r^{-(n+1)}\}$ cannot be explained for now. In North-South direction, the basis are the Legendre functions $P_{n,m}(\sin \phi)$.

$$= -\frac{GM}{2a} - \frac{GM}{R_{\mathrm{E}}}\left(\frac{R_{\mathrm{E}}}{r}\right)^3 C_{2,0}P_{2,0}(\sin\phi)\,.$$

The non-normalized Legendre function is of the form $P_{2,0}(\sin\phi) = \frac{1}{2}(3\sin^2\phi - 1)$. The argument $\sin\phi$ must be expressed here in Kepler elements for differentiation. In a spherical triangle we find the relation $\sin\phi = \sin I \sin u$.

$$R_{2,0} = \frac{1}{2}\frac{GM}{R_{\mathrm{E}}}\left(\frac{R_{\mathrm{E}}}{r}\right)^3 C_{2,0}(3\sin^2 u \sin^2 I - 1)$$

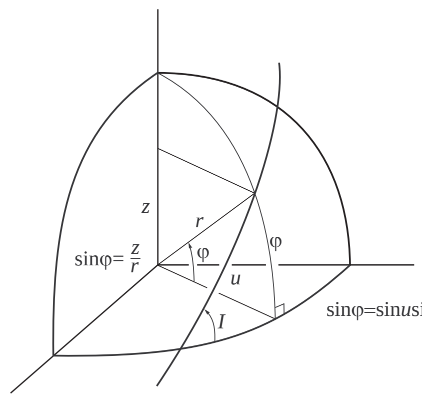

Figure 4.2.: Relation between latitude ϕ and the Kepler elements I and u in a spherical triangle.

Inserting the potential $R_{2,0}$ into the LPE leads to

$$\begin{aligned}\dot{\Omega} &= \frac{1}{nab\sin I}\frac{\partial R_{2,0}}{\partial I} \\ &= \frac{1}{2}\frac{1}{nab\sin I}\frac{n^2a^3}{R_{\mathrm{E}}}\left(\frac{R_{\mathrm{E}}}{r}\right)^3 C_{2,0}2\cdot 3 \underbrace{\sin^2 u}_{\frac{1}{2}(1-\cos(2u))} \cos I \sin I \\ &= \frac{3}{2}\frac{a^2n}{br}\left(\frac{R_{\mathrm{E}}}{r}\right)^2 C_{20}\cos I(1-\cos(2u))\,.\end{aligned}$$

The rate of the ascending node varies with two osculations per revolution, but it also shows a constant term, which coincides with previous qualitative analysis.

The time variable ascending node can be found by integration, i.e.

$$\Omega(t) = \Omega_0 + \int_{\tau_0}^{\tau} \dot{\Omega}\,\mathrm{d}t\,.$$

The oscillating component $\cos(2u)$ will cancel out, when we integrate the effect within one or multiple (integer) revolutions.

sekulärer Trend

The constant term in the disturbing potential $R_{2,0}$ generates a *secular trend*

$$\dot{\Omega} = \frac{3}{2} n \frac{C_{2,0}}{(1-e^2)^2} \left(\frac{R_\mathrm{E}}{r}\right)^2 \cos I \tag{4.1}$$

which corresponds to a long-term linear trend in the ascending node

$$\Omega(t) = \Omega_0 + \dot{\Omega}(t - t_0)\,.$$

In the following, we are only interested in the *secular effect* of the Earth's flattening, which is parameterized by the unnormalized coefficient $C_{20} = -1.08263 \cdot 10^{-3}$. The equations of motion (3.10a) to (3.10f) reduce to:

$$\dot{a} = 0 \tag{4.2a}$$

$$\dot{e} = 0 \tag{4.2b}$$

$$\dot{I} = 0 \tag{4.2c}$$

$$\dot{\omega} = \frac{3nC_{20}a_\mathrm{E}^2}{4(1-e^2)^2a^2}\left(1 - 5\cos^2 I\right) \qquad = n\frac{\kappa}{a^2}\left(1 - 5\cos^2 I\right) \tag{4.2d}$$

$$\dot{\Omega} = \frac{3nC_{20}a_\mathrm{E}^2}{2(1-e^2)^2a^2}\cos I \qquad = 2n\frac{\kappa}{a^2}\cos I \tag{4.2e}$$

$$\dot{M} = n - \frac{3nC_{20}a_\mathrm{E}^2}{4(1-e^2)^{3/2}a^2}\left(3\cos^2 I - 1\right) = n - n\sqrt{1-e^2}\frac{\kappa}{a^2}\left(3\cos^2 I - 1\right) \tag{4.2f}$$

$$\kappa := \frac{3C_{2,0}a_\mathrm{E}^2}{4(1-e^2)^2}$$

Discussion The flattening of the Earth has no secular effect on the shape and size of the orbit (a and e). The inclination of the orbital plane remains constant, too (I). There will be a precession of the orbital plane, though ($\dot{\Omega}$). Within the orbit, the flattening effect is twofold: the perigee starts to precess ($\dot{\omega}$) and the mean motion gets an additional term.

Exercise 4.2 *For a satellite at about 750 km height, following a near-circular orbit (e.g. $e = 0.01$), the above equations become:*

$$\dot{\omega} \approx 3.\!\!^\circ 35\left(5\cos^2 I - 1\right) \quad \textit{per day}$$

$$\dot{\Omega} \approx -6.\!\!^\circ 7 \cos I \quad \textit{per day}$$

$$\dot{M} \approx 14.\!\!^\circ 4 + \frac{3.\!\!^\circ 35}{360^\circ}\left(3\cos^2 I - 1\right) \quad \textit{revolutions per day}$$

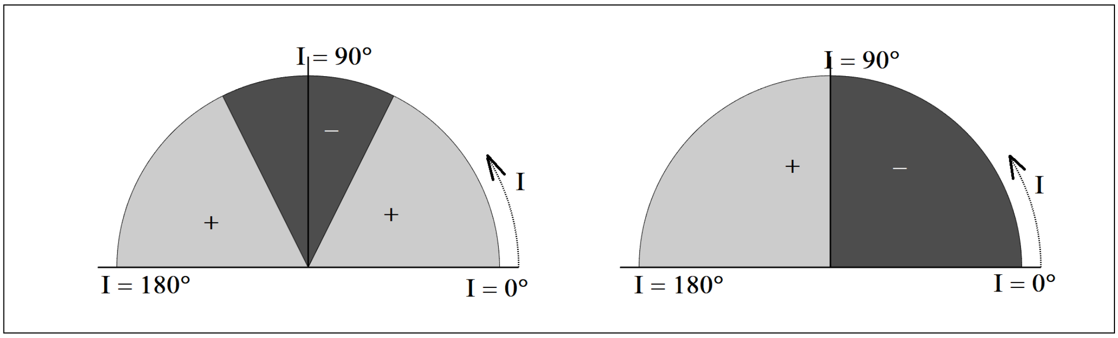

Figure 4.3.: Sign-analysis of $\dot{\omega} \propto \left(5\cos^2 I - 1\right)$ and $\dot{\Omega} \propto -\cos I$.

The secular rates of the Kepler elements due to Earth flattening constitute the next level of orbit design tools beyond Kepler's 3^{rd} law. Some applications of the above formulae:

Polar orbit For a polar orbit ($I = 90°$), the equatorial bulge has no effect on the ascending node. Its precession remains zero and the orbital plane keeps it orientation in inertial space.

Sun-synchronous orbit For remote sensing purposes (illumination angle) and engineering purposes (no moving solar paddles, no Earth shadow transitions) a sun-synchronous orbit is very useful. Sun-synchronicity is attained if the orbital plane precession is equal to the Earth's rotation around the sun, i.e. $\dot{\Omega} = 2\pi/\text{year}$, which is nearly 1° per day. For the above numerical example, this is achieved at the near-polar retrograde inclination of $98.^\circ5$. Examples of sun-synchronous orbits are ERS, Envisat, Landsat, GOCE, Sentinel-3 and many more.

Critical inclination Perigee precession does not occur if $5\cos^2 I = 1$, which leads to $I \approx 63.^\circ43$ and its complement $I \approx 116.^\circ57$. This inclination is used in altimetry, for instance. An interesting use of this property is made by the Russian system of Molniya communication satellites, which have a very large eccentricity ($e = 0.74$) and semi-major axis ($a = 26\,000$ km). The perigee at 270° is fixed by a critical inclination. Thus these satellites swing around the Southern hemisphere rapidly, after which they will be visible over the Northern hemisphere (Russia) for a long time.

Repeat orbit A repeat orbit performs β revolutions in α nodal days while the spatial sampling is determined by the inclination I. The concept is presented in the next section.

4.3. Repeat orbit

Wiederholungsbahn

Many Earth observations benefit from repeated data in space and time. A *repeat orbit* performs β revolutions in α nodal days while the spatial sampling is determined by the inclination I. The integers α and β are relative primes, i.e. they have no common divisor.

A number of geodetic satellites with repeat orbits are listed in table 4.1:

Table 4.1.: Satellites with repeat orbits

Satellite	β	α
geosynchronous	1	1
GPS	2	1
TOPEX	127	10
ERS	501	35
GOCE	979	61
Sentinel-3	385	27
CryoSat-2	5344	369
IceSat	1354 (119)	91 (8)

Bahn-Design

The flattening of the Earth is for most missions the dominant orbit perturbation, and must be considered in the *orbit design* if the parameter shall persist. The inclination I is fixed by the sampling requirements and also launch restrictions, while the eccentricity e tends in many missions to zero for homogeneous observations. The semi-major axis a is then determined by the repeat condition i.e. the ratio of α and β.

The semi-major axis of a repeat orbit is found in two steps:

1. A first approximation can be estimated by Kepler's third law already:

$$\boxed{\beta T_{\text{rev}} = \alpha T_{\text{day}}} \tag{4.3}$$

$$\Longrightarrow \frac{\beta}{\alpha} = \frac{T_{\text{day}}}{T_{\text{rev}}} = \frac{n_{\text{rev}}}{n_{\text{day}}} = \frac{n}{\omega_{\text{E}}}$$

$$\Longrightarrow n = \frac{\beta}{\alpha}\omega_{\text{E}} = \frac{2\pi\beta}{\alpha} \text{ per day}$$

Inserted in Kepler's third law, one obtains a semi-major axis a_0:

$$\Longrightarrow a_0 = \sqrt[3]{\frac{GM}{n^2}} = \sqrt[3]{\frac{GM\alpha^2}{\beta^2\omega_{\text{E}}^2}}$$

2. For a more precise estimate, the effect of the Earth flattening on the orbit must be considered. On the one hand, we express the mean motion n by the differentiated argument of latitude[2] $\dot{u} = \dot{\omega} + \dot{\nu}$. On the other hand, the sidereal day T_{day} is replace by the so called *nodal day*. A nodal day is the duration of the Earth's rotation around its axis relative to the (precessing) node. The angular velocity is $\omega_{\text{E}} - \dot{\Omega}$ and, hence, Knotentag

$$T_{\text{nodal}} = \frac{2\pi}{\omega_{\text{E}} - \dot{\Omega}} \, . \tag{4.4}$$

The repeat condition is then the ratio

$$\boxed{\tfrac{\beta}{\alpha} = \tfrac{T_{\text{nodal}}}{T_{\text{rev}}} \approx \tfrac{\dot{\omega}+\dot{M}}{\omega_{\text{E}}-\dot{\Omega}}} \tag{4.5}$$

$$\Longrightarrow \frac{\beta}{\alpha}(\omega_{\text{E}} - \dot{\Omega}) \approx \dot{\omega} + \dot{M} \tag{4.6}$$

Inserting the solution of the LPE on page 56 leads to

$$\begin{aligned}
\frac{\beta}{\alpha}\omega_{\text{E}} - 2\frac{\beta}{\alpha}n\frac{\kappa}{a^2}\cos I &\approx n\frac{\kappa}{a^2}\left(1 - 5\cos^2 I\right) + n - n\sqrt{1-e^2}\frac{\kappa}{a^2}\left(3\cos^2 I - 1\right) \\
n &\approx \frac{\beta}{\alpha}\omega_{\text{E}} + \frac{n}{a^2}\kappa\left[-2\frac{\beta}{\alpha}\cos I - \left(1 - 5\cos^2 I\right) + \sqrt{1-e^2}\left(3\cos^2 I - 1\right)\right] \\
\frac{\sqrt{GM}}{a^{3/2}} &\approx \frac{\beta}{\alpha}\omega_{\text{E}} + \frac{\sqrt{GM}}{a^{7/2}}\kappa\left[-2\frac{\beta}{\alpha}\cos I - \left(1 - 5\cos^2 I\right) + \sqrt{1-e^2}\left(3\cos^2 I - 1\right)\right]
\end{aligned}$$

The non-linear equation can be solved by an iteration, with the starting value a_0:

$$a_{i+1} \approx \left(\underbrace{\frac{\beta}{\alpha}\frac{\omega_{\text{E}}}{\sqrt{GM}}}_{(a_0)^{-3/2}} + \frac{\kappa}{a_i^{7/2}}\left[-2\frac{\beta}{\alpha}\cos I - \left(1 - 5\cos^2 I\right) + \sqrt{1-e^2}\left(3\cos^2 I - 1\right)\right]\right)^{-2/3} \tag{4.7}$$

Exercise 4.3 *Which semi-major axis a must be chosen for a repeat orbit with $\beta = 901$, $\alpha = 55$, when the eccentricity $e = 0.3$ and the inclination $I = 60$ are given?*

- *initial guess:* $a_0 = \sqrt[3]{\frac{GM\alpha^2}{\beta^2\omega_{\text{E}}^2}} = 6548780\,\text{m}$

[2]We ignore here the difference between mean and true anomaly: $\dot{\nu} = \frac{\mathrm{d}\nu}{\mathrm{d}t} = \frac{\mathrm{d}\nu}{\mathrm{d}M}\frac{\mathrm{d}M}{\mathrm{d}t} = \frac{ab}{r^2}\dot{M} \approx \dot{M}$

- *iteration leads to*

$$
\begin{aligned}
a_1 &= \left((a_0)^{-3/2} + \frac{\kappa}{a_0^{7/2}} [...] \right)^{-2/3} = 6483139\,\mathrm{m} \\
a_2 &= \left((a_0)^{-3/2} + \frac{\kappa}{a_1^{7/2}} [...] \right)^{-2/3} = 6480813\,\mathrm{m} \\
a_3 &= \left((a_0)^{-3/2} + \frac{\kappa}{a_2^{7/2}} [...] \right)^{-2/3} = 6480729\,\mathrm{m} \\
a_4 &= 6480726\,\mathrm{m} \\
a_5 &= 6480726\,\mathrm{m}
\end{aligned}
$$

Remark 4.1 *The iteration will quickly converge as the numerical value*

$$
\left| \kappa \frac{1}{a^{7/2}} \right| = \left| \frac{3C_{2,0} a_\mathrm{E}^2}{4(1-e^2)^2} \frac{1}{a^2 a^{3/2}} \right| = \left| \frac{3C_{2,0}}{4(1-e^2)^2} \left(\frac{a_\mathrm{E}}{a} \right)^2 \frac{1}{a^{3/2}} \right| \approx \frac{0.00075}{a^{3/2}} \left(\frac{a_\mathrm{E}}{a} \right)^2
$$

is significantly smaller than $a_0^{-3/2}$.

5. Non gravitational orbit perturbations

Non-gravitational orbit perturbations are difficult to model, and their integrated effect is often observed by on-board accelerometers in the geodetic space missions. The perturbations on satellites are caused by

- atmospheric drag
- solar radiation pressure
- Earth albedo

We will recognize, that the effect depends in particular on relative orientation, i.e. the effective area of the satellite—non-gravitational perturbations are also known as *surface forces*—, but also time-dependent parameters like the density of the atmosphere. Oberflächenkräfte

5.1. Atmospheric drag

In case of low Earth orbiters, the atmosphere is the largest non-gravitational effect. It is also the most difficult one to model, as the density is highly variable and poorly observed.

Figure 5.1.: Volume passed by the satellite in a time span Δt

In fig. 5.1 a simplified empirical model, we investigate the mass Δm of an atmospheric volume. This volume “hits” a surface A of our satellite, flying with velocity v. In the finite time span Δt the volume represent a mass and, hence, a finite linear impulse Δp:

$$\Delta m = \rho \Delta V = \rho A v \Delta t$$

An impulse will be exerted on the satellite

$$\Delta p = -v \Delta m = -\rho A v^2 \Delta t$$

which is related to the force

$$F = \frac{\Delta p}{\Delta t} = -\rho A v^2\,.$$

Dividing by the the satellite mass yields the specific force:

$$f = -\rho \frac{A}{m} v^2\,.$$

This concept must be improved by several steps:

- The density $\rho(\boldsymbol{r}, \boldsymbol{t})$ of the atmosphere is depending on position, time, but also temperature, Sun activity, particles distribution. A very coarse model is an exponential form $\rho_{\text{atm}} \approx \rho_0 \mathrm{e}^{-\frac{h}{H_0}}$ with a reference height h_0 and density ρ_0.

Table 5.1.: Density of upper atmosphere (*Seeber*, 2003, p. 103)

height [km]	density [g/km^3]
100	497400
200	255 – 316
300	17 – 35
400	2.2 – 7.5
500	0.4 – 2.0
600	0.081 – 0.639
700	0.020 – 0.218
800	0.007 – 0.081
900	0.003 – 0.036
1000	0.001 – 0.018

- The shape of the body influences the atmospheric drag. This is considered in a factor $\left(\frac{1}{2}C_{\text{D}}\right)$, where the term $\frac{1}{2}$ is extracted for consistency with theories in flight dynamics.
- The direction and magnitude of the force must be considered: v^2 becomes $\|\boldsymbol{v}\|\boldsymbol{v}$

- So far we assumed, that a satellite passed through an unmoved atmosphere in the inertial frame. In a better approximation, the atmosphere co-rotates with the Earth, on top of which also other atmospheric circulation may occur. Hence, the relative velocity $(\boldsymbol{v} - \boldsymbol{v}_{\text{atm}})$ must be known for modelling.

Integrating these steps leads to the specific atmospheric drag:

$$\boldsymbol{f}_{\text{drag}} = -\frac{1}{2} C_{\text{D}} \rho(\boldsymbol{r}, t) \frac{A}{m} (\boldsymbol{v} - \boldsymbol{v}_{\text{atm}}) \|\boldsymbol{v} - \boldsymbol{v}_{\text{atm}}\| \,. \tag{5.1}$$

Remark 5.1 *The product* $\left(C_{\text{D}} \frac{A}{m}\right)$ *is also known as* ballistic coefficient.

ballistischer Koeffizient

Remark 5.2 *The* area-to-mass ratio $\frac{A}{m}$ *is an important parameter for orbit design. Non-gravitational orbit perturbations are reduced if the ratio gets smaller. On the one hand, the size of the satellite is determined by the onboard instruments and payload, while the mass can be changed by materials. On the other hand, possible size and mass are also limited by the launch vehicles and costs.*

Flächen-zu-Massen-Verhältnis

5.2. Solar radiation pressure

The sun ($\odot$) emits permanently photons in all directions. These particles generate a solar flux

Photonenfluss

$$\Phi = \frac{\Delta E}{A \Delta t}$$

i.e. an amount of energy ΔE passing the area A in a time span Δt, which acts on satellites, but also on Moon or Earth.

In a simplified, mechanical interpretation each photon delivers an "impulse":

$$p_\nu = \frac{E_\nu}{c} \qquad (E_\nu = m_\nu c^2 = m_\nu c \cdot c = p_\nu c)$$

$$\Longrightarrow \Delta p = \frac{\Delta E}{c} = \frac{\Phi}{c} A \Delta t \qquad \text{linear momentum}$$

and also a force:

$$F = \frac{\Delta p}{\Delta t} = \frac{\Phi}{c} A$$

These impulses cause a pressure $P = \frac{F}{A}$ on the satellite surface. To highlight the sun as its "source", we write the in pressure as

$$P_\odot = \frac{\Phi}{c} \,.$$

Close to the Earth orbit, the solar flux is almost constant: $\Phi \approx 1367\,\frac{\mathrm{W}}{\mathrm{m}^2}$, which leads to the pressure $P_\odot \approx 4.56 \cdot 10^{-6}\,\frac{\mathrm{N}}{\mathrm{m}^2}$. Thus the basic specific force reads

$$\|\boldsymbol{f}\| = \frac{F}{m} = \frac{\Phi}{c}\frac{A}{m}\,. \tag{5.2}$$

Note that the area-to-mass ratio appears again.

Orientation of Surfaces – absorption or reflection

effektive Fläche

Each surface element has its particular normal vector $\boldsymbol{n}$, which forms an inner angle θ with the incoming light rays. Hence, the *effective area* is given by $A_{\mathrm{eff}} = A\cos\theta$.

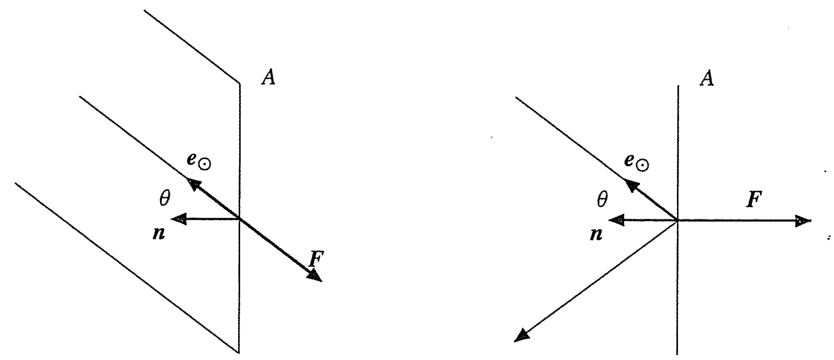

Figure 5.2.: Reflection and absorption of photons (*Montenbruck and Gill*, 2001, p.78).

Photons are either absorbed into the material of the surface (or generate electricity), which leads to the force

$$\boldsymbol{F}_{\mathrm{abs}} = -P_\odot \cos\theta A \boldsymbol{e}_\odot$$

or they are reflected by the same angle with

$$\boldsymbol{F}_{\mathrm{refl}} = -2P_\odot \cos\theta A \cos\theta \boldsymbol{n}\,.$$

Reflexionskoeffizient

The *reflection coefficient* (ϵ) describes the relative amount of reflected energy, while its counterpart $(1-\epsilon)$ describes the absorbed energy.

$$\Longrightarrow \boldsymbol{F}_{\mathrm{abs+refl}} = -P_\odot \cos\theta A\left[(1-\epsilon)\boldsymbol{e}_\odot + 2\epsilon\cos\theta\boldsymbol{n}\right]\,.$$

The coefficients depends on the material.

Table 5.2.: Absorption and reflection coefficients in satellite geodesy

material	– ϵ (reflection)	$1-\epsilon$ (absorption)	$C_R = 1+\epsilon$
solar panel –	0.21	0.79	1.21
antenna –	0.30	0.70	1.30
aluminum –	0.88	0.12	1.88

Distance to the Sun

The flux Φ of the Sun is attenuated quadratically with the distance, and the orbit of the Earth has an eccentricity of $e \approx 0.017$. Hence, the distance $r_\odot$ to the Sun varies around 3.3% between the perihelion $a(1-e) = 147\,\text{Gm}$ and the apohelion $a(1+e) = 152\,\text{Gm}$.

We consider the variation by the squared ratio of the actual radius and a mean distance $\bar{r}_\odot = 1\,\text{AU}$:

$$\boldsymbol{f} = \frac{\boldsymbol{F}}{m} = -P_\odot \left(\frac{\bar{r}_\odot}{r_\odot}\right)^2 \frac{A}{m} \cos\theta \Big[(1-\epsilon)\boldsymbol{e}_\odot + 2\epsilon\cos\theta \boldsymbol{n}\Big] \tag{5.3}$$

Remark 5.3 *Solar panels are usually large and often flat. If the panels are also oriented perpendicular to the incoming sun-light, the two vectors are aligned*

$$\boldsymbol{n} = \boldsymbol{e}_\odot = \frac{\boldsymbol{r}_\odot}{r_\odot}$$

with $\theta = 0$ and the specific force is simplified:

$$\begin{aligned} \boldsymbol{f} &= -P_\odot \left(\frac{\bar{r}_\odot}{r_\odot}\right)^2 \frac{A}{m} \left[(1-\epsilon)\boldsymbol{e}_\odot + 2\epsilon\boldsymbol{e}_\odot\right] = -P_\odot C_R \frac{A}{m} \left(\frac{\bar{r}_\odot}{r_\odot}\right)^2 \boldsymbol{e}_\odot \\ C_R &= 1+\epsilon \end{aligned} \tag{5.4}$$

Shadow function χ

So far, we assumed, that the each surface is in direct sunlight. In fact, there are always parts of the satellite which are not illuminated by the sun-light, either because of the relative orientation of the surface, or if the light is blocked by another body, in particular the Earth. This is taken into account by introducing the *shadow function*. The value of the shadow function varies between $0 \leq \chi \leq 1$ depending on the circumstances. If the

Schattenfunktion

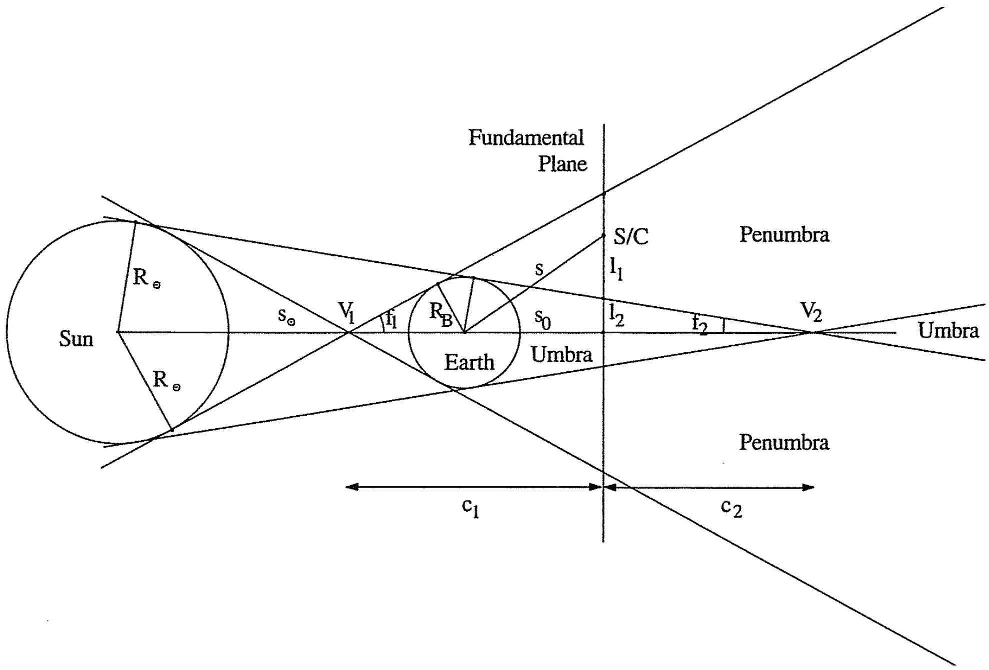

Figure 5.3.: The shadow function is derived via a geometrical model (*Montenbruck and Gill*, 2001, p. 80).

surface is fully illuminated, we find $\chi = 1$, while in the shadow $\chi = 0$ holds. There is also a transfer time, where the value is changing.

$$\boldsymbol{f} = \chi P_\odot \left(\frac{\bar{r}_\odot}{r_\odot}\right)^2 \frac{A}{m} \cos\theta \left[(1-\epsilon)\boldsymbol{e}_\odot + 2\epsilon\cos\theta\boldsymbol{n}\right]$$

Sonnensegel

Remark 5.4 Solar sails *are a (theoretical) concept of moving a space probe without onboard fuel only due to the reflection of sunlight on large mirrors, i.e by solar radiation pressure. The space probe* IKAROS *demonstrated by its flyby of Venus in 2010, that inner planets can be reached as well by solar sails. Another idea are "static satellites" which hover in a location like the polar regions, where geo-stationary satellites are not possible. Challenges are here the precise control of the solar sails, the stability of their construction, the restrictions in payload weight and also the very small accelerations.*

Exercise 5.1 *A balloon satellite*[1] *($C_\mathrm{D} \approx 2$) with the mass* $m = 46\,\mathrm{kg}$ *is launched into a circular orbit with* $h = 700\,\mathrm{km}$*. The spherical surface with radius* $R = 10\,\mathrm{m}$ *is made*

[1] Classic balloon satellites in 1960–1975 had a significant higher altitude, for example Echo 1 with $h = 1600\,\mathrm{km}$

by mylar with $\epsilon \approx 0.9$ and it acts as solar sail. Which non-gravitational force on the satellite is stronger?

- *effective area in all directions: $A = r^2\pi$ due to spherical shape*
- *maximum solar radiation pressure:*

$$\|\boldsymbol{f}_{\text{SRP,max}}\| = P_\odot C_R \frac{A}{m}\frac{\boldsymbol{r}_\odot}{r_\odot^3}\bar{r}_\odot^2 = 4.56\cdot 10^{-6}\,\frac{\text{N}}{\text{m}^2}(1+0.9)\frac{100\pi\,\text{m}^2}{46\,\text{kg}} = 5.92\cdot 10^{-5}\,\frac{\text{m}}{\text{s}^2}$$

- *atmospheric drag with table 5.1 (atmosphere without relative movements)*

$$\begin{aligned}\|\boldsymbol{f}_{\text{drag}}\| &= \frac{1}{2}C_{\text{D}}\rho(\boldsymbol{r},t)\frac{A}{m}v^2 = \frac{1}{2}C_{\text{D}}\rho(700\,\text{km})\frac{A}{m}\frac{GM}{r} = \\ &= \frac{1}{2}2\left(0.020\,\frac{0.001\text{kg}}{1000^3\text{m}^3}\right)\frac{100\pi\,\text{m}^2}{46\,\text{kg}}\frac{3.986005\cdot 10^{14}\,\frac{\text{m}^3}{\text{s}}}{6378136.6\,\text{m}+700000\,\text{m}} = 7.69\cdot 10^{-6}\,\frac{\text{m}}{\text{s}}\end{aligned}$$

At the first glimpse, the effect of the solar radiation pressure is significantly larger than the atmospheric drag. But we have used only the lower limit of the density; with the upper limit the effect of the drag will increase by one order of magnitude. It also should be pointed out, that the atmospheric drag acts permanently with same effect, i.e. lowering the orbital height. The solar radiation pressure might be blocked by the shadow of the Earth, and the effect on the orbit is variable and partly counterproductive.

5.3. Relativistic corrections

Special relativistic theory is beyond the scope of this course. Nevertheless, we find in (*Montenbruck and Gill*, 2001, p. 111) a post-Newton correction of the acceleration

$$\ddot{\boldsymbol{r}}_{\text{rel}} = -\frac{GM}{r^2}\left[\left(4\frac{GM}{c^2 r} - \frac{v^2}{c^2}\right)\boldsymbol{e}_r + 4\frac{v^2}{c^2}(\boldsymbol{e}_r\cdot\boldsymbol{e}_v)\boldsymbol{e}_v\right] \tag{5.5}$$

with the $c = 299\,792\,458\,\text{m/s}$ as speed of light and v as the scalar velocity of the satellite. The unit vectors $\boldsymbol{e}_r$ and $\boldsymbol{e}_v$ are pointing towards the position and velocity vectors, respectively.

Exercise 5.2 *Compare the relativistic effect and the acceleration due to gravity for a satellite on a circular orbit with an altitude of $h = 600\,\text{km}$.*

In case of a circular orbit the unit vectors $\boldsymbol{e}_r$ *and* $\boldsymbol{e}_v$ *are orthogonal, which eliminates the term* $(\boldsymbol{e}_r \cdot \boldsymbol{e}_v)\boldsymbol{e}_v$. *The scalar velocity* $v^2 = \frac{GM}{r}$ *is also known:*

$$\begin{aligned}\ddot{\boldsymbol{r}}_{\text{rel}} &= -\frac{GM}{r^2}\left(4\frac{GM}{c^2 r} - \frac{v^2}{c^2}\right)\boldsymbol{e}_r = \\ &= -\frac{GM}{r^2}\left(4\frac{GM}{c^2 r} - \frac{GM}{rc^2}\right)\boldsymbol{e}_r = \\ &= -\frac{GM}{r^2} 3\frac{GM}{c^2 r}\frac{\boldsymbol{r}}{\|\boldsymbol{r}\|}\end{aligned}$$

and

$$\|\ddot{\boldsymbol{r}}_{\text{rel}}\| = 3\frac{(GM)^2}{c^2 r^3}\bigg|_{h=600\,\text{km}} \approx 1.5608 \cdot 10^{-8}\,\frac{\text{m}}{\text{s}^2}\,.$$

The acceleration caused by gravity is $\ddot{\boldsymbol{r}} = -\frac{GM}{r^2}\frac{\boldsymbol{r}}{\|\boldsymbol{r}\|}$ *which leads to the ratio*

$$\begin{aligned}\frac{\ddot{\boldsymbol{r}}_{\text{rel}}}{\ddot{\boldsymbol{r}}} &= \frac{3\frac{GM}{c^2 r}}{1} \approx 0.013305\,\text{m} \cdot \frac{1}{r} \\ \implies \frac{\ddot{\boldsymbol{r}}_{\text{rel}}}{\ddot{\boldsymbol{r}}}\bigg|_{h=600\,\text{km}} &\approx 1.9067 \cdot 10^{-9}\end{aligned}$$

The relativistic acceleration is about 9 orders of magnitude smaller than the acceleration of the central term, which is also reflected in fig. 3.1.

6. The gravitational potential and its representation

The Lagrange Planetary equations (LPE) require the partial derivatives of the force function—or Hamiltonian—to all Kepler elements, i.e. $\nabla_{\boldsymbol{s}} F$. Thus, the main objective in this chapter is to transform $V(r, \theta, \lambda)$ into $V(a, e, I, \Omega, \omega, M) = V(\boldsymbol{s})$.

The Gauss version of the LPE requires forces in a local satellite frame, either $\boldsymbol{e}_{\mathrm{s}}$ or $\boldsymbol{e}_{\mathrm{t}}$. These can be generated by taking suitable derivatives of $V(\boldsymbol{s})$. Second derivatives in the local satellite frame will be presented, too. They are needed for gravity gradiometry.

6.1. Representation on the sphere

The gravitational potential is usually represented in a spherical harmonic. Such a representation turns out to be of advantage, since spherical harmonics possess the following properties:

- orthogonality,
- global support,
- harmonicity.

Because the geopotential fulfills the Laplace equation $\Delta V = 0$ outside the masses, the harmonicity of the spherical harmonics makes them natural base functions to V. Their orthogonality allows the analysis of the coefficients of the base functions.

For reasons of compactness *complex-valued* quantities will be employed here:

$$V(r, \theta, \lambda) = \frac{GM}{R} \sum_{l=0}^{\infty} \left(\frac{R_{\mathrm{E}}}{r} \right)^{l+1} \sum_{m=-l}^{l} K_{lm} Y_{lm}(\theta, \lambda) \,, \tag{6.1}$$

in which

$$\begin{aligned} r, \theta, \lambda &= \text{radius, co-latitude, longitude} \\ R &= \text{Earth's equatorial radius} \\ GM &= \text{gravitational constant times Earth's mass} \end{aligned}$$

$Y_{lm}(\theta,\lambda)$ = surface spherical harmonic of degree l and order m

K_{lm} = spherical harmonic coefficient, corresponding to $Y_{lm}(\theta,\lambda)$.

The coefficients K_{lm} constitute the *spherical harmonic spectrum* of the function V. They are the parameters of the gravitational field. The surface spherical harmonics $Y_{lm}(\theta,\lambda)$ are defined in the following way:

$$Y_{lm}(\theta,\lambda) = P_{l,|m|}(\cos\theta)\mathrm{e}^{im\lambda} . \tag{6.2}$$

It follows from this definition that for the complex conjugated it holds: $Y^*_{lm} = Y_{l,-m}$. Without explicitly using overbars, we assume that all complex quantities are (fully) normalized by the factor:

$$N_{lm} = \sqrt{(2l+1)\frac{(l-m)!}{(l+m)!}} . \tag{6.3}$$

Unnormalized spherical harmonic functions are multiplied by this factor to make them normalized. Unnormalized spherical harmonic coefficients are divided by (6.3). The orthogonality of the base functions is expressed by:

$$\frac{1}{4\pi}\iint\limits_{\sigma} Y_{l_1m_1}(\theta,\lambda)Y^*_{l_2m_2}(\theta,\lambda)\,\mathrm{d}\sigma = \delta_{l_1l_2}\delta_{m_1m_2} . \tag{6.4}$$

Remark 6.1 (Normalization conventions) *In literature, the factor $\frac{1}{4\pi}$ is sometimes taken care of in the normalization factor by incorporating a term $\sqrt{4\pi}$. Another difference between normalization factors, found in literature, is a factor $(-1)^m$. It is often used implicitly in the definition of the Legendre functions.*

In geodesy, one usually employs real-valued base functions and coefficients, cf. (*Heiskanen and Moritz*, 1967). The series (6.1) would become:

$$V(r,\theta,\lambda) = \frac{GM}{R}\sum_{l=0}^{\infty}\left(\frac{R_{\mathrm{E}}}{r}\right)^{l+1}\sum_{m=0}^{l}\left(C_{lm}\cos m\lambda + S_{lm}\sin m\lambda\right)P_{lm}(\cos\theta) , \tag{6.5}$$

with normalization factor:

$$N_{lm} = \sqrt{(2-\delta_{m0})(2l+1)\frac{(l-m)!}{(l+m)!}} . \tag{6.6}$$

The real- and complex-valued spherical harmonic coefficients, each with their *own* normalization, are linked by:

$$K_{lm} = \begin{cases} \frac{1}{2}(C_{lm} - iS_{lm}) , & m > 0 \\ C_{lm} , & m = 0 \\ \frac{1}{2}(C_{lm} + iS_{lm}) , & m < 0 \end{cases} , \tag{6.7}$$

such that $K_{lm} = K^*_{l,-m}$. Now it is easy to demonstrate the equality between complex and real-valued series expansions. If we ignore the dimensioning factor GM/R, the upward continuation term and the arguments of the spherical harmonics, we can write:

$$\begin{aligned}
V &= \sum_l \sum_{m=-l}^{l} K_{lm} Y_{lm} \\
&= \sum_l \sum_{m=0}^{l} K_{lm} Y_{lm} + K_{l,-m} Y_{l,-m} \\
&= \sum_l \sum_{m=0}^{l} K_{lm} Y_{lm} + K^*_{lm} Y^*_{lm} \\
&= \sum_l \sum_{m=0}^{l} K_{lm} Y_{lm} + (K_{lm} Y_{lm})^* \\
&= \sum_l \sum_{m=0}^{l} 2\Re \{K_{lm} Y_{lm}\} \\
&= \sum_l \sum_{m=0}^{l} 2\frac{1}{2}\Re \{(C_{lm} - iS_{lm})(\cos m\lambda + i \sin m\lambda)\} P_{lm}(\cos\theta) \\
&= \sum_l \sum_{m=0}^{l} (C_{lm} \cos m\lambda + S_{lm} \sin m\lambda) P_{lm}(\cos\theta)
\end{aligned}$$

We made a minor mistake in the second line for the case $m = 0$, that could have been repaired explicitly by dividing by $(1 + \delta_{m0})$. However, the definition (6.7) already takes care of this. The opposite mistake is made in the second last line.

Remark 6.2 (Complex vs. real) *From the derivations above the benefits of a series expansion in complex quantities is obvious: compactness and transparency of formulas. An added benefit in the next section will be the transformation properties of spherical harmonics under rotation of the coordinate system. Such transformation properties would be extremely laborious in real notation.*

6.2. Representation in Kepler elements

In order to transform the potential into a function of Kepler elements, two steps are required:

i) Rotate the spherical harmonics from the earth-fixed system into a coordinate system such that the orbit plane becomes the new equator and the new x-axis points towards the satellite. The following Euler rotation sequence is required:

$$\mathbf{R}_{313}(\Omega - \text{GAST}, I, \omega + \nu) = \mathbf{R}_3(\omega + \nu)\mathbf{R}_1(I)\mathbf{R}_3(\Omega - \text{GAST}) \text{ , or}$$
$$\mathbf{R}_{313}(\Lambda, I, u) = \mathbf{R}_3(u)\mathbf{R}_1(I)\mathbf{R}_3(\Lambda) \, ,$$

ii) Express $(R/r)^{l+1}\mathrm{e}^{ik\nu}$ as a Fourier series in the mean anomaly M, multiplied by $(R/a)^{l+1}$.

Step 1: Rotation of spherical harmonics. If we rotate the coordinate system around the 3rd axis over an angle α, $R_3(\alpha)$, the coordinates themselves change as:

$$\theta' = \theta \text{ , and } \lambda' = \lambda - \alpha \, .$$

Under this rotation, surface spherical harmonics transform as:

$$Y_{lm}(\theta, \lambda) = P_{lm}(\cos\theta)\mathrm{e}^{im\lambda} = P_{lm}(\cos\theta')\mathrm{e}^{im(\lambda' + \alpha)} = Y_{lm}(\theta', \lambda')\mathrm{e}^{im\alpha} \, . \tag{6.8}$$

Two of the three rotations can be dealt with now.

For rotations R_2 and R_1 things are not that simple. From representation theory we know that the transformation of a spherical harmonic $Y_{lm}(\theta, \lambda)$ of a specific degree l and order m in one frame requires all spherical harmonics $Y_{lk}(\theta', \lambda')$ of that same degree over all possible orders $-l \le k \le l$ in the rotated frame in a certain linear way. The linear mapping is expressed by *representation coefficients* d_{lmk} that are a function of the rotation angle. For a rotation $R_2(\alpha)$ we have the following transformation:

$$Y_{lm}(\theta, \lambda) = \sum_{k=-l}^{l} d_{lmk}(\alpha) Y_{lk}(\theta', \lambda') \, , \tag{6.9}$$

with

$$d_{lmk}(\alpha) = \left[\frac{(l+k)!(l-k)!}{(l+m)!(l-m)!}\right]^{\frac{1}{2}} \sum_{t=t_1}^{t_2} \binom{l+m}{t} \binom{l-m}{l-k-t} (-1)^t \, c^{2l-a} \, s^a \, ,$$

in which $c = \cos\frac{1}{2}\alpha$, $s = \sin\frac{1}{2}\alpha$, $a = k - m + 2t$, $t_1 = \max(0, m-k)$ and $t_2 = \min(l-k, l+m)$.

Note that (6.8) can be cast into a similar form when we use Kronecker deltas:

$$Y_{lm}(\theta, \lambda) = \sum_{k=-l}^{l} \delta_{mk} \mathrm{e}^{im\alpha} Y_{lk}(\theta', \lambda') \, .$$

Instead of a full $(2l+1) \times (2l+1)$ linear system we have a diagonal matrix only.

Since we need to perform the rotation $\mathbf{R}_1(I)$, (6.9) needs to be revised. A rotation around the 1st axis is achieved by a rotation around the 2nd axis if we properly pre- and postrotate by $\mathbf{R}_3(\pm\frac{1}{2}\pi)$:

$$\mathbf{R}_1(\alpha) = \mathbf{R}_3(\tfrac{1}{2}\pi)\mathbf{R}_2(\alpha)\mathbf{R}_3(-\tfrac{1}{2}\pi)\,.$$

Note that the rotation sequence is read from right to left. A spherical harmonic transforms under $\mathbf{R}_1(\alpha)$ therefore as follows:

$$Y_{lm}(\theta,\lambda) = \sum_{k=-l}^{l} \mathrm{e}^{-im\frac{1}{2}\pi} d_{lmk}(\alpha)\mathrm{e}^{ik\frac{1}{2}\pi} Y_{lk}(\theta',\lambda') = \sum_{k=-l}^{l} i^{k-m} d_{lmk}(\alpha) Y_{lk}(\theta',\lambda')\,. \quad (6.10)$$

In summary:

$$\begin{aligned} \boldsymbol{r}' &= \mathbf{R}_3(u)\mathbf{R}_1(I)\mathbf{R}_3(\Lambda)\boldsymbol{r} \\ &= \mathbf{R}_3(u+\tfrac{1}{2}\pi)\mathbf{R}_2(I)\mathbf{R}_3(\Lambda-\tfrac{1}{2}\pi)\boldsymbol{r} \qquad (6.11a) \\ \Longrightarrow \qquad Y_{lm}(\theta,\lambda) &= \sum_{k=-l}^{l} D_{lmk}(\Lambda,I,u) Y_{lk}(\theta',\lambda')\,, \qquad (6.11b) \\ \text{with} \quad D_{lmk}(\Lambda,I,u) &= i^{k-m} d_{lmk}(I)\mathrm{e}^{i(ku+m\Lambda)}\,. \qquad (6.11c) \end{aligned}$$

New coordinates. Using the time-variable elements $u(t)$ and $\Lambda(t)$, the rotation sequence will keep the new x-axis pointing to the satellite. Its orbital plane will instantaneously coincide with a new equator. The satellite's coordinates reduce to $\theta' = \frac{1}{2}\pi$ and $\lambda' = 0$, so that $Y_{lk}(\theta',\lambda') = P_{lk}(0)$. In principle the third rotation could have been omitted such that the representation coefficient $D_{lmk}(\Lambda, I, 0)$ should have been used in (6.11c). In that case the longitude in the new frame would have been $\lambda' = u$, leading to the same expression. In both cases the satellite is always on the rotated equator. In the second interpretation the argument of latitude would become the new longitude. In this view the name *argument of latitude* his highly misplaced.

Inserting the transformation (6.11b) and the representation coefficients (6.11c) into (6.1), combined with $\theta' = \frac{1}{2}\pi, \lambda' = 0$:

$$V(r,u,\Lambda,I) = \frac{GM}{R}\sum_{l=0}^{\infty}\left(\frac{R_{\mathrm{E}}}{r}\right)^{l+1}\sum_{m=-l}^{l}\sum_{k=-l}^{l} K_{lm} i^{k-m} d_{lmk}(I) P_{lk}(0)\mathrm{e}^{i(ku+m\Lambda)}\,. \quad (6.12)$$

Inclination functions. As a simplification a so-called *inclination function* is introduced:

$$F_{lmk}(I) = i^{k-m} d_{lmk}(I) P_{lk}(0) \,, \tag{6.13}$$

so that the along-orbit potential (6.12) is finally reduced to the series:

$$V(r,u,I,\Lambda) = \frac{GM}{R} \sum_{l=0}^{\infty} \left(\frac{R_{\mathrm{E}}}{r}\right)^{l+1} \sum_{m=-l}^{l} \sum_{k=-l}^{l} K_{lm} F_{lmk}(I) \mathrm{e}^{i(ku + m\Lambda)} \,. \tag{6.14}$$

The inclination functions (6.13) differ from Kaula's functions $F_{lmp}(I)$ (*Kaula*, 1966) in the following aspects:

- they are complex,
- they are normalized by the factor (6.3) (though written here without overbar),
- they make use of the index k.

The 3rd index of Kaula's inclination function, p, is due to the following. The inclination function $F_{lmk}(I)$ contains the equatorial Legendre function $P_{lk}(0)$. Legendre functions $P_{lm}(x)$ are either even or odd functions on the domain $x \in [-1;1]$ for $(l-m)$ even or odd, respectively. Thus, if $(l-m)$ is odd, $P_{lk}(0)$ will be zero and the whole inclination function becomes zero. Consequently the k-summation can be performed in steps of 2: $\sum_{k=-l,2}^{l}$. This fact allows the introduction of another index: $p = \frac{1}{2}(l-k)$ or $k = l - 2p$, which yields the summation $\sum_{p=0}^{l}$.

Remark 6.3 (p vs. k) *The p-index has two advantages: it is positive and it runs in unit steps. The third summation in (6.14) becomes $\sum_{p=0}^{l}$. The major disadvantage is that it does not have the meaning of* spherical harmonic order *(or* azimuthal order*) in the rotated system anymore. The index p is not a wavenumber, such as k. Thus, symmetries are lost, and formulae become more complicated. For instance* $\exp(i(ku+m\Lambda))$ *must be written as* $\exp(i((l-2p)u+m\Lambda))$*. The angular argument seems to depend on 3 indices in that case.*

Step 2: Eccentricity functions. So far, we have achieved an expression in terms of r, u, I, Λ, which is not the full set of Kepler elements yet. This partial results has to be complemented by the following transformation:

$$\frac{1}{r^{l+1}} \mathrm{e}^{ik\nu} = \frac{1}{a^{l+1}} \sum_{q=-\infty}^{\infty} G_{lkq}(e) \mathrm{e}^{i(k+q)M} \,, \tag{6.15}$$

which can be regarded as a Fourier transformation of the function $\mathrm{e}^{ik\nu}/r^{l+1}$. The Fourier coefficients $G_{lkq}(e)$ are called *eccentricity functions*. This transformation finalizes the required form of the geopotential in terms of Kepler elements:

$$V(\boldsymbol{s}) = \frac{GM}{R} \sum_{l=0}^{\infty} \sum_{m=-l}^{l} \sum_{k=-l,2}^{l} \sum_{q=-\infty}^{\infty} \left(\frac{R_{\mathrm{E}}}{a}\right)^{l+1} K_{lm} F_{lmk}(I) G_{lkq}(e) \mathrm{e}^{i\psi_{mkq}} \tag{6.16a}$$

$$\psi_{mkq} = k\omega + (k+q)M + m\Lambda \tag{6.16b}$$

The fourth summation over q runs in principle from $-\infty$ to ∞. However, the eccentricity functions decay rapidly according to:

$$G_{lkq}(e) \sim \mathcal{O}(e^{|q|}) \,.$$

Therefore, the q-summation can be limited for most geodetic satellites to $|q| \leq 1$ or 2 at most. Note that the *metric* Kepler elements (a, e, I) appear in the upward continuation, eccentricity and inclination functions, whereas the *angular* Kepler elements define the angular variable ψ_{mkq}.

If the p-index is used for a Kaula-type of inclination function, the eccentricity function becomes $G_{lpq}(e)$. Moreover, the composite angle ψ_{mkq} turns into:

$$\psi_{lmpq} = (l-2p)\omega + (l-2p+q)M + m\Lambda \,.$$

The apparent dependence of ψ on the degree l is artificial.

Real-valued expression. If we return to real-valued coefficients and functions, the inclination functions need to become real too. Only the term i^{k-m} in (6.13) needs to be adapted. Since l and k have the same parity, due to $P_{lk}(0) = 0$ for $l-k$ odd, we can write:

$$i^{k-m} = i^{l-2p-m} = (-1)^p \, i^{l-m} = (-1)^{\frac{l-k}{2}} \, i^{l-m} \,.$$

The power of (-1) can be absorbed into the definition of a real-valued inclination function. The power of i needs to be taken care of by a case distinction between $l-m$ even or odd and by a proper selection of either C_{lm} or S_{lm}. After some manipulations (6.16a) is recast into:

$$V(\boldsymbol{s}) = \frac{GM}{R} \sum_{l=0}^{\infty} \sum_{m=0}^{l} \sum_{k=-l,2}^{l} \sum_{q=-\infty}^{\infty} \left(\frac{R_{\mathrm{E}}}{a}\right)^{l+1} F_{lmk}(I) G_{lkq}(e) S_{lmkq}(\omega, \Omega, M)$$

$$S_{lmkq}(\omega, \Omega, M) = \left[\begin{pmatrix} C_{lm} \\ -S_{lm} \end{pmatrix} \cos\psi_{mkq} + \begin{pmatrix} S_{lm} \\ C_{lm} \end{pmatrix} \sin\psi_{mkq} \right]_{l-m \text{ odd}}^{l-m \text{ even}} \tag{6.17}$$

with the same definition of ψ_{mkq}. Again, one may use the p-index in order to have $\sum_{p=0}^{l}$ as the 3rd summation. Also, recall that real-valued quantities use a slightly different normalization factor.

6.3. Lumped coefficient representation

Let us return to (6.14), i.e. the expression of the geopotential in terms Kepler elements before introducing the eccentricity functions. The part $\exp(i(ku + m\Lambda))$ reminds of a 2D-Fourier series. The argument of latitude u and the longitude of the ascending node Λ attain values in the range $[0; 2\pi)$. Topologically, the product $[0; 2\pi) \times [0; 2\pi)$ yields a torus, which is the proper domain of a 2D-Fourier series. Indeed the potential can be recast into a 2D-Fourier expression, if the following Fourier coefficients are introduced:

$$A^V_{mk} = \sum_{l=\max(|m|,|k|)}^{\infty} H^V_{lmk} K_{lm} \,, \tag{6.18a}$$

$$\text{with} \quad H^V_{lmk} = \frac{GM}{R} \left(\frac{R_\mathrm{E}}{r} \right)^{l+1} F_{lmk}(I) \,. \tag{6.18b}$$

With these quantities, the potential reduces to the series:

$$V(u, \Lambda) = \sum_{m=-\infty}^{\infty} \sum_{k=-\infty}^{\infty} A^V_{mk} \mathrm{e}^{i\psi_{mk}} \,, \tag{6.18c}$$

$$\psi_{mk} = ku + m\Lambda \,. \tag{6.18d}$$

Just like (6.14), the above equations are valid for any orbit. They are not necessarily restricted to circular orbits. The 2D-Fourier expression (6.18) makes only sense, though, on an orbit with constant I and r. This is the concept of a *nominal orbit*. Only then do the H^V_{lmk} and correspondingly the Fourier coefficients A^V_{mk} become time independent.

The Fourier coefficients A^V_{mk} are usually referred to in literature as *lumped* coefficients, since they are a sum (over degree l). All potential coefficients K_{lm} of a specific order m are lumped in a linear way into A^V_{mk}. The coefficients H^V_{lmk} are denoted *transfer* coefficients here. They transfer the spherical harmonic spectrum into a Fourier spectrum. They are also known as *sensitivity* and *influence* coefficients.

Both A_{mk} and H_{lmk} are labelled by a super index V, referring to the geopotential V. In the next section, we will see that the same formulation can be applied to any functional of the geopotential. Only the transfer coefficients is specific to a particular functional.

Remark 6.4 (Lumped coefficients) *The word* lumped *merely indicates an accumulation of numbers, e.g. here a linear combination of potential coefficients over degree l, in general. Nevertheless a host of definitions and notations of lumped coefficients exists.*

An early reference where lumped coefficients are determined and discussed, is (*Gooding*, 1971). See (*Klokočník et al.*, 1990) for a list of lumped coefficients from several resonant orbit perturbations. Also in (*Heiskanen and Moritz*, 1967) lumped coefficients are discussed; zonal lumped coefficients, to be precise, that include non-linearities.

6.4. Pocket guide of dynamic satellite geodesy

Not only the potential, but also its functionals can be represented by a 2D-Fourier series, similar to (6.18). For $f^{\#}$, in which the label # represents a specific functional, the spectral decomposition is:

$$f^{\#} = \sum_{m=-\infty}^{\infty} \sum_{k=-\infty}^{\infty} A^{\#}_{mk} \mathrm{e}^{i(ku + m\Lambda)} \text{ , with} \tag{6.19a}$$

$$A^{\#}_{mk} = \sum_{l=\max(|m|,|k|)}^{\infty} H^{\#}_{lmk} K_{lm} \,. \tag{6.19b}$$

By means of the above equations, a linear observation model is established, that links functionals of the geopotential to the fundamental parameters, the spherical harmonic coefficients. The link is in the spectral domain. The elementary building blocks in this approach are transfer coefficients, similar to (6.18b). The linear model provides a basic tool for gravity field analyses. E.g. the recovery capability of future satellite missions can be assessed, or the influence of gravity field uncertainties on other functionals.

Pocket guide vs. Meissl scheme A collection of transfer coefficients $H^{\#}_{lmk}$ for all relevant functionals—observable or not—will be denoted as a *pocket guide* (PG) to dynamic satellite geodesy. Such a PG reminds of the *Meissl scheme*, cf. (*Rummel and van Gelderen*, 1995), which presents the spectral characteristics of the first and second order derivatives of the geopotential. This scheme enables to link observable gravity-related quantities to the geopotential field. A major difference between the PG and the Meissl-scheme is, that the former links SH coefficients to Fourier coefficients, whereas the latter stays in one spectral domain, either spherical harmonic or Fourier. Consequently, the transfer coefficients do not solely depend on SH degree l. In general, the spherical harmonic orders m and k are involved as well. The transfer coefficients can not be considered as eigenvalues of a linear operator, representing the observable, as in the case of the Meissl-scheme.

6.5. Derivatives of the geopotential

In this section the transfer coefficients of the first and second spatial derivatives of the potential are derived in the local satellite frame: x quasi along-track, y cross-track and z radial.

Since the satellite is in free fall, the gradient of the potential, ∇V, is not an observable functional. Nevertheless, the gradient vector—and consequently its transfer coefficients—are highly relevant. They supply the force function to the dynamic equations. In particular, with the derivatives in the satellite frame, the resulting gradient vector can directly be used in Gauss-type equations of motion. In 6.5.1 the transfer coefficients of all gradient components will be derived.

Gravity gradiometry is the measurement of the gradient of the gravity vector, which is a gradient by itself. The gradient of a gradient of a potential is a matrix or tensor of second derivatives. The gravity gradient tensor is also referred to as *Hesse matrix* in mathematics or *Marussi tensor* in physical geodesy. In 6.5.2, the transfer coefficients of all tensor components will be derived, also in the local satellite frame.

6.5.1. First derivatives: gravitational attraction

Before applying the gradient operator $\nabla = [\frac{\partial}{\partial x}\ \frac{\partial}{\partial y}\ \frac{\partial}{\partial z}]^{\mathsf{T}} = [\partial_x \quad \partial_y \quad \partial_z\ ]^{\mathsf{T}}$ to the geopotential expression (6.14) or to (6.18a)–(6.18d), it is recalled that in the rotated geocentric system u plays the role of longitude, θ' that of co-latitude (although its nominal value is fixed at $\frac{1}{2}\pi$) and r is the radial coordinate of course. Thus the gradient operator in the satellite frame becomes:

$$\nabla = \begin{pmatrix} \dfrac{\partial}{\partial x} \\ \dfrac{\partial}{\partial y} \\ \dfrac{\partial}{\partial z} \end{pmatrix} = \begin{pmatrix} \dfrac{1}{r}\dfrac{\partial}{\partial u} \\ -\dfrac{1}{r}\dfrac{\partial}{\partial \theta'} \\ \dfrac{\partial}{\partial r} \end{pmatrix} .$$

Let the potential be written as $V = \sum_{lmk} V_{lmk}$. Then the mechanism for deriving transfer coefficients is explained for the x and z components:

$$\begin{aligned} \partial_x V_{lmk} &= \frac{1}{r}\frac{\partial V_{lmk}}{\partial u} &&= \frac{1}{r}\frac{\partial V_{lmk}}{\partial \mathrm{e}^{i\psi_{mk}}}\frac{\partial \mathrm{e}^{i\psi_{mk}}}{\partial u} &&= \frac{ik}{r}V_{lmk}\,, \\ \partial_z V_{lmk} &= \frac{\partial V_{lmk}}{\partial r} &&= \frac{\partial V_{lmk}}{\partial (R/r)^{l+1}}\frac{\partial (R/r)^{l+1}}{\partial r} &&= -\frac{l+1}{r}V_{lmk}\,. \end{aligned}$$

So the along-track component of the gradient, $\partial_x V$, will be characterized by a term ik/r, and the radial derivative by the usual $-(l+1)/r$.

Cross-track derivative. The cross-track component requires special attention. The θ'-coordinate is hidden in the inclination function $F_{lmk}(I)$, (6.13). It is therefore convenient to introduce a cross-track derivative of the inclination function, denoted as $F^*_{lmk}(I)$, cf. (*Sneeuw*, 1992):

$$F^*_{lmk}(I) = -\frac{\partial F_{lmk}(I)}{\partial \theta'} = i^{k-m+2} d_{lmk}(I) \left. \frac{\mathrm{d}P_{lk}(\cos\theta')}{\mathrm{d}\theta'} \right|_{\theta'=\pi/2} .$$

With the parameter $t = \cos\theta$ the derivatives are: $\frac{\mathrm{d}P_{lk}(t)}{\mathrm{d}t} = -\frac{\mathrm{d}P_{lk}(\cos\theta)}{\sin\theta \mathrm{d}\theta}$. At the equator ($\theta = \pi/2$, or $t = 0$) no confusion about the sinθ factor can arise. Let the derivative with respect to t be simply called $\bar{P}'_{lk}(0)$, then the *cross-track inclination function* is defined as:

$$F^*_{lmk}(I) = i^{k-m} d_{lmk}(I) P'_{lk}(0) . \tag{6.20}$$

When applying recursions of derivatives of Legendre functions, e.g. (*Ilk*, 1983), to the equator, one obtains:

$$(1-t^2)\frac{\mathrm{d}P_{lk}(t)}{\mathrm{d}t} = \sqrt{1-t^2} P_{l,k+1}(t) - ktP_{lk}(t) \quad \stackrel{t=0}{\Longrightarrow} \quad P'_{lk}(0) = P_{l,k+1}(0) . \tag{6.21}$$

So the derivative P'_{lk} will be an even function for $l-k$ odd and an odd one for $l-k$ even. Thus the cross-track inclination functions will vanish for $l-k$ even. This would allow the introduction of a Kaula-like cross-track inclination function $F^*_{lmp}(I)$.

Alternative cross-track derivatives. Other approaches, circumventing the introduction of $F^*_{lmk}(I)$, exist. Colombo (1986) suggested as cross-track derivative the expression

$$\frac{\partial}{\partial y} = \frac{1}{r \sin u} \frac{\partial}{\partial I} ,$$

which shows singularities in u. See also (*Betti and Sansò*, 1989, *Rummel et al.*, 1993). Depending on coordinate choice, better worked out in (*Koop*, 1993) or (*Balmino et al.*, 1996) other expressions can be derived, e.g. the following singular one:

$$\frac{\partial}{\partial y} = \frac{1}{r \cos u \sin I} \left(\cos I \frac{\partial}{\partial u} - \frac{\partial}{\partial \Lambda} \right) .$$

By multiplying the former by $\sin^2 u$, the latter by $\cos^2 u$ and adding the result, *Schrama* (1989) derived the *regular* expression:

$$\frac{\partial}{\partial y} = \frac{1}{r} \left[\sin u \frac{\partial}{\partial I} + \frac{\cos u}{\sin I} \left(\cos I \frac{\partial}{\partial u} - \frac{\partial}{\partial \Lambda} \right) \right] ,$$

which leads to a corresponding cross-track inclination function:

$$F^*_{lmk}(I) = \frac{1}{2}\left[\frac{(k-1)\cos I - m}{\sin I}\right]\bar{F}_{lm,k-1}(I) - \frac{1}{2}\bar{F}'_{lm,k-1}(I) + \frac{1}{2}\left[\frac{(k+1)\cos I - m}{\sin I}\right]\bar{F}_{lm,k+1}(I) + \frac{1}{2}\bar{F}'_{lm,k+1}(I)\,, \tag{6.22}$$

where the primes denote differention with respect to inclination I. Although numerical equivalence between the real version of (6.20) and (6.22) could be verified, it was proven analytically in (*Balmino et al.*, 1996) that this last expression consists in fact of a twofold definition:

$$F^*_{lmk}(I) = \left[\frac{(k-1)\cos I - m}{\sin I}\right]\bar{F}_{lm,k-1}(I) - \bar{F}'_{lm,k-1}(I)\,, \tag{6.23a}$$

$$F^*_{lmk}(I) = \left[\frac{(k+1)\cos I - m}{\sin I}\right]\bar{F}_{lm,k+1}(I) + \bar{F}'_{lm,k+1}(I)\,. \tag{6.23b}$$

In summary, the spectral characteristics of the gradient operator in the local satellite frame are given by the following transfer coefficients:

$$\partial_x \quad : \quad H^x_{lmk} = \frac{GM}{R^2}\left(\frac{R_\text{E}}{r}\right)^{l+2} \quad [ik] \quad F_{lmk}(I) \tag{6.24a}$$

$$\partial_y \quad : \quad H^y_{lmk} = \frac{GM}{R^2}\left(\frac{R_\text{E}}{r}\right)^{l+2} \quad [1] \quad F^*_{lmk}(I) \tag{6.24b}$$

$$\partial_z \quad : \quad H^z_{lmk} = \frac{GM}{R^2}\left(\frac{R_\text{E}}{r}\right)^{l+2} \quad [-(l+1)] \quad F_{lmk}(I) \tag{6.24c}$$

Remark 6.5 (Nomenclature) *The different parts in these transfer coefficients will be denoted in the sequel as* dimensioning term *containing (GM, R),* upward continuation term *(a power of R/r),* specific transfer *and* inclination function part. *Especially the specific transfer is characteristic for a given observable.*

According to this nomenclature, the specific transfer of the potential is 1, cf. equation (6.18b). Both H^x_{lmk} and H^z_{lmk} show a transfer of $\mathcal{O}(l,k)$ which is specific to first derivatives in general. Higher frequencies are amplified. The same holds true for H^y_{lmk}, though hidden in $F^*_{lmk}(I)$. Equations (6.23a) indicate already that $F^*_{lmk}(I) \sim \mathcal{O}(l,k) \times F_{lmk}(I)$. This becomes clearer for the second cross-track derivative, cf. next section. Note also that only the radial derivative is isotropic, i.e. only depends on degree l. Its specific transfer is invariant under rotations of the coordinate system like (6.11b). This is not the case for V_x and V_y, when considered as scalar fields.

6.5.2. Second derivatives: the gravity gradient tensor

- In contrast to the first derivatives, the second derivatives of the geopotential field are observable quantities. The observation of these is called *gravity gradiometry*, whose technical realization is described e.g. in (Rummel, 1986a). For a historical overview of measurement principles and proposed satellite gradiometer missions, refer to *Forward* (1973), *Rummel* (1986).

The gravity gradient tensor of second derivatives reads:

$$\boldsymbol{V} = \begin{pmatrix} V_{xx} & V_{xy} & V_{xz} \\ V_{yx} & V_{yy} & V_{yz} \\ V_{zx} & V_{zy} & V_{zz} \end{pmatrix} . \tag{6.25}$$

The sub-indices denote differentiation with respect to the specified coordinates. The tensor $\boldsymbol{V}$ is symmetric. Due to Laplace's equation $\Delta V = V_{xx} + V_{yy} + V_{zz} = 0$, it is also trace-free. In local spherical coordinates (r, u, θ') the tensor can be expressed as, e.g. (*Koop*, 1993, eqn. (3.10)):

$$\boldsymbol{V} = \begin{pmatrix} \frac{1}{r^2}V_{uu} + \frac{1}{r}V_r & -\frac{1}{r^2}V_{\theta' u} & \frac{1}{r}V_{ur} - \frac{1}{r^2}V_u \\ & \frac{1}{r^2}V_{\theta'\theta'} + \frac{1}{r}V_r & -\frac{1}{r}V_{\theta' r} + \frac{1}{r^2}V_{\theta'} \\ \text{symm.} & & V_{rr} \end{pmatrix} . \tag{6.26}$$

Again, use has been made of the fact that the satellite is always on the rotated equator $\theta' = \frac{1}{2}\pi$. With Laplace's equation one can avoid a second differentiation with respect to the θ'-coordinate by writing:

$$V_{yy} = -V_{xx} - V_{zz} = -\frac{1}{r^2}V_{uu} - \frac{1}{r}V_r - V_{rr} .$$

As usual, the purely radial derivative is the simplest one. It is spectrally characterized by: $(l{+}1)(l{+}2)/r^2$. The operator ∂_{xx} will return the term: $-[k^2{+}(l{+}1)]/r^2$. The second cross-track derivative ∂_{yy} thus gives with Laplace $[k^2 + (l+1) - (l+1)(l+2)]/r^2 = [k^2 - (l+1)^2]/r^2$. The *spectral transfer* for ∂_{xz} becomes: $[-ik(l+1) - ik]/r^2 = -ik(l+2)/r^2$. The components V_{xy} and V_{yz} make use of $\partial_{\theta'}$, which requires the use of $F^*_{lmk}(I)$ again. Starting from the expression for V_y, one further ik/r-term is required to obtain V_{xy}. For V_{yz} one needs an extra $[-(l+1) - 1]/r = -(l+2)/r$. The full set of transfer coefficients, describing the single components of the gravity gradient tensor is thus given by:

$$\partial_{xx} \quad : \quad H^{xx}_{lmk} = \frac{GM}{R^3}\left(\frac{R_\mathrm{E}}{r}\right)^{l+3} [-(k^2 + l + 1)] \; F_{lmk}(I) \tag{6.27a}$$

$$\partial_{yy} \quad : \quad H^{yy}_{lmk} = \frac{GM}{R^3}\left(\frac{R_\mathrm{E}}{r}\right)^{l+3} [k^2 - (l + 1)^2] \; F_{lmk}(I) \tag{6.27b}$$

$$\partial_{zz} \quad : \quad H^{zz}_{lmk} = \frac{GM}{R^3}\left(\frac{R_\mathrm{E}}{r}\right)^{l+3} \quad [(l+1)(l+2)] \quad F_{lmk}(I) \tag{6.27c}$$

$$\partial_{xy} \quad : \quad H^{xy}_{lmk} = \frac{GM}{R^3}\left(\frac{R_\mathrm{E}}{r}\right)^{l+3} \quad [ik] \quad F^*_{lmk}(I) \tag{6.27d}$$

$$\partial_{xz} \quad : \quad H^{xz}_{lmk} = \frac{GM}{R^3}\left(\frac{R_\mathrm{E}}{r}\right)^{l+3} \quad [-ik(l+2)] \quad F_{lmk}(I) \tag{6.27e}$$

$$\partial_{yz} \quad : \quad H^{yz}_{lmk} = \frac{GM}{R^3}\left(\frac{R_\mathrm{E}}{r}\right)^{l+3} \quad [-(l+2)] \quad F^*_{lmk}(I) \tag{6.27f}$$

The specific transfer is of order $\mathcal{O}(l^2, lk, k^2)$, as can be expected for second derivatives. This is also true for H^{xy}_{lmk} and H^{yz}_{lmk}, that make use of $F^*_{lmk}(I)$. Again, the purely radial derivative is the only isotropic component. Adding the specific transfers of the diagonal components yields the Laplace equation in the spectral domain:

$$-(k^2 + l + 1) + k^2 - (l+1)^2 + (l+1)(l+2) = 0\,.$$

Alternative cross-track gravity gradient. An alternative derivation of V_{yy} could have been obtained directly, i.e. without the Laplace equation, by a second cross-track differentation. A new inclination function, say $F^{**}_{lmk}(I)$ is required, defined as:

$$F^{**}_{lmk}(I) = \frac{\partial^2 F_{lmk}(I)}{\partial \theta'^2} = i^{k-m} d_{lmk}(I) \bar{P}''_{lk}(0)\,.$$

From known recursions (*Ilk*, 1983), we have for the second latitudinal derivative of the unnormalized Legendre function at the equator:

$$P''_{lk}(0) = [k^2 - l(l+1)] P_{lk}(0)\,.$$

A normalized version of this expression must be inserted in the definition of $F^{**}_{lmk}(I)$ above, yielding the specific transfer $[k^2 - l(l+1)]$ of the second cross-track derivative $V_{\theta'\theta'}$. Since $V_{yy} = V_{\theta'\theta'}/r^2 + V_r/r$ one ends up with exactly the same transfer, as derived above with the Laplace equation, namely $[k^2 - (l+1)^2]/r^2$. Moreover, it demonstrates again that $F^*_{lmk}(I)$ is of order $\mathcal{O}(l,k)$, since the second cross-track derivative has a transfer of $\mathcal{O}(l^2, lk, k^2)$.

Space-stable gradiometry. The transfer coefficients (6.27) pertain to tensor components in the local satellite frame. Especially for local-level orientations, such as Earth-pointing, these expressions are useful. In principle any other orientation can be deduced from them, since a tensor $\boldsymbol{V}$ is transformed into another coordinate system by:

$$\boldsymbol{V}' = \mathbf{R}\boldsymbol{V}\mathbf{R}^\mathsf{T}\,,$$

cf. (*Koop*, 1993), in which $\mathbf{R}$ is the rotation matrix between the two systems. For instance the rotation sequence

$$\mathbf{R} = \mathbf{R}_3(-\Lambda)\mathbf{R}_1(-I)\mathbf{R}_3(-u)\,,$$

which is the inverse of the rotations from 6.2, may be used to transform the gravity gradient tensor back into an Earth-fixed reference frame. Note, however, that the angles u and Λ are time-dependent. The derivation of transfer functions becomes cumbersome. An alternative approach, based on the work of *Hotine* (1969), is followed by *Ilk* (1983) and (*Bettadpur*, 1991, 1995).

7. Gravitational orbit perturbations

We are now able to write down the equations of motion of a satellite in a gravitational field. To that end we need to take the partial derivatives of the gravitational potential (6.16a) to all Kepler elements and combine them according to the LPE. The first step we take in 7.1 is to solve the LPE for the main effect, that is the secular orbit change due to the flattening of the Earth. In the subsequent section 7.2 we will derive the remaining gravitational orbit perturbations from linear perturbation theory (LPT). In 7.3 we will discuss the orbit perturbation spectrum and related aspects like resonance.

7.1. The J_2 secular reference orbit

The main deviation from a central gravitational field GM/r is caused by the dynamic flattening of the Earth. In the GRS80 normal field the flattening is represented by the dimensionless constant $J_2 = 1.082\,63 \cdot 10^{-3}$. For actual gravity fields, it is represented by the spherical harmonic coefficient $C_{2,0} = K_{2,0} \approx -J_2$. To be precise, these are non-normalized coefficients. A division by $\sqrt{5}$ would normalize them.

The gravitational field produced by $K_{2,0}$ reads:

$$V_{2,0}(\boldsymbol{s}) = \frac{GM}{R_\mathrm{E}} \left(\frac{R_\mathrm{E}}{a}\right)^3 K_{2,0} \sum_{k=-2,2}^{2} \sum_{q=-\infty}^{\infty} F_{2,0,k}(I) G_{2,k,q}(e) \mathrm{e}^{i[k\omega + (k+q)M]} \,.$$

It can be expected that periodic excitations give mainly rise to periodic perturbations. Thus the main perturbation can be expected from the zero-frequency term with $k = q = 0$:

$$\begin{aligned} R = V_{2,0,0,0}(a,e,I) &= \frac{GM}{R_\mathrm{E}} \left(\frac{R_\mathrm{E}}{a}\right)^3 K_{2,0} F_{2,0,0}(I) G_{2,0,0}(e) \\ &= \frac{GM}{R_\mathrm{E}} \left(\frac{R_\mathrm{E}}{a}\right)^3 C_{2,0} \left(\frac{3}{4}\sin^2 I - \frac{1}{2}\right) (1-e^2)^{-\frac{3}{2}} \end{aligned}$$

The LPE require the partial derivatives of this expression. The partial derivatives w.r.t.

the angular variables are all zero. Only the following remain:

$$\frac{\partial R}{\partial a} = -3GM\frac{R_{\mathrm{E}}^2}{a^4}C_{2,0}\left(\frac{3}{4}\sin^2 I - \frac{1}{2}\right)(1-e^2)^{-\frac{3}{2}} \tag{7.1a}$$

$$\frac{\partial R}{\partial I} = GM\frac{R_{\mathrm{E}}^2}{a^3}C_{2,0}\frac{3}{2}\sin I\cos I(1-e^2)^{-\frac{3}{2}} \tag{7.1b}$$

$$\frac{\partial R}{\partial e} = 3eGM\frac{R_{\mathrm{E}}^2}{a^3}C_{2,0}\left(\frac{3}{4}\sin^2 I - \frac{1}{2}\right)(1-e^2)^{-\frac{5}{2}} \tag{7.1c}$$

These partial derivatives are to be inserted in equations ((3.10a) to (3.10f)). Substituting $GM = n^2a^3$ and performing the necessary simplifications will yield the LPE for secular orbital motion due to the flattening of the Earth:

$$\dot{a} = 0 \tag{7.2a}$$

$$\dot{e} = 0 \tag{7.2b}$$

$$\dot{I} = 0 \tag{7.2c}$$

$$\dot{\omega} = \frac{3}{4}nC_{2,0}\frac{1}{(1-e^2)^2}\left(\frac{R_{\mathrm{E}}}{a}\right)^2(1-5\cos^2 I) \tag{7.2d}$$

$$\dot{\Omega} = \frac{3}{2}nC_{2,0}\frac{1}{(1-e^2)^2}\left(\frac{R_{\mathrm{E}}}{a}\right)^2\cos I \tag{7.2e}$$

$$\dot{M} = n - \frac{3}{4}nC_{2,0}\frac{1}{(1-e^2)^{\frac{3}{2}}}\left(\frac{R_{\mathrm{E}}}{a}\right)^2(3\cos^2 I - 1) \tag{7.2f}$$

The first three of these equations are trivially solved: a, e and I are constant. The orbit does not change its size and shape under the influence of the Earth's flattening. Nor does the inclination change. With the metric Kepler elements constant, the right hand sides of the remaining three LPE become constant too. The full set of differential equations (7.2a) is easily integrable to:

$$a(t) = a_0 \tag{7.3a}$$

$$e(t) = e_0 \tag{7.3b}$$

$$I(t) = I_0 \tag{7.3c}$$

$$\omega(t) = \omega(t_0) + \dot{\omega}(t-t_0)\,, \tag{7.3d}$$

$$\Omega(t) = \Omega(t_0) + \dot{\Omega}(t-t_0)\,, \tag{7.3e}$$

$$M(t) = M(t_0) + \dot{M}(t-t_0)\,, \tag{7.3f}$$

with the above indicated rates. The nodal line will precess at a constant rate $\dot{\Omega}$. Also the perigee will precess linearly in time. Moreover, the flattened Earth causes the mean anomaly to accelerate (or decelerate). An orbit with these constant angular rates is called *secular*. In summary, the secular J_2-orbit is characterized by:

$$\text{secular } J_2 \text{ orbit:} \quad \boxed{\begin{array}{r} a, e, I \text{ constant} \\ \dot{\omega}, \dot{\Omega}, \dot{M} \text{ constant} \end{array}} \tag{7.4}$$

Perigee precession. The perigee precession rate depends on the inclination. It can be made to zero if $\cos^2 I = \frac{1}{5}$, resulting in the *critical inclinations* $I = 63\overset{\circ}{.}4$ or $I = 116\overset{\circ}{.}6$. For lower inclinations—orbital plane closer to the equator—the perigee precession rate becomes positive: both $(1 - 5\cos^2 I)$ and $C_{2,0}$ are negative. For higher inclinations—orbital plane closer to the poles—$\dot{\omega}$ is negative.

The Russian communication satellite system Molniya makes a clever use of this property. Molniya satellites are in a highly eccentric orbit ($e \approx 0.74$). After sweeping through perigee, they will move slowly and be visible for a long time. To ensure that this occurs over Russia, or over the Northern hemisphere in general, the perigee must be fixed over the Southern hemisphere at $\omega = 270°$. This is done by choosing an inclination of $63\overset{\circ}{.}4$.

Perigee precession will also occur for equatorial orbits, or, in a heliocentric setting, for ecliptical orbits. Thus the relativistic perigee advance of Mercury's orbit around the sun, may be obscured by an inadequately known gravitational flattening of the Sun.

Nodal precession. The nodal precession is proportional to $\cos I$. Thus, the plane of polar orbits will not change. This can be expected, since the rotationally symmetric flattened Earth does not exert a gravitational torque on a polar orbit. For prograde orbits, the nodes will move clockwise ($\dot{\Omega} < 0$), whereas $\dot{\Omega} > 0$ for retrograde orbits.

Mean motion change. Similarly, the mean motion change due to the Earth's flattening is proportional to $(3\cos^2 I - 1)$. On orbits with an inclination lower than $54\overset{\circ}{.}7$ or higher than $125\overset{\circ}{.}3$ the satellite will actually move faster than the mean motion n. In between these inclinations, the satellite is held back by the gravitational torque.

Remark 7.1 (Numerical example) *For a satellite at about 750 km height, following a near-circular orbit (e.g. $e = 0.01$), the angular rates (7.2a) typically become:*

$$\begin{aligned} \dot{\omega} &\approx 3\overset{\circ}{.}35 \left(5\cos^2 I - 1\right) \text{ per day} \\ \dot{\Omega} &\approx -6\overset{\circ}{.}7 \cos I \text{ per day} \\ \dot{M} &\approx 14.4 + \frac{3\overset{\circ}{.}35}{360°}\left(3\cos^2 I - 1\right) \text{ revolutions per day} \end{aligned}$$

7.2. Periodic gravity perturbations in linear approach

With the main orbit perturbation described by the J_2 secular orbit, we will now derive periodic orbit perturbations due to the remaining spherical harmonic contributions V_{lmkq}, including the periodic J_2 effects $V_{2,0,k,q}$. Since the LPE will be non-linear we will apply *linear perturbation theory* (LPT). The algorithm is as follows:

- Take the partial derivatives of (6.16a) to the Kepler elements,
- Insert the partial derivatives into the LPE ((3.10a) to (3.10f)),
- Evaluate the right hand side of the resulting non-linear equations on the J_2 reference orbit, thus leading to a linear system,
- Replace the integration to time by integration to the angular variable ψ_{mkq}.

The resulting LPT solution is an *approximation* to the real orbit perturbations, because of the linearization on the reference orbit. In principle, the LPT solution might be inserted again into the right side of the LPE. The method of *successive approximation* would lead to higher approximations. This process is extremely laborious, though.

Partial derivatives. In the following we will abbreviate $F_{lmk}(I)$ into F and $G_{lkq}(e)$ into G. Primes will denote derivatives of the functions towards their argument. We will also recast the power of the upward continuation in (6.16a) by adjusting the dimensioning factor.

$$
\begin{aligned}
\frac{\partial V}{\partial a} &= \frac{GM}{a^2} \sum_{lmkq} [-(l+1)] \left(\frac{R_\mathrm{E}}{a}\right)^l FGK_{lm} \mathrm{e}^{i\psi_{mkq}} \\
\frac{\partial V}{\partial e} &= \frac{GM}{a} \sum_{lmkq} \left(\frac{R_\mathrm{E}}{a}\right)^l FG' K_{lm} \mathrm{e}^{i\psi_{mkq}} \\
\frac{\partial V}{\partial I} &= \frac{GM}{a} \sum_{lmkq} \left(\frac{R_\mathrm{E}}{a}\right)^l F' G K_{lm} \mathrm{e}^{i\psi_{mkq}} \\
\frac{\partial V}{\partial \omega} &= \frac{GM}{a} \sum_{lmkq} \left(\frac{R_\mathrm{E}}{a}\right)^l FG[ik] K_{lm} \mathrm{e}^{i\psi_{mkq}} \\
\frac{\partial V}{\partial \Omega} &= \frac{GM}{a} \sum_{lmkq} \left(\frac{R_\mathrm{E}}{a}\right)^l FG[im] K_{lm} \mathrm{e}^{i\psi_{mkq}} \\
\frac{\partial V}{\partial M} &= \frac{GM}{a} \sum_{lmkq} \left(\frac{R_\mathrm{E}}{a}\right)^l FG[i(k+q)] K_{lm} \mathrm{e}^{i\psi_{mkq}}
\end{aligned}
$$

Insertion into LPE. Collecting all derivatives, combining them into the equations ((3.10a) to (3.10f)) and simplifying some factors using $GM = n^2 a^3$ leads to the following set of Lagrange Planetary Equations:

$$\dot{a} = 2na \sum_{lmkq} \left(\frac{R_{\mathrm{E}}}{a}\right)^l FGK_{lm}\,[k+q]\; i\,\mathrm{e}^{i\psi_{mkq}} \tag{7.5a}$$

$$\dot{e} = \frac{n}{e} \sum_{lmkq} \left(\frac{R_{\mathrm{E}}}{a}\right)^l FGK_{lm} \left[(1-e^2)(k+q) - \sqrt{1-e^2}k\right] i\,\mathrm{e}^{i\psi_{mkq}} \tag{7.5b}$$

$$\dot{I} = \frac{n}{\sin I\sqrt{1-e^2}} \sum_{lmkq} \left(\frac{R_{\mathrm{E}}}{a}\right)^l FGK_{lm}\,[k\cos I - m]\; i\,\mathrm{e}^{i\psi_{mkq}} \tag{7.5c}$$

$$\dot{\omega} = n \sum_{lmkq} \left(\frac{R_{\mathrm{E}}}{a}\right)^l \left[F\frac{\sqrt{1-e^2}}{e}G' - F'\frac{\cot I}{\sqrt{1-e^2}}G\right] K_{lm}\mathrm{e}^{i\psi_{mkq}} \tag{7.5d}$$

$$\dot{\Omega} = \frac{n}{\sin I\sqrt{1-e^2}} \sum_{lmkq} \left(\frac{R_{\mathrm{E}}}{a}\right)^l F'GK_{lm}\mathrm{e}^{i\psi_{mkq}} \tag{7.5e}$$

$$\dot{M} = n - n \sum_{lmkq} \left(\frac{R_{\mathrm{E}}}{a}\right)^l F\left[\frac{1-e^2}{e}G' - 2(l+1)G\right] K_{lm}\mathrm{e}^{i\psi_{mkq}} \tag{7.5f}$$

Linear Perturbation Theory. The above LPE (7.5a) are nonlinear ordinary differential equations. They can be solved in linear approximation. The J_2 reference orbit (7.3a) is considered as the zero-order approximation, i.e. a *trajectory of Taylor points*. The remaining orbit perturbations are expected to be relatively small, that is, the real orbit is expected to oscillate around the reference orbit.

Remark 7.2 *Naturally, all zonal coefficients will contribute a zero-frequency (DC) term with $m = k = q = 0$. Although they will be several orders of magnitude smaller than the J_2-effect, they will cause secular perturbations nevertheless. Thus it may be wise to incorporate the DC contributions from other zonal coefficients into the definition of the reference orbit, too.*

Now, the right hand side of (7.5a) is evaluated with with constant a, e and I. At the same time, since the time t appears linearly in the complex exponentials, the time integration is replaced by an integration towards the angular variable ψ_{mkq}:

$$\int \mathrm{d}t = \int \frac{\mathrm{d}t}{\mathrm{d}\psi}\,\mathrm{d}\psi = \int \frac{1}{\dot{\psi}}\,\mathrm{d}\psi = \frac{1}{\dot{\psi}} \int \mathrm{d}\psi\,,$$

$$\text{with} \quad \dot{\psi} = \dot{\psi}_{mkq} = k\dot{\omega} + (k+q)\dot{M} + m(\dot{\Lambda})\,.$$

The whole set of differential equations immediately becomes linear. A straightforward integration yields for each $\{lmkq\}$-combination:

$$\Delta a_{lmkq} = \frac{n}{\dot{\psi}_{mkq}} 2a \left(\frac{R_{\mathrm{E}}}{a}\right)^l FGK_{lm}\,[k+q]\,\mathrm{e}^{i\psi_{mkq}} \tag{7.6a}$$

$$\Delta e_{lmkq} = \frac{n}{\dot{\psi}_{mkq}} \frac{1}{e} \left(\frac{R_{\mathrm{E}}}{a}\right)^l FGK_{lm} \left[(1-e^2)(k+q) - \sqrt{1-e^2}k\right] \mathrm{e}^{i\psi_{mkq}} \tag{7.6b}$$

$$\Delta I_{lmkq} = \frac{n}{\dot{\psi}_{mkq}} \frac{1}{\sin I\sqrt{1-e^2}} \left(\frac{R_{\mathrm{E}}}{a}\right)^l FGK_{lm}\,[k\cos I - m]\,\mathrm{e}^{i\psi_{mkq}} \tag{7.6c}$$

$$\Delta \omega_{lmkq} = \frac{n}{\dot{\psi}_{mkq}} \left(\frac{R_{\mathrm{E}}}{a}\right)^l \left[F\frac{\sqrt{1-e^2}}{e}G' - F'\frac{\cot I}{\sqrt{1-e^2}}G\right] K_{lm}\,[-i]\,\mathrm{e}^{i\psi_{mkq}} \tag{7.6d}$$

$$\Delta \Omega_{lmkq} = \frac{n}{\dot{\psi}_{mkq}} \frac{1}{\sin I\sqrt{1-e^2}} \left(\frac{R_{\mathrm{E}}}{a}\right)^l F'GK_{lm}\,[-i]\,\mathrm{e}^{i\psi_{mkq}} \tag{7.6e}$$

$$\Delta M_{lmkq} = \frac{n}{\dot{\psi}_{mkq}} \left(\frac{R_{\mathrm{E}}}{a}\right)^l F\left[2(l+1)G - \frac{1-e^2}{e}G'\right] K_{lm}\,[-i]\,\mathrm{e}^{i\psi_{mkq}} \tag{7.6f}$$

The Δ's have to be understood as perturbations to the J_2 reference orbit. In order to achieve the full orbit in linear perturbation theory we have to add the combined summations to the reference orbit :

$$\boldsymbol{s}(t) = \boldsymbol{s}_0 + \dot{\boldsymbol{s}}(t-t_0) + \sum_{l=2}^{\infty}\sum_{m=-l}^{l}\sum_{k=-l}^{l}\sum_{q=-\infty}^{\infty} \Delta\boldsymbol{s}_{lmkq}\,. \tag{7.7}$$

Remark 7.3 (Linear orbit perturbations accuracy) *The above orbit perturbation solution was achieved through linearization. The orbit perturbations (7.6a) are said to be linear. The main deviation from the zero-order solution, i.e. the J_2 reference orbit, are the periodic effects due to $C_{2,0}$, which are of the order $\mathcal{O}(J_2) = 10^{-3}$. Thus, the zero-order solution achieves roughly a relative accuracy of 10^{-3}. The linear solution has a relative precision of 10^{-6}. The main approximation error is $\mathcal{O}(J_2^2)$.*

Real-valued solutions. To express the linear perturbations (7.6a) in terms of real-valued quantities, similar to (6.17), the following adaptations have to be made:

- The summation over m in (7.7) starts at $m = 0$.

- Combine terms with $K_{lm}\mathrm{e}^{i(ku+m\Lambda)}$ into S_{lmkq}, as defined in (6.17).
- Combine terms with $K_{lm}\,[-i]\,\mathrm{e}^{i\psi_{mkq}}$ into $\bar{S}_{lmkq} = \int S_{lmkq}\,\mathrm{d}\psi_{mkq}$.
- Usually the k-summation is changed into a p-summation, including $F_{lmp}(I)$ and $G_{lpq}(e)$.

Again it is seen that complex-valued expressions are far more compact. They are also more transparent. For instance, the terms $[-i]$ that stem from the integration of $\mathrm{e}^{i\psi_{mkq}}$ are a simple phase-shift: $-i = \mathrm{e}^{-i\frac{\pi}{2}}$. In the real-valued case, the integration from S_{lmkq} into $\bar{S}_{lmkq}$ requires a more complicated interchange of C_{lm}, S_{lm}, and cosines and sines.

7.3. The orbit perturbation spectrum

Linear system. In linear perturbation theory, the originally non-linear equations of motion (7.5a) were linearized at the J_2 reference orbit. As a consequence (7.5a) became a set of linear ODE. One characteristic of linear systems is that an input forcing at a certain frequency causes an output disturbance at the same frequency. Indeed, if the Kepler elements are perturbed at a specific frequency $\dot{\psi}_{mkq}$, cf. the RHS of (7.5a), the resulting orbit perturbation (7.6a) will be at the same frequency.

In order to emphasize the spectral character of the orbit perturbations in a Fourier sense, we can go back to a lumped coefficient expression again as in (6.18). The main step is to turn the outer l-summation in (7.7) into an inner summation:

$$\sum_{l=2}^{\infty}\sum_{m=-l}^{l}\sum_{k=-l}^{l}\sum_{q=-\infty}^{\infty} \rightarrow \sum_{m=-\infty}^{\infty}\sum_{k=-\infty}^{\infty}\sum_{q=-\infty}^{\infty}\sum_{l=\max(|m|,|k|)}^{\infty},$$

perform the summation (i.e. lump) over the degree l, and collect the appropriate terms into a corresponding transfer coefficient. As an example, we can write for the perturbed semi-major axis:

$$\text{Fourier series:} \qquad a(t) = \sum_{m=-\infty}^{\infty}\sum_{k=-\infty}^{\infty}\sum_{q=-\infty}^{\infty} A^a_{mkq}\mathrm{e}^{i\dot{\psi}_{mkq}(t-t_0)}$$

$$\text{lumped coefficients:} \qquad A^a_{mkq} = \sum_{l=\max(|m|,|k|)}^{\infty} H^a_{lmkq}K_{lm}$$

$$\text{transfer coefficients:} \qquad H^a_{lmkq} = \frac{n}{\dot{\psi}_{mkq}}2a\left(\frac{R_\mathrm{E}}{a}\right)^l F_{lmk}(I)G_{lkq}(e)\,[k+q]$$

Which spherical harmonic coefficients contribute to a (lumped) Fourier coefficient $A^{\#}_{mkq}$ at the frequency $\dot{\psi}_{mkq}$? The frequency does not involve the degree l. Thus, if the $\{mkq\}$-

combination is fixed, all spherical harmonic coefficients K_{lm} of that specific order m will contribute, i.e. all degrees larger than m. Because of the vanishing inclination functions $F_{lmk}(I)$ when $(l-k)$ is odd, it will be either only the even or the odd degrees that contribute.

Perturbation spectrum. The perturbation frequencies $\dot{\psi}_{mkq}$ are composite frequencies:

$$\dot{\psi}_{mkq} = k\dot{\omega} + (k+q)\dot{M} + m(\dot{\Omega} - \dot{\text{GAST}}) \,, \text{ or} \tag{7.8a}$$

$$= (k+q)(\dot{\omega} + \dot{M}) + m\dot{\Lambda} - q\dot{\omega} \,. \tag{7.8b}$$

The perigee drift $\dot{\omega}$ and the nodal drift $\dot{\Omega}$ are small: typically a few degrees per day. The freqency $\dot{\text{GAST}}$ is the daily rotation rate, i.e. 360° per siderial day. Since this is far larger than the nodal rate (in absolute value), the *nodal daily rate* $\dot{\Lambda} \approx -\dot{\text{GAST}}$. The frequency $\dot{M}$ is the largest. For LEO satellites it is approximately 16 times faster than the daily rate.

The rewritten version (7.8b) is illustrative. The main frequency lines will be at an integer amount of $(\dot{\omega} + \dot{M})$, i.e. the orbital revolution frequency. These main peaks are interspersed with frequency lines $m\dot{\Lambda}$. On top of that, the orbit perturbations will be modulated by the apsidal frequency $q\dot{\omega}$.

For near-circular orbits the terms with $q \neq 0$ will become small. The simplified perturbation spectrum reads:

$$\dot{\psi}_{mk} = k\dot{u} + m\dot{\Lambda} \,. \tag{7.8c}$$

Resonance. The linear orbit perturbations (7.6a) all contain a denominator $\dot{\psi}_{mkq}$. That means that the input forcing is greatly amplified for the low frequency spectrum. For an actual forcing at DC, i.e. the zero-frequency, the amplification would be infinite. This behaviour is called *resonance*, which is a common phenomenon in dynamical systems. If the dynamical system is excited close to the zero-frequency we have *near-resonance* or *shallow resonance*.

In case of exact resonance, the linear perturbation solution is invalid. A forcing at DC can simply not be represented by the type of oscillatory solutions as in (7.6a). Instead, a zero-frequency forcing will likely result in secular orbit perturbations similar to the $C_{2,0}$ effect in 7.1. In case of near-resonance the linear perturbation theory does not necessarily break down, though care should be taken.

When does (near-)resonance occur? If we analyse the simplified frequency (7.8c), we can distinguish the following cases:

zonals With $m = 0$ we have $\dot{\psi}_{0,k} = k\dot{u}$. Trivially, a zero frequency arises for $k = 0$, cf. 7.1. Thus, all even degree zonal coefficients will contribute.

***m*-dailies** As mentioned before, the nodal-daily frequency $\dot{\Lambda}$ are nearly 16 times smaller than the orbital revolution rate. Thus, if $k = 0$ the frequencies $\dot{\psi}_{m,0} = m\dot{\Lambda}$ are close to zero, in particular for very low order m. Thus, low order coefficients give rise to near-resonance at a frequency of m cycles per day (CPD), hence the name m-dailies.

repeat orbits In general, resonance occurs if

$$\dot{\psi}_{mk} = 0 \Rightarrow k\dot{u} = -m\Lambda \Rightarrow \frac{k}{m} = \frac{-\dot{\Lambda}}{\dot{u}} = \frac{T_u}{T_\Lambda}\,,$$

in which T_u denotes the orbital revolution period and T_Λ is one nodal day.

Now the ratio $\frac{k}{m}$ is an integer ratio. Thus the resonance condition can be met—i.e. we can find a suitable $\{mk\}$-combination—if the above periods T_u and T_Λ are in an integer ratio is well:

$$\frac{\dot{u}}{-\dot{\Lambda}} = \frac{T_\Lambda}{T_u} = \frac{\beta}{\alpha}\,. \tag{7.9}$$

This mathematical *commensurability* means geometrically a *repeat orbit*. After β revolutions exactly α nodal days have passed. The integers α and β have to be *relative primes*, i.e. they can not have a common divisor.

Repeat orbits. The repeat ratio β/α will be close to 16 for LEO orbits, e.g. 49/3 or 31/2. For repeat orbits the simplified spectrum $\dot{\psi}_{mk}$ can be simplified even further:

$$\dot{\psi}_{mk} = k\dot{u} + m\dot{\Lambda} = \dot{u}\left(k + m\frac{\dot{\Lambda}}{\dot{u}}\right) = \dot{u}\left(k - m\frac{\alpha}{\beta}\right) = \frac{\dot{u}}{\beta}(k\beta - m\alpha)\,. \tag{7.10}$$

Since $(k\beta - m\alpha)$ is solely composed of integers, we can map them onto a single integer n. The base frequency $\dot{u}/\beta$ pertains to one full repeat period (of α nodal days $= \beta$ revolutions). With:

$$(k\beta - m\alpha) \mapsto n \quad \Rightarrow \quad \dot{\psi}_{mk} \mapsto \dot{\psi}_n = n\frac{\dot{u}}{\beta}\,.$$

Even if the repeat orbit condition (7.9) is not met, there will always be specific $\{mk\}$-combinations that, for the given $\dot{u}$ and $\dot{\Lambda}$, give rise to the near-resonance situation $\dot{\psi}_{mk} \approx 0$. That will particularly occur when

$$m = \gamma\,\mathrm{int}\left(\frac{\beta}{\alpha}\right), \quad \gamma = 1, 2, \ldots$$

As an example, suppose we have a 49/3 repeat ratio. Now take the situation $k = 1$ and $m = \text{int}(\frac{49}{3}) = 16$. Then we get a near resonant frequency of

$$(k\beta - m\alpha) = (1 \cdot 49 - 16 \cdot 3) = 1 \implies \dot{\psi}_{16,1} = \frac{\dot{u}}{49}\,,$$

which is even smaller than the 1-daily near-resonance.

8. A viable alternative: Hill Equations

The standard procedure in dynamic satellite geodesy is to develop a linear perturbation theory in terms of Kepler[1] elements. To this end, the Newton[2] equations of motion $\ddot{\boldsymbol{r}} = \boldsymbol{a}$ are transformed into equations of motion of the form:

$$\dot{\boldsymbol{s}} = \boldsymbol{f}(\boldsymbol{s}), \quad \boldsymbol{s} = (a, e, I, \Omega, \omega, M) .$$

These are the so-called Lagrange[3] planetary equations, a set of 6 first-order coupled non-linear ordinary differential equations (ODE). They are solved by noticing that the major gravitational perturbation is due to the dynamic flattening of the Earth (expressed by J_2), causing the Kepler orbit to precess with $\dot{\Omega}$, $\dot{\omega}$ and $\dot{M}$ all proportional to J_2. The non-linear ODE are linearized on this precessing or secular reference orbit. This is the procedure followed in *Kaula* (1966) and most other textbooks.

Here we will follow a different approach. Most satellites of geodetic interest are following a near-circular orbit. Therefore, we will use a set of equations that describes motion in a reference frame, that co-rotates with the satellite on a circular path. These are the Hill[4] equations, that were revived for geodetic purposes by O.L. Colombo, E.J.O. Schrama and others.

8.1. Acceleration in a rotating reference frame

Let us consider the situation of motion in a *rotating* reference frame and let us associate this rotating frame with a triad that is rotating uniformly on a nominal circular orbit, for the time being. Inertial coordinates, velocities and accelerations will be denoted with the index i. Satellite-frame quantities get the index s. Now suppose that a *time-dependent*

[1] Johannes Kepler (1571–1630). Gave the first mathematical description of (planetary) orbits: *i)* Planets move on an elliptical orbit around the sun in one of the focal points, *ii)* The line between sun and planet sweeps equal areas in equal times, and *iii)* The ratio between the cube of the semi-major axis and the square of the revolution period is constant.

[2] Sir Isaac Newton (1642–1727).

[3] Comte Louis de Lagrange (1736–1813). French-Italian mathematician and astronomer.

[4] George William Hill (1838–1914), American mathematician. He developed his eponymous equations to describe lunar motion in his *Researches in the Lunar Theory* (1878), American Journal of Mathematics, vol. 1, pp. 5–26, 129–147, 245–260

rotation matrix $\mathbf{R} = \mathbf{R}(\alpha(t))$, applied to the inertial vector $\boldsymbol{r}_i$, results in the Earth-fixed vector $\boldsymbol{r}_s$. We would be interested in velocities and accelerations in the rotating frame. The time derivations must be performed in the inertial frame, though.

From $\mathbf{R}\boldsymbol{r}_i = \boldsymbol{r}_s$ we get:

$$\boldsymbol{r}_i = \mathbf{R}^\mathsf{T}\boldsymbol{r}_s \tag{8.1a}$$

$$\Downarrow \text{ time derivative}$$

$$\dot{\boldsymbol{r}}_i = \mathbf{R}^\mathsf{T}\dot{\boldsymbol{r}}_s + \dot{\mathbf{R}}^\mathsf{T}\boldsymbol{r}_s \tag{8.1b}$$

$$\Downarrow \text{ multiply by } \mathbf{R}$$

$$\begin{aligned}\mathbf{R}\dot{\boldsymbol{r}}_i &= \dot{\boldsymbol{r}}_s + \mathbf{R}\dot{\mathbf{R}}^\mathsf{T}\boldsymbol{r}_s \\ &= \dot{\boldsymbol{r}}_s + \boldsymbol{\Omega}\boldsymbol{r}_s\end{aligned} \tag{8.1c}$$

The matrix $\boldsymbol{\Omega} = \mathbf{R}\dot{\mathbf{R}}^\mathsf{T}$ is called *Cartan*[5] *matrix*. It describes the rotation rate, as can be seen from the following simple 2D example with $\alpha(t) = \omega t$:

$$\mathbf{R} = \begin{pmatrix} \cos\omega t & \sin\omega t \\ -\sin\omega t & \cos\omega t \end{pmatrix}$$

$$\Rightarrow \boldsymbol{\Omega} = \begin{pmatrix} \cos\omega t & \sin\omega t \\ -\sin\omega t & \cos\omega t \end{pmatrix} \omega \begin{pmatrix} -\sin\omega t & -\cos\omega t \\ \cos\omega t & -\sin\omega t \end{pmatrix} = \begin{pmatrix} 0 & -\omega \\ \omega & 0 \end{pmatrix}$$

It is useful to introduce $\boldsymbol{\Omega}$. In the next time differentiation step we can now distinguish between time dependent rotation matrices and time variable rotation rate. Let's pick up the previous derivation again:

$$\Downarrow \text{ multiply by } \mathbf{R}^\mathsf{T}$$

$$\dot{\boldsymbol{r}}_i = \mathbf{R}^\mathsf{T}\dot{\boldsymbol{r}}_s + \mathbf{R}^\mathsf{T}\boldsymbol{\Omega}\boldsymbol{r}_s \tag{8.1d}$$

$$\Downarrow \text{ time derivative}$$

$$\begin{aligned}\ddot{\boldsymbol{r}}_i &= \mathbf{R}^\mathsf{T}\ddot{\boldsymbol{r}}_s + \dot{\mathbf{R}}^\mathsf{T}\dot{\boldsymbol{r}}_s + \dot{\mathbf{R}}^\mathsf{T}\boldsymbol{\Omega}\boldsymbol{r}_s + \mathbf{R}^\mathsf{T}\dot{\boldsymbol{\Omega}}\boldsymbol{r}_s + \mathbf{R}^\mathsf{T}\boldsymbol{\Omega}\dot{\boldsymbol{r}}_s \\ &= \mathbf{R}^\mathsf{T}\ddot{\boldsymbol{r}}_s + 2\dot{\mathbf{R}}^\mathsf{T}\dot{\boldsymbol{r}}_s + \dot{\mathbf{R}}^\mathsf{T}\boldsymbol{\Omega}\boldsymbol{r}_s + \mathbf{R}^\mathsf{T}\dot{\boldsymbol{\Omega}}\boldsymbol{r}_s\end{aligned} \tag{8.1e}$$

$$\Downarrow \text{ multiply by } \mathbf{R}$$

$$\mathbf{R}\ddot{\boldsymbol{r}}_i = \ddot{\boldsymbol{r}}_s + 2\boldsymbol{\Omega}\dot{\boldsymbol{r}}_s + \boldsymbol{\Omega}\boldsymbol{\Omega}\boldsymbol{r}_s + \dot{\boldsymbol{\Omega}}\boldsymbol{r}_s \tag{8.1f}$$

This equation tells us that acceleration in the rotating e-frame equals acceleration in the inertial i-frame—in the proper orientation, though—when 3 more terms are added. The additional terms are called *inertial* accelerations Analyzing (8.1f) we can distinguish the four terms at the right hand side:

[5]Élie Joseph Cartan (1869–1951), French mathematician.

- $\mathbf{R}\ddot{\boldsymbol{r}}_i$ is the inertial acceleration vector, expressed in the orientation of the rotating frame.
- $2\boldsymbol{\Omega}\dot{\boldsymbol{r}}_s$ is the so-called *Coriolis* acceleration, which is due to motion in the rotating frame.
- $\boldsymbol{\Omega}\boldsymbol{\Omega}\boldsymbol{r}_s$ is the *centrifugal* acceleration, determined by the position in the rotating frame.
- $\dot{\boldsymbol{\Omega}}\boldsymbol{r}_s$ is sometimes referred to as *Euler* acceleration or inertial acceleration of rotation. It is due to a non-constant rotation rate.

Remark 8.1 *Equation (8.1f) can be generalized to moving frames with time-variable origin. If the linear acceleration of the e-frame's origin is expressed in the i-frame with* $\ddot{\boldsymbol{b}}_i$*, the only change to be made to (8.1f) is* $\mathbf{R}\ddot{\boldsymbol{r}}_i \rightarrow \mathbf{R}(\ddot{\boldsymbol{r}}_i - \ddot{\boldsymbol{b}}_i)$*.*

Properties of the Cartan matrix $\boldsymbol{\Omega}$. Cartan matrices are skew-symmetric, i.e. $\boldsymbol{\Omega}^\mathsf{T} = -\boldsymbol{\Omega}$. This can be seen in the simple 2D example above already. But it also follows from the orthogonality of rotation matrices:

$$\mathbf{R}\mathbf{R}^\mathsf{T} = I \implies \frac{\mathrm{d}}{\mathrm{d}t}(\mathbf{R}\mathbf{R}^\mathsf{T}) = \underbrace{\dot{\mathbf{R}}\mathbf{R}^\mathsf{T}}_{\boldsymbol{\Omega}^\mathsf{T}} + \underbrace{\mathbf{R}\dot{\mathbf{R}}^\mathsf{T}}_{\boldsymbol{\Omega}} = \mathbf{0} \implies \boldsymbol{\Omega}^\mathsf{T} = -\boldsymbol{\Omega}\,. \tag{8.2}$$

A second interesting property is the fact that multiplication of a vector with the Cartan matrix equals the cross product of the vector with a corresponding rotation vector:

$$\boldsymbol{\Omega}\boldsymbol{r} = \boldsymbol{\omega} \times \boldsymbol{r} \tag{8.3}$$

This property becomes clear from writing out the 3 Cartan matrices, corresponding to the three independent rotation matrices:

$$\left.\begin{array}{l}
\mathbf{R}_1(\omega_1 t) \;\Rightarrow\; \boldsymbol{\Omega}_1 = \begin{pmatrix} 0 & 0 & 0 \\ 0 & 0 & -\omega_1 \\ 0 & \omega_1 & 0 \end{pmatrix} \\
\mathbf{R}_2(\omega_2 t) \;\Rightarrow\; \boldsymbol{\Omega}_2 = \begin{pmatrix} 0 & 0 & \omega_2 \\ 0 & 0 & 0 \\ -\omega_2 & 0 & 0 \end{pmatrix} \\
\mathbf{R}_3(\omega_3 t) \;\Rightarrow\; \boldsymbol{\Omega}_3 = \begin{pmatrix} 0 & -\omega_3 & 0 \\ \omega_3 & 0 & 0 \\ 0 & 0 & 0 \end{pmatrix}
\end{array}\right\} \quad \stackrel{\text{general}}{\Longrightarrow} \quad \boldsymbol{\Omega} = \begin{pmatrix} 0 & -\omega_3 & \omega_2 \\ \omega_3 & 0 & -\omega_1 \\ -\omega_2 & \omega_1 & 0 \end{pmatrix}. \tag{8.4}$$

Indeed, when a general rotation vector $\boldsymbol{\omega} = (\omega_1, \omega_2, \omega_3)^\mathsf{T}$ is defined, we see that:

$$\begin{pmatrix} 0 & -\omega_3 & \omega_2 \\ \omega_3 & 0 & -\omega_1 \\ -\omega_2 & \omega_1 & 0 \end{pmatrix} \begin{pmatrix} x \\ y \\ z \end{pmatrix} = \begin{pmatrix} \omega_1 \\ \omega_2 \\ \omega_3 \end{pmatrix} \times \begin{pmatrix} x \\ y \\ z \end{pmatrix} .$$

The skew-symmetry (8.2) of Ω is related to the fact $\boldsymbol{\omega} \times \boldsymbol{r} = -\boldsymbol{r} \times \boldsymbol{\omega}$.

Exercise 8.1 *Convince yourself that the above Cartan matrices $\boldsymbol{\Omega}_i$ are correct, by doing the derivation yourself.*

Using property (8.3), the velocity (8.1c) and acceleration (8.1f) may be recast into the perhaps more familiar form:

$$\mathbf{R}\dot{\boldsymbol{r}}_i = \dot{\boldsymbol{r}}_s + \boldsymbol{\omega} \times \boldsymbol{r}_s \tag{8.5a}$$

$$\mathbf{R}\ddot{\boldsymbol{r}}_i = \ddot{\boldsymbol{r}}_s + 2\boldsymbol{\omega} \times \dot{\boldsymbol{r}}_s + \boldsymbol{\omega} \times (\boldsymbol{\omega} \times \boldsymbol{r}_s) + \dot{\boldsymbol{\omega}} \times \boldsymbol{r}_s \tag{8.5b}$$

8.2. Hill equations

Rotation. As inertial system we will use the so-called *perifocal* system, which has its $x_i y_i$-plane in the orbital plane with the x_i-axis pointing towards the perigee. Thus the z_i axis is aligned with the angular momentum vector. This may not be the conventional inertial system, but it is a convenient one for the following discussion. If you don't like the perifocal frame you have to perform the following rotations first:

$$\boldsymbol{r}_i = \mathbf{R}_3(\omega)\mathbf{R}_1(I)\mathbf{R}_3(\Omega)\boldsymbol{r}_{i_0} ,$$

with Ω the right ascension of the ascending node, I the inclination, ω the argument of perigee (not to be mistaken for the rotation rate), and the index i_0 referring to the conventional inertial system.

The s-frame will be rotating around the $z_i = z_s$-axis at a constant rotation rate n that we will later identify with a satellite's mean motion. Thus, the rotation angle is nt:

$$\boldsymbol{r}_s = \mathbf{R}_3(nt)\boldsymbol{r}_i . \tag{8.6}$$

$$\boldsymbol{\Omega} = \begin{pmatrix} 0 & -n & 0 \\ n & 0 & 0 \\ 0 & 0 & 0 \end{pmatrix} \quad \text{and} \quad \dot{\boldsymbol{\Omega}} = \mathbf{0} .$$

The three inertial accelerations, due to the rotation of the Earth, become:

$$\text{Coriolis:} \qquad -2\boldsymbol{\Omega}\dot{\boldsymbol{r}}_s = 2n\begin{pmatrix} \dot{y}_s \\ -\dot{x}_s \\ 0 \end{pmatrix} \tag{8.7a}$$

$$\text{centrifugal:} \quad -\boldsymbol{\Omega}\boldsymbol{\Omega}\boldsymbol{r}_s = n^2\begin{pmatrix} x_s \\ y_s \\ 0 \end{pmatrix} \tag{8.7b}$$

$$\text{Euler:} \qquad -\dot{\boldsymbol{\Omega}}\boldsymbol{r}_s = \mathbf{0} \tag{8.7c}$$

Translation. Now let's introduce a *nominal orbit* of constant radius R, which should not be mistaken for the rotation matrix $\mathbf{R}$. A satellite on this orbit would move with uniform angular velocity n, according to Kepler's third law: $n^2R^3 = GM$.

The origin of the s-frame is now translated to the nominal orbit over the x_s-axis. While the frame is revolving on the nominal orbit, the x_s axis continuously points in the radial direction, the y_s-axis is in along-track, whereas the z_s axis points cross-track. As mentioned before, the translation induces an additional origin acceleration. Since we are dealing with circular motion this is a *centripetal* acceleration. In the orientation of the s-frame it is purely radial (in negative direction:) $\mathbf{R}\ddot{\boldsymbol{b}}_i = (-n^2R, 0, 0)^{\mathsf{T}}$.

Permutation. In local frames, we usually want the z-coordinate in the vertical direction. Thus we now permute the coordinates according to fig. 8.1. At the same time we will drop the index s.

$$\begin{aligned} y_s &\to x = \text{along-track} \\ z_s &\to y = \text{cross-track} \\ x_s &\to z = \text{radial} \end{aligned}$$

Hill equations: kinematics. Notice that sofar we have only dealt with kinematics, i.e. a description of position, velocity and acceleration under the transformation from the inertial to the satellite frame. We do not have *equations of motion* yet, that will only come up as soon as we introduce dynamics (a force) as well.

Combining all the kinematic information we have, we arrive at the following:

$$\left.\begin{aligned} &\ddot{x} + 2n\dot{z} - n^2x &= \\ &\ddot{y} &= \\ &\ddot{z} - 2n\dot{x} - n^2z - n^2R &= \end{aligned}\right\} \mathbf{R}\ddot{\boldsymbol{r}}_i \tag{8.8}$$

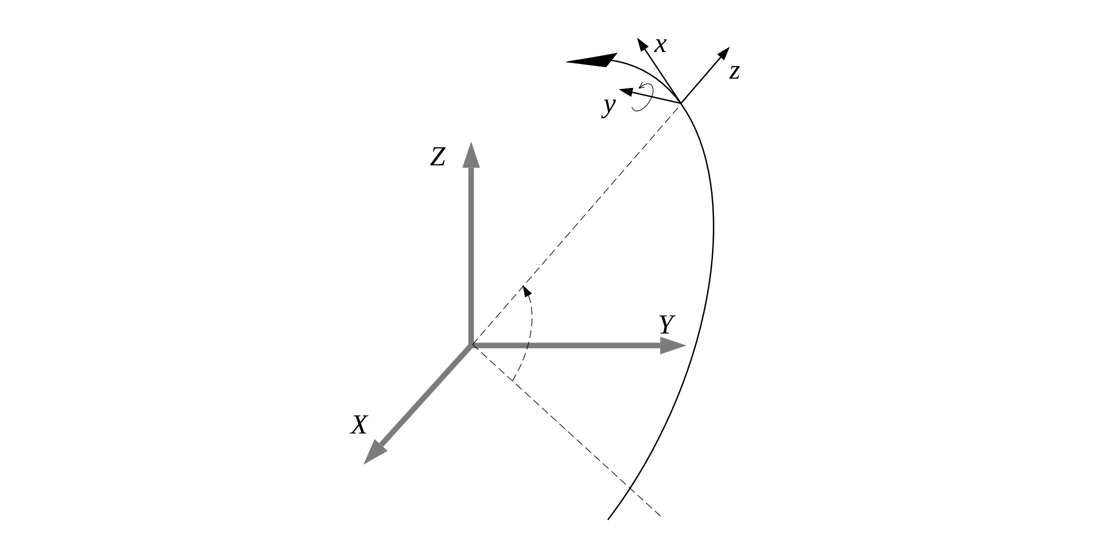

Figure 8.1.: The local orbital triad: x along-track, y cross-track and z radial.

Hill equations: dynamics. Now let's turn to the right hand side. In inertial space, the equations of motion are simply Newton's equations. We assume that the force is composed of a central field term $U(\boldsymbol{r}) = GM/r$, with $r = |\boldsymbol{r}|$ and a term that contains all other forces, both gravitational and non-gravitational:

$$\ddot{\boldsymbol{r}}_i = \nabla_i U(\boldsymbol{r}_i) + \boldsymbol{f}_i = -\frac{GM}{r^3}\boldsymbol{r}_i + \boldsymbol{f}_i\,. \tag{8.9}$$

According to (8.8) we need to rotate this with the matrix $\mathbf{R}$. At the same time we will *linearize* this on the circular nominal orbit:

$$\begin{aligned}
\mathbf{R}\,\ddot{\boldsymbol{r}}_i &= \nabla_s U(\boldsymbol{r})_{|r=R} + \nabla_s^2 U(\boldsymbol{r})_{|r=R}\cdot\boldsymbol{r}_s + \boldsymbol{f}_s + \mathcal{O}(r_s^2)\\
&= -\frac{GM}{R^2}\begin{pmatrix}0\\0\\1\end{pmatrix} + \frac{GM}{R^3}\begin{pmatrix}-1&0&0\\0&-1&0\\0&0&2\end{pmatrix}\begin{pmatrix}x\\y\\z\end{pmatrix} + \begin{pmatrix}f_x\\f_y\\f_z\end{pmatrix}\\
&= -n^2\begin{pmatrix}0\\0\\R\end{pmatrix} + n^2\begin{pmatrix}-x\\-y\\2z\end{pmatrix} + \begin{pmatrix}f_x\\f_y\\f_z\end{pmatrix}.
\end{aligned}$$

In the last step we used Kepler's third again, i.e. $n^2R^3 = GM$. Now inserting the linearized dynamics into (8.8) results in:

$$\boxed{\begin{array}{llll} \ddot{x} & + \; 2n\dot{z} & & = f_x \\ \ddot{y} & & + \; n^2 y & = f_y \\ \ddot{z} & - \; 2n\dot{x} & - \; 3n^2 z & = f_z \end{array}} \tag{8.10}$$

These are known as *Hill equations*. They describe satellite motion in a satellite frame that is co-rotating on a circular path at uniform speed n. Note that they are *approximated* equations of motion due to

- the linearization of ∇U on the circular orbit,
- constant radius approximation of the gravity gradient tensor $\nabla^2 U$.

From (8.10) it is obvious that the motion in the orbital plane (x, z) is coupled. The cross-track motion equation is that of a harmonic oscillator.

8.3. Solutions of the Hill equations

The key advantage of Hill equations (HE) is that they are linear ordinary differential equations with constant coefficients. That means that we will be able to find an analytical solution. Thus we can find an exact solution to approximated equations of motion. This is in contrast to the Lagrange Planetary Equations. They are exact equations of motions that need to be solved by linear approximation.

The HE are second order ODEs. For this type of equations the following strategy solution usually works:

i) Write the 3 second order equations as 6 first order equations. Actually, since the y-equation is decoupled one can setup two separate sets of first order equations.

ii) Write the set of equations as $\dot{\boldsymbol{u}} = \mathbf{A}\boldsymbol{u}$.

iii) Perform eigenvalue decomposition on $\mathbf{A} = \mathbf{Q}\boldsymbol{\Lambda}\mathbf{Q}^{-1}$.

iv) Transform $\dot{\boldsymbol{u}} = \mathbf{A}\boldsymbol{u}$ into $\mathbf{Q}^{-1}\dot{\boldsymbol{u}} = \boldsymbol{\Lambda}\mathbf{Q}^{-1}\boldsymbol{u}$ or simply $\dot{\boldsymbol{v}} = \boldsymbol{\Lambda}\boldsymbol{v}$.

v) Solve the decoupled equations by: $v_n = c_n e^{\lambda_n t}$ or in vector-matrix form: $\boldsymbol{v} = e^{\Lambda t}\boldsymbol{c}$.

vi) Transform back using the eigenvector matrix $\mathbf{Q}$: $\boldsymbol{u} = \mathbf{Q}\boldsymbol{v} = \mathbf{Q}e^{\Lambda t}\boldsymbol{c}$ or in index form $\boldsymbol{u} = \sum_n c_n e^{\lambda_n t}\boldsymbol{q}_n$.

The problem is: that doesn't work for the coupled in-plane equations. One can set up the 4×4 matrix $\mathbf{A}$:

$$\mathbf{A} = \begin{pmatrix} 0 & 0 & 1 & 0 \\ 0 & 0 & 0 & 1 \\ 0 & 0 & 0 & -2n \\ 0 & 3n^2 & 2n & 0 \end{pmatrix}$$

The characteristic polynomial of this matrix is:

$$\det(\mathbf{A} - \lambda \mathbf{I}) = \lambda^2(\lambda^2 + n^2) = 0\,.$$

This gives the 4 eigenvalues $\lambda_1 = in$, $\lambda_2 = -in$ and $\lambda_{3,4} = 0$. This is were the trouble starts. For the first two eigenvalues one can find eigenvectors. To the double zero-eigenvalue, however, one can only find a single eigenvector. In mathematical terms: the algebraic multiplicity (2 eigenvalues) is larger than the geometric multiplicity (1 eigenvalue).

For this type of pathological matrices there is a way out: the *Jordan*[6] *decomposition*. Where the eigenvalue decomposition achieves a full decoupling or diagonalization, the Jordan decomposition tries to decouple as much as possible. That usually involves putting the number 1 in the first (few) off-diagonals. In terms of solutions one can expect to see terms with $t\mathrm{e}^{\lambda_n t}$, $t^2\mathrm{e}^{\lambda_n t}$, etc. next to the usual $\mathrm{e}^{\lambda_n t}$. In our case, with $\lambda_{3,4} = 0$, we can therefore expect to see terms that are linear in time.

8.3.1. The homogeneous solution

We start with the homogeneous Hill equations, i.e. the non-perturbed equations:

$$\begin{aligned} \ddot{x} + 2n\dot{z} \qquad\quad &= 0 \\ \ddot{y} \qquad\qquad + n^2 y &= 0 \\ \ddot{z} - 2n\dot{x} - 3n^2 z &= 0 \end{aligned} \tag{8.11}$$

Their solution reads:

$$x(t) = \frac{2}{n}\dot{z}_0 \cos nt + \left(\frac{4}{n}\dot{x}_0 + 6z_0\right)\sin nt - (3\dot{x}_0 + 6nz_0)t + x_0 - \frac{2}{n}\dot{z}_0 \tag{8.12a}$$

$$y(t) = y_0 \cos nt + \frac{\dot{y}_0}{n}\sin nt \tag{8.12b}$$

$$z(t) = \left(-\frac{2}{n}\dot{x}_0 - 3z_0\right)\cos nt + \frac{\dot{z}_0}{n}\sin nt + \frac{2}{n}\dot{x}_0 + 4z_0 \tag{8.12c}$$

The solution mainly consists of periodic motion at the orbit frequency n. But indeed the x-component contains a term linear in t. Again, it is seen that x- and z-motion is coupled, whereas y behaves as a pure oscillator independent from the other terms.

[6] Marie Ennemond Camille Jordan (1838–1922), French mathematician.

The amplitudes of the sines and cosines as well as the constant terms and the drift are purely dependent on the initial state elements. Note that these initial state elements are given in the co-rotating satellite frame. Thus, the homogeneous solution (8.12a) can be used for initial state problems, e.g.:

- docking manoeuvres,
- Δv thrusts,
- configuration flight design.

The homogeneous response is visualized in fig. 8.2.

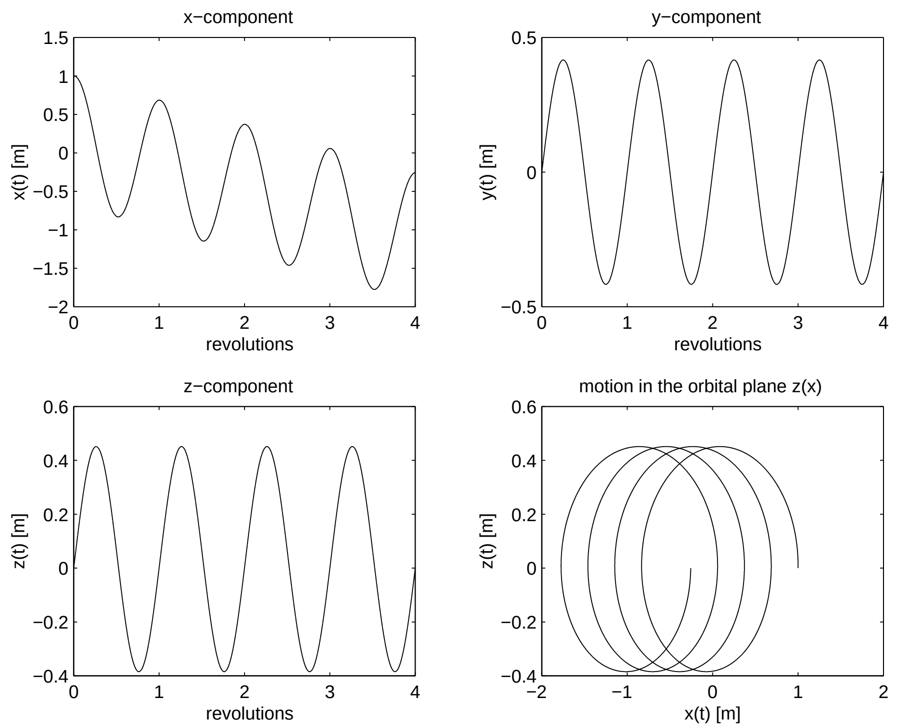

Figure 8.2.: Homogeneous solution.

8.3.2. The particular solution

Suppose the orbit is perturbed by a force that can be decomposed into a Fourier series. This is for instance the case with gravitational forces, cf. next chapter. Since the HE is a system of linear ODE's an forcing (the input) at a certain frequency will result in an orbit perturbation (the output) at the same frequency. Thus we only need to investigate the behaviour of the equations of motion at one specific disturbing frequency ω (not to be mistaken for rotation rate nor for argument of perigee). Then we can apply the superposition principle, or spectral synthesis, to achieve a full solution.

$$\begin{aligned} \ddot{x} + 2n\dot{z} \quad\quad\quad &= A_x \cos\omega t + B_x \sin\omega t \\ \ddot{y} \quad\quad + n^2 y &= A_y \cos\omega t + B_y \sin\omega t \\ \ddot{z} - 2n\dot{x} - 3n^2 z &= A_z \cos\omega t + B_z \sin\omega t \end{aligned} \tag{8.13}$$

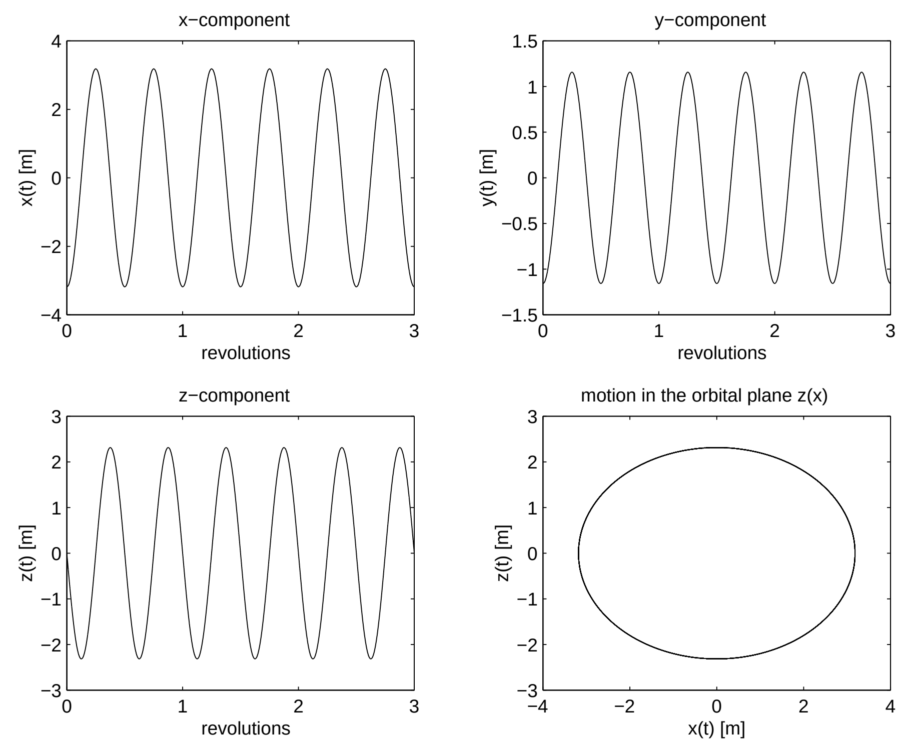

Figure 8.3.: Particular solution with disturbance at $\omega = 2n$.

The solution to (8.13) reads:

$$x(t) = \frac{(3n^2 + \omega^2)A_x + 2\omega n B_z}{\omega^2(n^2 - \omega^2)} \cos\omega t + \frac{(3n^2 + \omega^2)B_x - 2\omega n A_z}{\omega^2(n^2 - \omega^2)} \sin\omega t \tag{8.14a}$$

$$y(t) = \frac{A_y}{n^2 - \omega^2} \cos\omega t + \frac{B_y}{n^2 - \omega^2} \sin\omega t \tag{8.14b}$$

$$z(t) = \frac{\omega A_z - 2nB_x}{\omega(n^2 - \omega^2)} \cos\omega t + \frac{\omega B_z + 2nA_x}{\omega(n^2 - \omega^2)} \sin\omega t \tag{8.14c}$$

Again one can see that the two components in the orbital plane, x and z are coupled. Inspecting the denominators in the perturbation amplitudes, we notice a huge amplification close to the frequencies $\omega = 0$ and $\omega = \pm n$. This amplification is called *resonance*. The several resonances are visualized in fig. 8.4. It occurs if the satellite is excited at the zero frequency (DC) or a the orbital frequency itself. These are the eigenfrequencies of the system, that were already identified by the eigenvectors $-in$, 0, and in. For these frequencies the solution becomes invalid and we will seek another solution for resonant forcing later on.

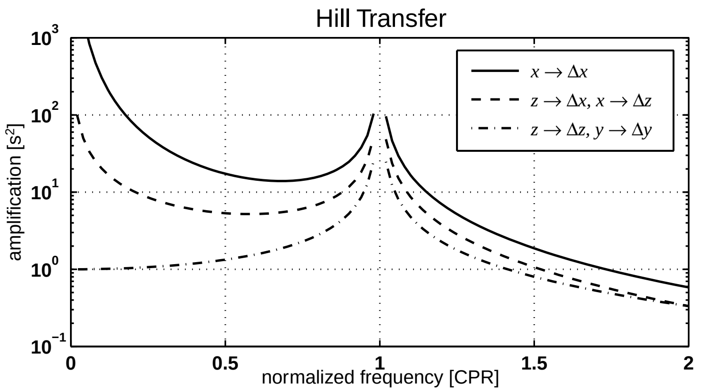

Figure 8.4.: Resonances of the Hill equations.

8.3.3. The complete solution

A complete solution will consist of a combination of particular and homogeneous solution. The homogeneous solution lies in the null space of the set of ODE. Thus one can always add the homogeneous solution (8.12a) without changing the right hand side of equations (8.13). The complete solutions reads:

$$\begin{aligned} x(t) = & \left(2\frac{\dot{z}_0}{n} - \frac{4A_x}{n^2-\omega^2} - \frac{2\omega B_x}{n(n^2-\omega^2)}\right)\cos nt \\ & + \left(6z_0 + 4\frac{\dot{x}_0}{n} + \frac{2A_z}{n^2-\omega^2} - \frac{4\omega B_x}{n(n^2-\omega^2)}\right)\sin nt \\ & + \frac{1}{\omega^2(n^2-\omega^2)}\left((3n^2+\omega^2)A_x + 2\omega n B_z\right)\cos\omega t \end{aligned}$$

$$
\begin{aligned}
&+\frac{1}{\omega^2(n^2-\omega^2)}\left((3n^2+\omega^2)B_x+2\omega nA_z\right)\sin\omega t \\
&+\left(-6nz_0-3\frac{B_x}{\omega}-3\dot{x}_0\right)t+x_0-3\frac{A_x}{\omega^2}-2\frac{B_z}{\omega n}-2\frac{\dot{z}_0}{n} \qquad (8.15a)
\end{aligned}
$$

$$
\begin{aligned}
y(t) &= \left(y_0-\frac{A_y}{n^2-\omega^2}\right)\cos nt+\left(\frac{\dot{y}_0}{n}-\frac{\omega B_y}{n(n^2-\omega^2)}\right)\sin nt \\
&+\frac{1}{n^2-\omega^2}\left(A_y\cos\omega t+B_y\sin\omega t\right) \qquad (8.15b)
\end{aligned}
$$

$$
\begin{aligned}
z(t) &= \left(-3z_0-2\frac{\dot{x}_0}{n}-\frac{A_z}{n^2-\omega^2}+\frac{2\omega B_x}{n(n^2-\omega^2)}\right)\cos nt \\
&+\left(\frac{\dot{z}_0}{n}-\frac{2A_x}{n^2-\omega^2}-\frac{\omega B_z}{n(n^2-\omega^2)}\right)\sin nt \\
&+\frac{1}{\omega(n^2-\omega^2)}\left(\omega A_z-2nB_x\right)\cos\omega t \\
&+\frac{1}{\omega(n^2-\omega^2)}\left(\omega B_z+2nA_x\right)\sin\omega t+4z_0+2\frac{B_x}{n\omega}+2\frac{\dot{x}_0}{n} \qquad (8.15c)
\end{aligned}
$$

As can be seen in the solution (8.15a) and in fig. 8.5 the complete solution is a superposition of two components: one at the orbital frequency n and one at the disturbing frequency ω.

8.3.4. The resonant solution

As mentioned before, the amplification for disturbances at $\omega \to -n, 0, +n$ becomes infinite. This is only a mathematical shortcoming of our solution so far. In order to investigate resonance, we have to assume a forcing at the resonant frequencies. The corresponding Hill equations read:

$$
\begin{array}{lllll}
\ddot{x} & + & 2n\dot{z} & & = A_x\cos nt+B_x\sin nt+C_x \\
\ddot{y} & & & +\, n^2y & = A_y\cos nt+B_y\sin nt+C_y \\
\ddot{z} & - & 2n\dot{x} & -\, 3n^2z & = A_z\cos nt+B_z\sin nt+C_z
\end{array} \qquad (8.16)
$$

These ODE are solved by:

$$
\begin{aligned}
x(t) &= \left(\frac{1}{n^2}(2n\dot{z}_0-4C_x+3A_x+2B_z)+\frac{1}{n}(-2B_x+A_z)t\right)\cos nt \\
&+\left(\frac{1}{n^2}(6n^2z_0+4n\dot{x}_0+5B_x+2C_z-A_z)+\frac{1}{n}(2A_x+B_z)t\right)\sin nt
\end{aligned}
$$

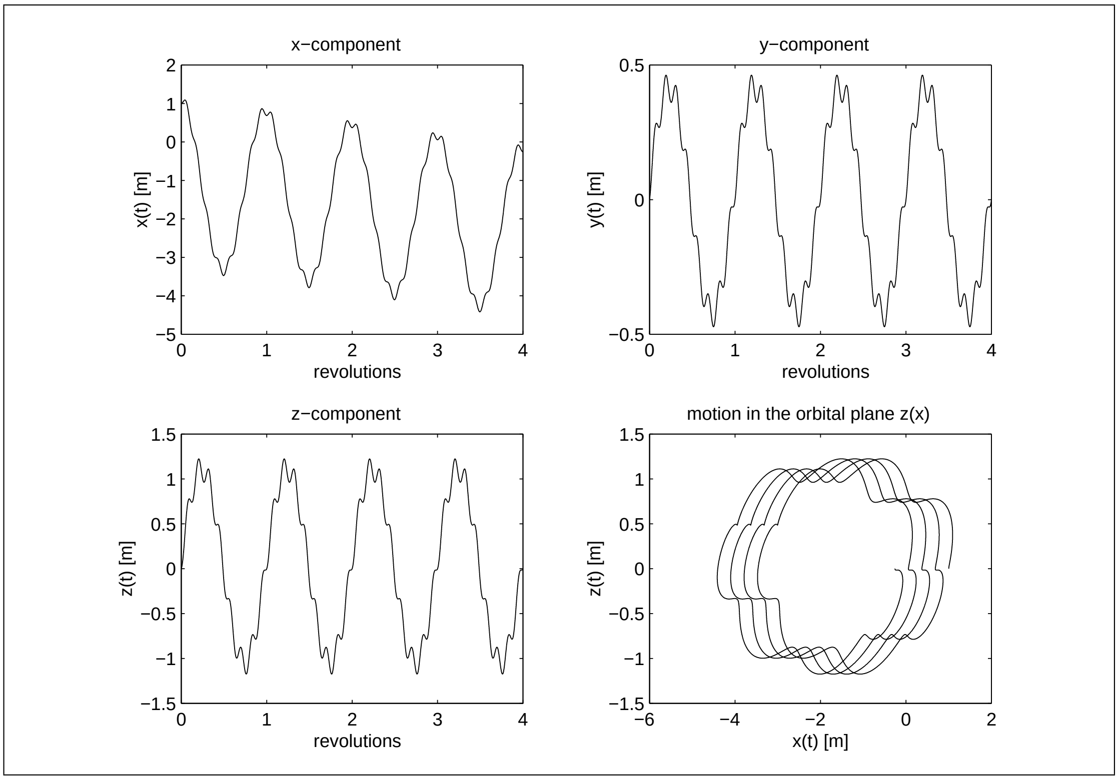

Figure 8.5.: Complete solution with arbitrary ω.

$$+\frac{1}{n^2}(n^2 x_0 - 2n\dot{z}_0 + 4C_x - 3A_x - 2B_z)$$

$$+\frac{1}{n}(-6n^2 z_0 - 3n\dot{x}_0 - B_x - 2C_z)t - \frac{3}{2}C_x t^2 \tag{8.17a}$$

$$y(t) = \left(y_0 - \frac{C_y}{n^2} - \frac{1}{2n}B_y t\right)\cos nt + \left(\frac{\dot{y}_0}{n} + \frac{B_y}{2n^2} + \frac{1}{2n}A_y t\right)\sin nt + \frac{1}{n^2}C_y \tag{8.17b}$$

$$z(t) = \left(\frac{1}{n^2}(-3n^2 z_0 - 2n\dot{x}_0 - 2B_x - C_z) - \frac{1}{2n}(2A_x + B_z)t\right)\cos nt$$

$$+\left(\frac{1}{2n^2}(2n\dot{z}_0 - 4C_x + 2A_x + B_z) + \frac{1}{2n}(-2B_x + A_z)t\right)\sin nt$$

$$+\frac{1}{n^2}(4n^2 z_0 + 2n\dot{x}_0 + 2B_x + C_z) + \frac{2}{n}C_x t \tag{8.17c}$$

This solution contains amplitudes that grow linearly in time, see also fig. 8.6. This is characteristic for resonance. In terms of Kepler elements, these growing amplitudes express secular orbit elements $\dot{\omega}, \dot{\Omega}, \dot{M}$.

The resonant equations are useful to investigate the behaviour of satellites under non-gravitational forces like air drag or solar radiation pressure.

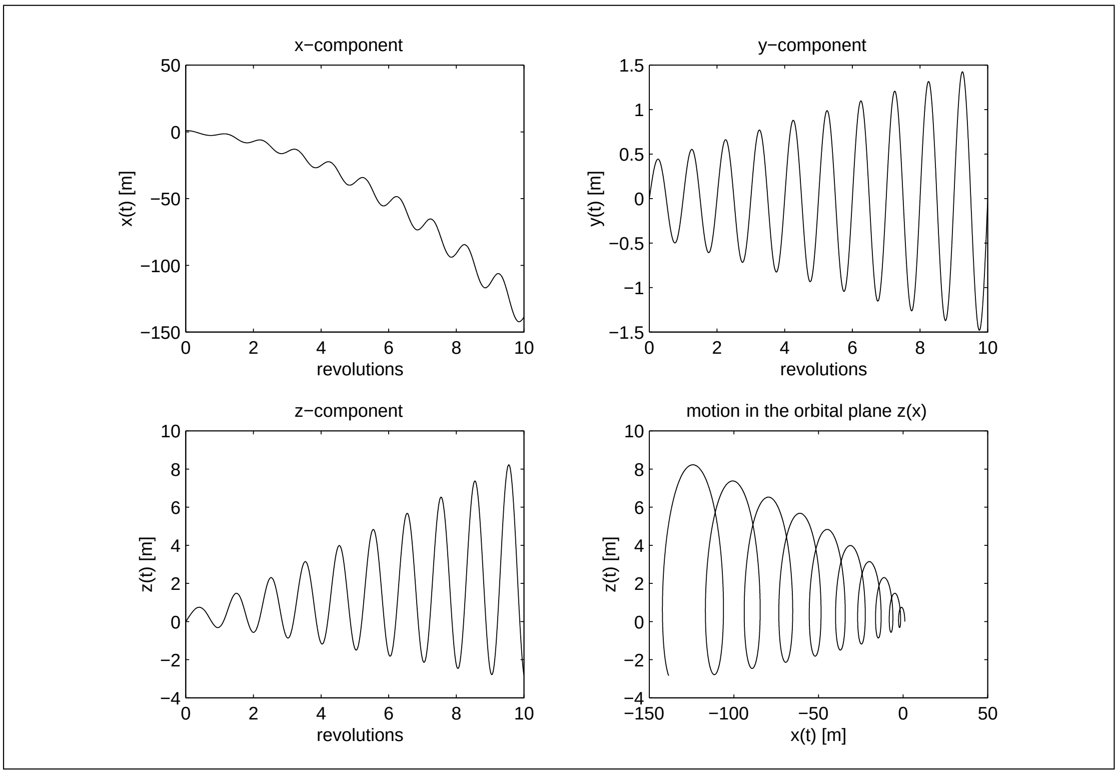

Figure 8.6.: Resonant solution.

A. Modeling CHAMP, GRACE and GOCE observables

A.1. The Jacobi integral

The vis-viva equation described the total energy of a Kepler orbit. For real satellite orbits in a real and rotating Earth gravity field, the total energy will not be constant. Nevertheless, a constant of the motion can be found: the so-called Jacobi integral. It can be used to determine the gravity potential, more specifically the disturbing potential, as soon as the orbit is given in terms of position and velocity (and disturbing forces).

The Jacobi integral is a constant of the motion in a rotating frame. Here we will use an extended version that includes dissipative forces. The derivation of the Jacobi integral starts from the equation of motion in a rotating frame, whose rotation is prescribed by the vector $\boldsymbol{\omega}$. The kinematics in a rotating frame were derived in 8.1 in order to obtain the Hill equations of motion. In the following discussion, however, $\boldsymbol{\omega}$ denotes the Earth's rotation vector, which is assumed to be constant in direction and rate: $\omega = (0\ 0\ \omega_{\mathrm{E}})^{\mathsf{T}}$.

$$\ddot{\boldsymbol{r}} = \boldsymbol{f} + \boldsymbol{g} - \boldsymbol{\omega} \times (\boldsymbol{\omega} \times \boldsymbol{r}) - 2\boldsymbol{\omega} \times \dot{\boldsymbol{r}} - \dot{\boldsymbol{\omega}} \times \boldsymbol{r}\,, \tag{A.1a}$$

in which we have, at the right hand side, the dissipative force (per unit mass) $\boldsymbol{f}$, gravitational attraction $\boldsymbol{g}$, centrifugal, Coriolis and Euler acceleration, respectively. The gravitational attraction and the centrifugal acceleration are both conservative vector fields and can therefore be written as the gradient of the gravitational potential V and the centrifugal potential $Z = \frac{1}{2}\omega^2(x^2 + y^2)$, respectively. The vectors $\boldsymbol{r}$, $\dot{\boldsymbol{r}}$ and $\ddot{\boldsymbol{r}}$ are positions, velocities and accelerations in the rotating frame. The Earth rotation $\boldsymbol{\omega}$ is assumed to be constant, such that the Euler term cancels. Thus (A.1a) reduces to:

$$\ddot{\boldsymbol{r}} = \boldsymbol{f} + \nabla V + \nabla Z - 2\boldsymbol{\omega} \times \dot{\boldsymbol{r}} \tag{A.1b}$$

In 2.3 Newton's equation of motion was premultiplied by $\dot{\boldsymbol{r}} \cdot \ldots$ in order to establish energy conservation in the Kepler problem. We will now apply the same trick to (A.1a) in order to derive the Jacobi integral. Multiplying by the velocity $\dot{\boldsymbol{r}}$ the part with the Coriolis acceleration will drop out:

$$\dot{\boldsymbol{r}} \cdot \ddot{\boldsymbol{r}} = \dot{\boldsymbol{r}} \cdot \boldsymbol{f} + \dot{\boldsymbol{r}} \cdot (\nabla V + \nabla Z) - 2\dot{\boldsymbol{r}} \cdot (\boldsymbol{\omega} \times \dot{\boldsymbol{r}}) \tag{A.2}$$

$$= \dot{\boldsymbol{r}} \cdot \boldsymbol{f} + \frac{\mathrm{d}(V+Z)}{\mathrm{d}t} - \frac{\partial(V+Z)}{\partial t}$$

The latter step is due to the fact that the total time derivative of a potential is written as:

$$\frac{\mathrm{d}\Phi}{\mathrm{d}t} = \frac{\partial \Phi}{\partial \boldsymbol{r}} \cdot \frac{\mathrm{d}\boldsymbol{r}}{\mathrm{d}t} + \frac{\partial \Phi}{\partial t} = \dot{\boldsymbol{r}} \cdot \nabla\Phi + \frac{\partial \Phi}{\partial t} \ .$$

Because of the constant $\boldsymbol{\omega}$ the centrifugal potential has no explicit time derivative $\partial Z/\partial t$. Thus, upon integration, we are left with:

$$\int \dot{\boldsymbol{r}} \cdot \ddot{\boldsymbol{r}} \,\mathrm{d}t = \int \left(\dot{\boldsymbol{r}} \cdot \boldsymbol{f} - \frac{\partial V}{\partial t} \right) \mathrm{d}t + V + Z + c \ .$$

The integration constant c is called *Jacobi constant*. The left hand side is the kinetic energy (per unit mass) $\frac{1}{2}\dot{\boldsymbol{r}} \cdot \dot{\boldsymbol{r}}$. The gravitational potential is split up in a normal (gravitational) part and a disturbance: $V = U + T$. Rearrangement gives:

$$T + c = E_{\mathrm{kin}} - U - Z - \int \boldsymbol{f} \cdot \mathrm{d}\boldsymbol{r} - \int \frac{\partial V}{\partial t} \,\mathrm{d}t \tag{A.3}$$

Equation (A.3) is the basis for gravity field determination using the energy balance approach. At the left we have the unknown disturbing potential, up till an unknown constant. All terms at the right are determined from CHAMP data or existing models:

- E_{kin} requires orbit velocities $\dot{\boldsymbol{r}}$,
- U, the normal gravitational potential, requires satellite positions $\boldsymbol{r}$,
- Z, the centrifugal potential at the satellite's location is also calculated from $\boldsymbol{r}$,
- $\int \boldsymbol{f} \cdot \mathrm{d}\boldsymbol{r}$ is the dissipated energy, which is an integral of CHAMP's accelerometer data $\boldsymbol{f}$ along the orbit,
- $\int \partial_t V \,\mathrm{d}t$ is the integral along the orbit of the gradient of time-variable potentials. It contains known sources (tides, 3$^{\mathrm{rd}}$ bodies), that can be corrected in (A.3), and unknown gravity field changes.

A.2. Range, range rate and range acceleration

Whereas 8.1 described kinematics in a moving frame, we will now be concerned with the relative kinematics of a baseline between two satellites. We will discuss the intersatellite *range* and its first and second time derivative *range rate* and *range acceleration*. At the same time we will see how the baseline direction changes.

The baseline vector between two satellites is $\boldsymbol{\rho}_{12} = \boldsymbol{r}_2 - \boldsymbol{r}_1$. The normalized baseline vector then becomes:

$$\boldsymbol{e}_{12} = \frac{\boldsymbol{\rho}_{12}}{\|\boldsymbol{\rho}_{12}\|} = \frac{\boldsymbol{\rho}_{12}}{\rho_{12}} \ .$$

Remark A.1 (notation) *The quantities with indices 1 and 2 indicate* differences *between satellite 1 and 2. If it is clear from the context, the indices are dropped.*

range

The vectorial baseline is the scalar range times the unit vector in the direction of the baseline.

$$\boldsymbol{\rho} = \rho\hat{\mathbf{e}} \quad \Longrightarrow \quad \rho = \boldsymbol{\rho} \cdot \hat{\mathbf{e}} \tag{A.4}$$

baseline

The baseline direction $\hat{\boldsymbol{e}} = \boldsymbol{\rho}/\rho$ is a unit vector:

$$\hat{\boldsymbol{e}} \cdot \hat{\boldsymbol{e}} = 1 \quad \Longrightarrow \quad \hat{\boldsymbol{e}} \cdot \dot{\hat{\boldsymbol{e}}} = 0\,.$$

Hence, the time derivative $\dot{\hat{\boldsymbol{e}}}$ of the baseline vector is perpendicular to the baseline itself. The vector $\dot{\hat{\boldsymbol{e}}}$ itself is not a unit vector.

range rate

The scalar range rate $\dot{\rho}$ is *not* the length of the relative velocity vector $\dot{\boldsymbol{\rho}}$. Instead it is the projection of the relative velocity onto the baseline.

$$\dot{\boldsymbol{\rho}} = \dot{\rho}\hat{\mathbf{e}} + \rho\dot{\hat{\mathbf{e}}} \quad \Longrightarrow \quad \dot{\boldsymbol{\rho}} \cdot \hat{\mathbf{e}} = \dot{\rho}\underbrace{\hat{\mathbf{e}} \cdot \hat{\mathbf{e}}}_{1} + \rho\underbrace{\dot{\hat{\mathbf{e}}} \cdot \hat{\mathbf{e}}}_{0} \quad \Longrightarrow \quad \dot{\rho} = \dot{\boldsymbol{\rho}} \cdot \hat{\mathbf{e}}\,. \tag{A.5}$$

An elementary way of writing this is: $\boldsymbol{\rho} \cdot \dot{\boldsymbol{\rho}} = \rho\dot{\rho}$.

baseline (again)

The above shows that the vector $\dot{\hat{\boldsymbol{e}}} = \frac{1}{\rho}(\dot{\boldsymbol{\rho}} - \dot{\rho}\hat{\boldsymbol{e}})$ is obtained by subtracting the projection of $\dot{\boldsymbol{\rho}}$ onto $\hat{\boldsymbol{e}}$ from the relative velocity vector $\dot{\boldsymbol{\rho}}$ itself. The result will indeed be perpendicular to $\hat{\boldsymbol{e}}$. This is nicely visualized in fig. A.1. The perpendicular component of the relative velocity is called $\boldsymbol{c}$, for cross-track, defined as:

$$\boldsymbol{c} = \dot{\boldsymbol{\rho}} - \dot{\rho}\hat{\mathbf{e}} = \rho\dot{\hat{\mathbf{e}}}\,.$$

range acceleration

A further time differentiation yields

$$\begin{aligned} \ddot{\rho} &= \ddot{\boldsymbol{\rho}} \cdot \hat{\mathbf{e}} + \dot{\boldsymbol{\rho}} \cdot \dot{\hat{\mathbf{e}}} \;=\; \ddot{\boldsymbol{\rho}} \cdot \hat{\mathbf{e}} + \dot{\boldsymbol{\rho}} \cdot \frac{1}{\rho}(\dot{\boldsymbol{\rho}} - \dot{\rho}\hat{\mathbf{e}}) \\ \Longrightarrow \ddot{\rho} &= \ddot{\boldsymbol{\rho}} \cdot \hat{\mathbf{e}} + \frac{1}{\rho}\left(\dot{\boldsymbol{\rho}} \cdot \dot{\boldsymbol{\rho}} - \dot{\rho}^2\right)\,. \end{aligned} \tag{A.6}$$

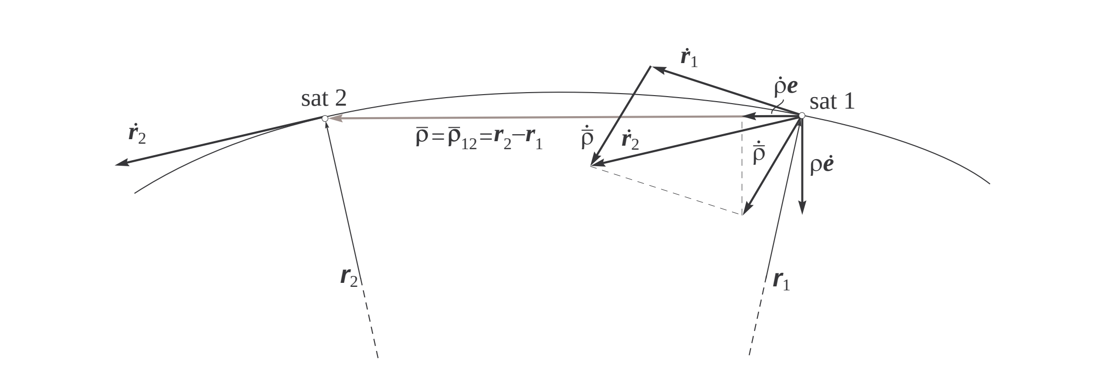

Figure A.1.: Position difference $\boldsymbol{\rho}$, range ρ, differential velocity $\dot{\boldsymbol{\rho}}$ and range rate $\dot{\rho}$.

Using the perpendicular vector $\boldsymbol{c}$ again, this is summarized into

$$\ddot{\rho} = \ddot{\boldsymbol{\rho}} \cdot \hat{\boldsymbol{e}} + \frac{1}{\rho}\boldsymbol{c} \cdot \boldsymbol{c}\,.$$

A.3. Spaceborne gravimetry

Inserting Newton's equations of motion—in differential mode—into the above range acceleration yields the basic SST equation for differential gravimetry

$$\begin{aligned} \ddot{\boldsymbol{r}}_2 - \ddot{\boldsymbol{r}}_1 &= \nabla V_2 - \nabla V_1 \\ \Longrightarrow\ \ddot{\boldsymbol{\rho}}_{12} &= \nabla V_{12} \\ \Longrightarrow\ \ddot{\rho} &= \nabla V_{12} \cdot \hat{\boldsymbol{e}} + \frac{1}{\rho}\left(\dot{\boldsymbol{\rho}} \cdot \dot{\boldsymbol{\rho}} - \dot{\rho}^2\right)\,. \end{aligned}$$

The observable range acceleration $\ddot{\rho}$, corrected for perpendicular velocity terms, equals the projection of the gradient difference onto the baseline. For low-low SST like GRACE the main problem is the size of the perpendicular velocity correction. It is larger than the range acceleration by orders of magnitude. It represents the (differential) centrifugal acceleration, projected onto the baseline.

But apart from numerical complications, the above formula demonstrates that in principle a GRACE-type observable can be considered as *spaceborne gravimetry*. Terrestrial gravimetry determines the length of the gravity vector, which is the projection of the gravity vector along the *plumb line*: $g = \boldsymbol{g} \cdot \boldsymbol{e}_r = \nabla V \cdot \boldsymbol{e}_r$. In spaceborne gravimetry we have something similar, although in differential mode: the projection of the gravity difference onto the baseline.

Lotlinie

A.4. GRACE-type gradiometry

The right hand side of the above equation was the difference of a gradient. When we divide this by the baseline length we obtain a gradient of a gradient, at least in linear approximation. Thus the range accelerometry can be interpreted as gravity gradiometry. Denoting the gravitational gradient tensor as $\boldsymbol{V}$, one obtains:

$$\frac{1}{\rho}\ddot{\rho} = \boldsymbol{e}^{\mathrm{T}}\boldsymbol{V}\boldsymbol{e} + \frac{1}{\rho^2}\left(\dot{\boldsymbol{\rho}}\cdot\dot{\boldsymbol{\rho}} - \dot{\rho}^2\right) + \text{lin.error}\,.$$

By using a priori gravity field information the linearization error can be controlled, depending on maximum degree, baseline length and accuracy requirement.

In the gravity gradiometry literature, the observable tensor is usually expressed as:

$$\boldsymbol{\Gamma} = \boldsymbol{V} + \boldsymbol{\Omega}^2 + \dot{\boldsymbol{\Omega}}\,,$$

with the latter two terms representing centrifugal and Euler acceleration differences. If we adopt a Hill frame (x quasi along-track, y cross-track and z radial) the range acceleration observable becomes along-track gradiometry:

$$\frac{1}{\rho}\ddot{\rho} = V_{xx} - (\omega_y^2 + \omega_z^2) + \text{lin.error}\,.$$

This shows again that the velocity correction terms represent the differential centrifugal acceleration:

$$\frac{1}{\rho^2}(\boldsymbol{c}\cdot\boldsymbol{c}) = -(\omega_y^2 + \omega_z^2)\,.$$

For a LEO leader-follower configuration the nominal values of these terms are:

$$\begin{aligned}\omega_y &= 1\,\text{CPR} = 0.18\,\text{mHz}\\ \omega_z &= 0\end{aligned}$$

Note that the centrifugal terms are independent of baseline length.

A.5. GOCE gradiometry

Today, the information about the global gravity field is mainly derived from positions and velocities of satellites or the inter-satellite measurements like ranges or range-rates. Satellite gravity gradiometry enables the direct observation of field quantities in space.

GOCE (Gravity field and steady-state Ocean Circulation Explorer) was the first space mission with an onboard satellite gravity gradiometer (SGG). This instrument consist of six accelerometers, which are located equidistantly to the satellite's center of mass on three orthogonal axis. The different locations leads to slightly different accelerations due to gravity. By measuring the differential accelerations, a tensor of the second derivatives of the gravitational potential is approximated.

B. Coordinate Systems in Satellite Geodesy

B.1. Coordinate systems

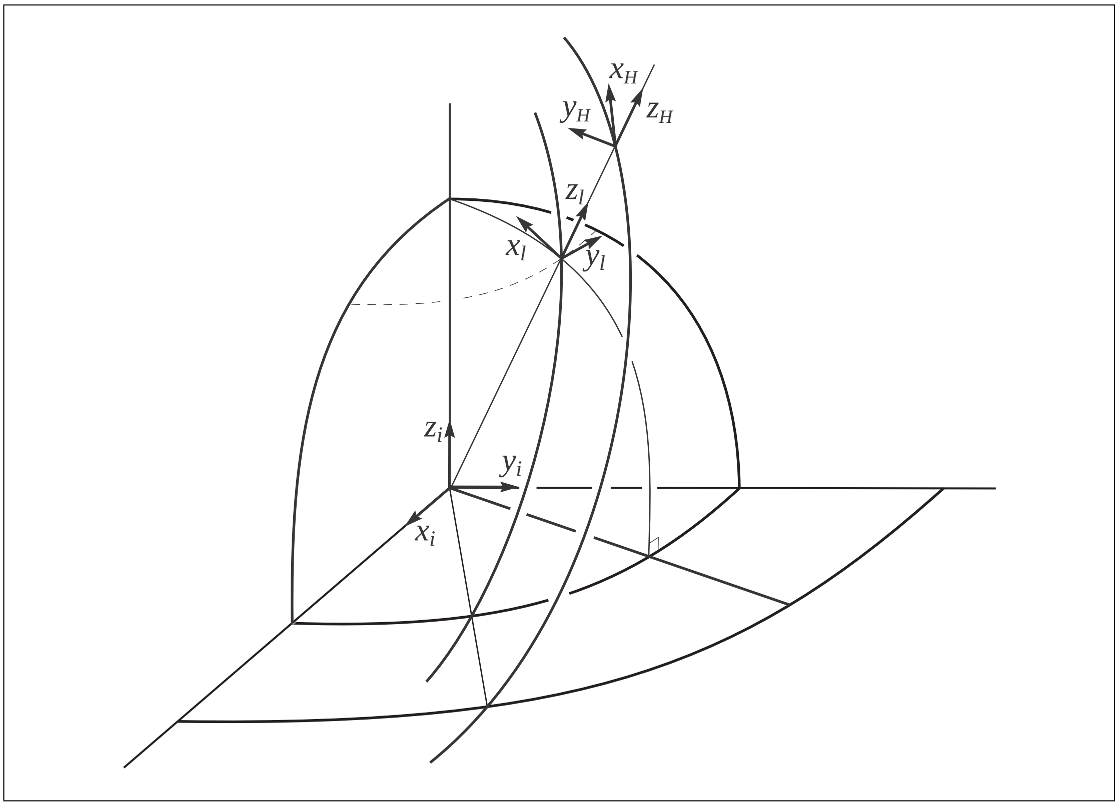

Figure B.1.: Coordinate systems in satellite geodesy.

Several coordinate systems are used in satellite geodesy:

$\{\hat{e}_i\}$ **inertial system** Inertialsystem

Newton's laws of physics hold only in inertial systems. In these systems, the directions towards stars and the angles of the Kepler orbit are defined. Also the numerical orbit integration is usually performed in an inertial system.

Several inertial systems are in use, which might be classified w.r.t to the center (geocentric vs. barycenter of the solar system) or their plane $z = 0$ (equatorial plane vs. plane of ecliptic).

For satellites around the Earth, we prefer a geocentric system with the equatorial plane:

- $\hat{\boldsymbol{e}}_{i=1}$ and $\hat{\boldsymbol{e}}_{i=2}$ span the equatorial plane,
- $\hat{\boldsymbol{e}}_{i=1}$ points towards the vernal equinox ♈,
- $\hat{\boldsymbol{e}}_{i=3}$ points to the celestial pol,
- $\mathbf{0}$ in the geocenter.

More precisely, we might further distinguish between *mean inertial reference system at epoch* T_0 (effect of precession), a *mean instantaneous reference system at epoch* T_0 (effect of nutation) and a *true instantaneous reference system*.

Erdfestes System

$\{\hat{\boldsymbol{e}}_e\}$ **Earth-fixed system**

The gravity field of the Earth is an important source of orbit perturbations and also a research goal of satellite geodesy. The field is related to the mass distributions within the Earth and shall be described in Earth-related coordinates. The difference between the geocentric inertial system and an Earth-fixed system is the rotation of the Earth, in particular around the angle GAST

- $\hat{\boldsymbol{e}}_{e=1}$ and $\hat{\boldsymbol{e}}_{e=2}$ span the equatorial plane,
- $\hat{\boldsymbol{e}}_{e=1}$ points towards intersection of equatorial plane and a chosen meridian (e.g. Greenwich meridian),
- $\hat{\boldsymbol{e}}_{e=3}$ points towards North pole ,
- $\mathbf{0}$ in the geocenter.

In a more precise model, also the polar motion must be considered.

$\{\hat{\boldsymbol{e}}_l\}$ **Local North Oriented System**

The local North oriented system is an Earth fixed system in a chosen location, e.g. a ground station. The axis are defined in a tangential plane (w.r.t. sphere or ellipsoid):

- $\hat{\boldsymbol{e}}_{l=1}$: North direction, defined by North-South tangent to meridian,
- $\hat{\boldsymbol{e}}_{l=2}$: East direction defined by East-West tangent to parallel circle,
- $\hat{\boldsymbol{e}}_{l=3}$: up direction (normal to sphere or ellipsoid),

Please note, that the North-East-Up (NEU) system is a left-handed system.

$\{\hat{e}_H\}$ **Hill-system**
The Hill-system is introduced as a satellite based system, in which a linearized equation of motion can be solved in closed formulas. The system rotates with a constant angular rate and it is pointing to a nominal orbit close to the current satellite position.

- $\hat{\boldsymbol{e}}_{H=1}$ complementary quasi-along track,
- $\hat{\boldsymbol{e}}_{H=2}$: direction of $\boldsymbol{L}$,
- $\hat{\boldsymbol{e}}_{H=3}$: radial direction.

$\{\hat{e}_t\}$ **tangential (satellite) system**
Orbit perturbations which are acting in flight direction are modeled in a tangential frame for simplicity.

- $\hat{\boldsymbol{e}}_{t=1}$: along track, direction of $\boldsymbol{v}$
- $\hat{\boldsymbol{e}}_{t=2}$: direction of $\boldsymbol{L}$,
- $\hat{\boldsymbol{e}}_{t=3}$: quasi radial direction.

In the following, we ignore the different centers of the systems and also the correction for precession, nutation and polar motion. Hence, the transformation between two systems are only rotations and reflections.

B.2. Transformation between systems

A vector in the inertial system is transformed into its Earth-fixed counter part by the rotation around the angle GAST

$$\boldsymbol{r}_e = \mathbf{R}_3(\text{GAST})\boldsymbol{r}_i, \tag{B.1}$$

if we ignore nutation, precession and polar motion. A transformation into the local North oriented system requires a rotation towards the location (λ, ϕ) and a reflection of the x-axis by a permutation matrix $\mathbf{S}_1$ to consider the left handed system:

$$\boldsymbol{r}_l = \mathbf{S}_1\mathbf{R}_2\left(\frac{\pi}{2} - \phi\right)\mathbf{R}_3(\lambda)\boldsymbol{r}_e = \mathbf{S}_1\mathbf{R}_2\left(\frac{\pi}{2} - \phi\right)\mathbf{R}_3(\lambda + \text{GAST})\boldsymbol{r}_i. \tag{B.2}$$

The rotations between the inertial system and the Hill system were already discussed in Section 8.2:

$$\boldsymbol{r}_H = \mathbf{R}_3(nt)\mathbf{R}_3(\omega)\mathbf{R}_1(I)\mathbf{R}_3(\Omega)\boldsymbol{r}_i = \mathbf{R}_3(u)\mathbf{R}_1(I)\mathbf{R}_3(\Omega)\boldsymbol{r}_i \tag{B.3}$$

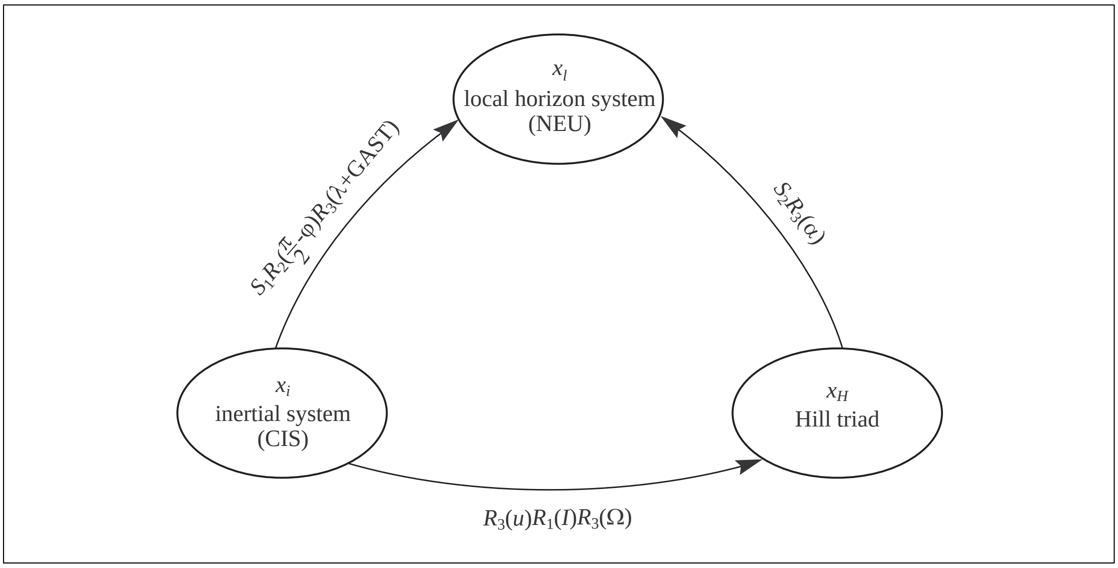

Figure B.2.: Relation between CIS, NEU and Hill-system.

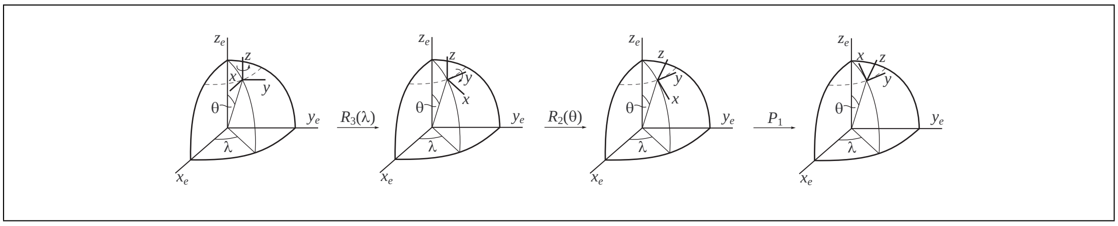

Figure B.3.: Transformation of the global Earth-fixed system into the local North oriented system.

where n is the mean motion of the nominal orbit. If the satellite is identified with the coordinate system, we can set $u = nt + \omega$ here.

The $\hat{\boldsymbol{e}}_{H=3}$-axis of the Hill-system and the $\hat{\boldsymbol{e}}_{l=3}$-axis of the local North oriented system are parallel. The first system is right-handed, while the second one is left-handed. Hence, the transformation is a rotation around the common z-axis with an angle α and another permutation to reflect the second axis:

$$\boldsymbol{r}_l = \mathbf{S}_2\mathbf{R}_3(\alpha)\boldsymbol{r}_H \,. \tag{B.4}$$

The angle α will be discussed in the following section.

The tangential satellite system is almost identical will the Hill-system, with a rotation around the y-axis

$$\boldsymbol{r}_t = \mathbf{R}_2(\kappa)\boldsymbol{r}_H \tag{B.5}$$

with $\tan\kappa = \frac{e\sin\nu}{1+e\cos\nu}$.

In many cases, there is one coordinate system, where the disturbing force or the equation of motion are relative simple to represent. However, a transformation into a common system might be necessary for the analysis or the orbit integration. With this chain of rotations (and reflections), we can now transform any disturbing force of satellite geodesy in all standard coordinate systems.

Interpretation of the angle α

We find the angle α in the fundamental triangle in the inertial system, which is formed by the meridian through the location (λ, ϕ), the equator, and the circular orbit passing the same location.

In this spherical triangle with a right angle, we know the angles u, ϕ and the angle I. Hence, we can calculate

$$\frac{\sin u}{\sin 90°} = \frac{\sin\phi}{\sin I}$$
$$\Longrightarrow \sin\phi = \sin I \sin u\,.$$

Remark B.1 *Please note, that the angle α is defined in a spherical triangle and in the inertial system! The corresponding intersection angle between the ground track and the meridian in a map projection changes its value due to the rotation of the Earth during the satellite's revolution.*

Exercise B.1 *Define a circular orbit and investigate the chain of rotations*

$$\mathbf{S}_1\mathbf{R}_2\left(\frac{\pi}{2}-\phi\right)\mathbf{R}_3(\lambda+\textsc{gast}) \overset{!}{=} \mathbf{S}_2\mathbf{R}_3\mathbf{R}_3(u)\mathbf{R}_1(I)\mathbf{R}_3(\Omega)$$

numerically.

B.3. Gradient

If a conservative vector field is described by its potential, then the acceleration is calculated by the gradient operator acting on the field. A gradient operator can be derived for any coordinate system.

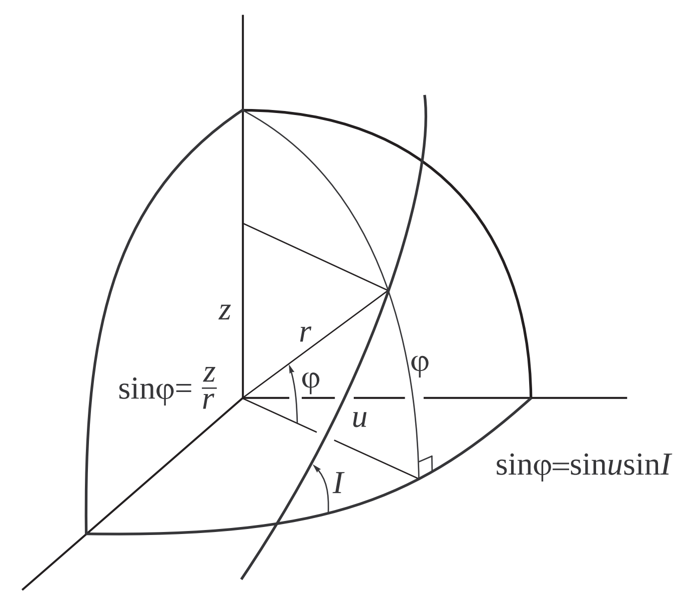

Figure B.4.: fundamental triangle

In Cartesian coordinates the gradient of a field quantity $f(x_i, y_i, z_i)$ is simply the vector of the partial derivatives: $\nabla_i f(x_i, y_i, z_i) = (\frac{\partial f}{\partial x_i}, \frac{\partial f}{\partial y_i}, \frac{\partial f}{\partial z_i})$, when we assume a inertial system.

In satellite geodesy we might want express the gradient in terms of Earth-fixed spherical coordinate or terms of Kepler elements:

$$\nabla_i = \begin{pmatrix} \frac{\partial}{\partial x_i} \\ \frac{\partial}{\partial y_i} \\ \frac{\partial}{\partial z_i} \end{pmatrix}, \qquad \nabla_l = \begin{pmatrix} \frac{\partial}{r \partial \phi} \\ \frac{\partial}{r \cos\phi \partial \lambda} \\ \frac{\partial}{\partial r} \end{pmatrix}, \qquad \nabla_H \approx \begin{pmatrix} \frac{\partial}{r \partial u} \\ \frac{\partial}{r \cos\phi \partial I} \\ \frac{\partial}{\partial r} \end{pmatrix} \tag{B.6}$$

C. Numerical integration

Newton's equation of motion $\ddot{\boldsymbol{r}} = \boldsymbol{f}(\boldsymbol{r}, \dot{\boldsymbol{r}}, ...)$ is an ordinary differential equation (ODE) of second order. In many cases, these equations cannot be solved by closed formulas, as the equations are non-linear or coupled. Hence, numerical methods are applied to approximate the solution of the ODEs.

Every linear or explicit ODE $\boldsymbol{y}'' = \boldsymbol{f}(\boldsymbol{y}, \boldsymbol{y}', ...)$ — with initial values — can be traced back to a system of first order:

$$\boldsymbol{y}' = \boldsymbol{F}(x, \boldsymbol{y}) \tag{C.1}$$

$$\boldsymbol{y}(x_0) = \boldsymbol{y}_0. \tag{C.2}$$

The initial value problem can be solved by numerical methods. The result will be a set of discrete points $(\tilde{x}_\ell, \tilde{\boldsymbol{u}}_\ell)$ with $\ell = 0, 1, 2, ..., L$ instead of the continuous function $\boldsymbol{y}(x)$. For "well-behaved problems" the set can approximate the real solution $\tilde{\boldsymbol{u}}_\ell \approx \boldsymbol{y}(\tilde{x}_\ell)$.

Exercise C.1 *Re-write the Euler-Cauchy differential equation $16t^2\ddot{y} + 8t\dot{y} + y = 0$ into a system of first order.*

We isolate the highest derivative:

$$16t^2\ddot{y} + 8t\dot{y} + y = 0 \Rightarrow \ddot{y} = -\frac{1}{2t}\dot{y} - \frac{1}{16t^2}y$$

and introduce new variables $v = y$ and $w = \dot{v}$. This provides

$$\begin{aligned} \frac{\mathrm{d}v}{\mathrm{d}t} &= w \\ \frac{\mathrm{d}w}{\mathrm{d}t} &= -\frac{1}{2t}w - \frac{1}{16t^2}v \end{aligned}$$

or in matrix vector form:

$$\underbrace{\begin{pmatrix} \dot{v} \\ \dot{w} \end{pmatrix}}_{\dot{\boldsymbol{y}}(t)} = \begin{pmatrix} 0 & 1 \\ \frac{-1}{16t^2} & \frac{-1}{2t} \end{pmatrix} \underbrace{\begin{pmatrix} v \\ w \end{pmatrix}}_{\boldsymbol{y}(t)}. \tag{C.3}$$

Remark C.1 *A strict matrix vector form is only possible for linear ODEs.*

An initial value problem is equivalent to the integral equation

$$\boldsymbol{y} = \boldsymbol{y}_0 + \int_{x_0}^{x} \boldsymbol{F}(x, \boldsymbol{y}(\xi))\,\mathrm{d}\xi\,. \tag{C.4}$$

Many numerical methods have been derived for different types of problems. They can be ordered by the following aspects:

- fixed/adaptive stepwidth h,
- one-step or multistep methods,
- implicit/explicit methods.

In the following, we sketch only one-step methods, where the value $\boldsymbol{u}_\ell$ is calculated from $\boldsymbol{u}_{\ell-1}$ and with a fixed stepwidth h.

Remark C.2 *Please note, that all internal methods of* MATLAB *like* `ode45` *and* `ode113` *use adaptive stepwidth. If a fixed stepwidth is entered in the function call, this is only considered by interpolation, not in the algorithm.*

C.1. Methods of Euler

C.1.1. Explicit Euler method (Euler polygon)

1. First we re-write the differential equations into a system of first order $\boldsymbol{F}(t, \boldsymbol{y})$ by introducing new variables.
2. We replace the $\boldsymbol{y}$ by its discrete counterpart $\boldsymbol{u}_\ell$ to distinguish the solutions.
3. A stepwidth h is selected or defined by the question.
4. a) Replacing the derivatives by "forward differences" leads to

$$\boldsymbol{u}'_{\ell-1} = \boldsymbol{F}(x_{\ell-1}, \boldsymbol{u}_{\ell-1}) \approx \frac{\boldsymbol{u}_\ell - \boldsymbol{u}_{\ell-1}}{h} + \mathcal{O}(h) \tag{C.5}$$

$$\Rightarrow \boldsymbol{u}_\ell = \boldsymbol{u}_{\ell-1} + h\boldsymbol{F}(x_{\ell-1}, \boldsymbol{u}_{\ell-1}) \qquad \ell = 1, 2, ..., L\,. \tag{C.6}$$

Together with $\boldsymbol{y}(x_0) = \boldsymbol{u}_0$, this provides a simple approximation of the solution by an explicit Euler polygon. The method is "explicit", because the formula is already solved for the new value $\boldsymbol{u}_\ell$ on the left.

Exercise C.2 *Approximate a solution of the ODE*

$$\dot{y}(t) = y - y^2 \qquad \& \quad y(0) = 0.5$$

by the explicit Euler method and with a stepwidth $h = 0.4$.

The differential equation is of first order and in one variable, so the re-writing is not necessary. For consistency we not down $\boldsymbol{F}(t_{\ell-1}, \boldsymbol{u}_{\ell-1}) = \boldsymbol{u}_{\ell-1} - \boldsymbol{u}_{\ell-1}^2$ with $\boldsymbol{u}_0 = 0.5$.

The first steps of the forward Euler method (polygon) provide

$$\begin{aligned}
\boldsymbol{u}_1 &= \boldsymbol{u}_0 + h\boldsymbol{F}(t_0, \boldsymbol{u}_0) = 0.5 + 0.4(0.5 - 0.5^2) = 0.60 \\
\boldsymbol{u}_2 &= \boldsymbol{u}_1 + h\boldsymbol{F}(t_1, \boldsymbol{u}_1) = 0.6 + 0.4(0.6 - 0.6^2) = 0.69 \\
\boldsymbol{u}_3 &= \boldsymbol{u}_2 + h\boldsymbol{F}(t_2, \boldsymbol{u}_2) = 0.69 + 0.4(0.69 - 0.69^2) \approx 0.7807
\end{aligned}$$

C.1.2. Backward Euler method

1. – 3. Analogously to the forward Euler method
4. b) Replacing the derivatives by "backward differences" leads to

$$\boldsymbol{u}'_\ell = \boldsymbol{F}(x_{\ell-1}, \boldsymbol{u}_{\ell-1}) \approx \frac{\boldsymbol{u}_\ell - \boldsymbol{u}_{\ell-1}}{h} + \mathcal{O}(h) \tag{C.7}$$

$$\Rightarrow \boldsymbol{u}_\ell = \boldsymbol{u}_{\ell-1} + h\boldsymbol{F}(x_\ell, \boldsymbol{u}_\ell) \qquad \ell = 1, 2, ..., L\,. \tag{C.8}$$

   As the desired values $\boldsymbol{u}_\ell$ occur on both sides—once within the non-linear function $\boldsymbol{F}(..)$—, it is an implicit method and we have to solve now a non-linear equation in every step.

C.2. Accuracy, convergence and stability

At first glance, it might be promising to reduce the stepwidth for getting a better solution. But this will not always help, because there is a difference between convergence and stability. In practical applications like solving the equation of motion of an IMU, the stepwidth is also fixed by the sampling.

For demonstration, we apply the two Euler methods on the problem

$$y' = \mu y \qquad \& \quad y(0) = 1 \tag{C.9}$$

with the exact solution $y = \mathrm{e}^{\mu x}$.

With the explicit Euler method we obtain

$$\begin{aligned}
u_0 &= 1 \\
u_1 &= 1 + h(\mu 1) \\
u_2 &= 1 + h\mu + hf(x_1, u_1) = 1 + h\mu + h\mu(1 + h\mu) = (1 + h\mu)^2 \\
&\vdots \\
u_L &= (1 + h\mu)^L .
\end{aligned}$$

For a fixed value $\bar{x} \in \mathbb{R}$ and sufficient small stepwidth, the method is converging to the correct answer: We set $h = \frac{\bar{x}}{L}$ and obtain

$$u_L = \left(1 + \mu\frac{\bar{x}}{L}\right)^L \to \mathrm{e}^{\mu\bar{x}} \quad \text{for } L \to \infty . \tag{C.10}$$

Table C.1.: Approximation of $y' = -1000y$ with a stepwidth $h = 0.01$ via the forward Euler method

t_ℓ	u_ℓ	e^{-1000t_ℓ}
0.01	-9	$4.5400 \cdot 10^{-5}$
0.02	81	$2.0612 \cdot 10^{-9}$
0.03	-729	$9.3576 \cdot 10^{-14}$
0.04	6561	$4.2484 \cdot 10^{-18}$
0.05	-59049	$1.9287 \cdot 10^{-22}$

For a fixed value $h > 0$, the correctness might not be guaranteed. In particular for large negative values of μ we might have a problem. Due to $|1 + h\mu| > 1$ the "solution" u_ℓ will increase in magnitude and also oscillate.

In this example, the method is converging for $h \to 0$, but numerical unstable for fixed values $h > 0$.

The implicit Euler method provides

$$\begin{aligned}
u_0 &= 1 \\
u_1 &= 1 + h\mu u_1 \Rightarrow u_1 = \frac{1}{1 - \mu h} \\
u_2 &= u_1 + h\mu u_2 \Rightarrow u_2 = \frac{u_1}{1 - h\mu} = \frac{1}{(1 - \mu h)^2}
\end{aligned}$$

$$\vdots$$
$$u_L = u_{L-1} + h\mu u_L \Rightarrow u_L = \frac{1}{(1-\mu h)^L}\,.$$

Again the method/solution is converging to the correct function for a fixed value $\bar{x} \in \mathbb{R}$. We set $h = \frac{\bar{x}}{L}$ and obtain

$$u_L = \left(1 - \mu\frac{\bar{x}}{L}\right)^{-L} = \left(1 + \mu\frac{\bar{x}}{L'}\right)^{L'} \to \mathrm{e}^{\mu x} \quad \text{for } L' \to \infty\,.$$

For negative values μ the solution is tending to zero now without oscillations.

Table C.2.: Approximation of $y' = -1000y$ with a stepwidth $h = 0.01$ via the backward Euler method

t_ℓ	u_ℓ	e^{-1000t_ℓ}
0.01	$9.0909 \cdot 10^{-2}$	$4.5400 \cdot 10^{-5}$
0.02	$8.2645 \cdot 10^{-3}$	$2.0612 \cdot 10^{-9}$
0.03	$7.5131 \cdot 10^{-4}$	$9.3576 \cdot 10^{-14}$
0.04	$6.8301 \cdot 10^{-5}$	$4.2484 \cdot 10^{-18}$
0.05	$6.2092 \cdot 10^{-6}$	$1.9287 \cdot 10^{-22}$

For this example, the implicit method is converging for $h \to 0$ and numerical stable for fixed values $h > 0$.

C.3. Explicit Runge-Kutta method

A general form of explicit one-step methods was described by Runge and Kutta. In each step — within the interval $[x_\ell, x_{\ell+1}]$ — the approximation is defined by

$$\begin{aligned}
\boldsymbol{u}_{\ell+1} &= \boldsymbol{u}_\ell + h\sum_{i=1}^{m} \gamma_i \boldsymbol{k}_i(x_\ell, \boldsymbol{u}_\ell) \qquad \text{(C.11)}\\
\boldsymbol{k}_1 &= \boldsymbol{F}(x_\ell, \boldsymbol{u}_\ell)\\
\boldsymbol{k}_2 &= \boldsymbol{F}(x_\ell + \alpha_2 h, \boldsymbol{u}_\ell + h\beta_{21}\boldsymbol{k}_1)\\
\boldsymbol{k}_3 &= \boldsymbol{F}(x_\ell + \alpha_3 h, \boldsymbol{u}_\ell + h(\beta_{31}\boldsymbol{k}_1 + \beta_{32}\boldsymbol{k}_2))\\
&\vdots\\
\boldsymbol{k}_m &= \boldsymbol{F}\left(x_\ell + \alpha_m h, \boldsymbol{u}_\ell + h\left(\sum_{j=1}^{m-1} \beta_{m,j}\boldsymbol{k}_j\right)\right)\,.
\end{aligned}$$

The method requires a set of parameters $\left\{\gamma_1, \gamma_2, ..., \gamma_m . \alpha_2, \alpha_3, ...\alpha_m, \beta_{21}, \beta_{32}, , ..., \beta_{m,m-1}\right\}$. These $(2m-1+m(m-1)/2)$ parameters are not completely independent. In particular it must hold

- $\gamma_1 + \gamma_2 + ... + \gamma_n = 1$ (consistency)
- $\alpha_i = \sum_{i-1}^{j=1} \beta_{i,j}$ (approximation of the derivatives is of the order $\mathcal{O}(h^2)$)

The most popular version is the Runge-Kutta method of order 4, which often provides a reasonable approximation with an acceptable effort (and the parameters are 'simple' and symmetric: $\alpha_2 = \alpha_3 = 0.5 = \beta_{21} = \beta_{32}$)

The parameters are often noted down in a so called butcher tableau. The tableau for the explicit Runge-Kutta method of order 4 is given by

$$
\begin{array}{c|cccc}
\boxed{\alpha_k} \quad 0 & & & & \\
1/2 & 1/2 & & & \boxed{\beta_{ki}} \\
1/2 & 0 & 1/2 & & \\
1 & 0 & 0 & 1 & \\
\hline
 & 1/6 & 1/3 & 1/3 & 1/6 \quad \boxed{\gamma_{ik}}
\end{array}
\tag{C.12}
$$

Remark C.3 *In each step we use only $(x_\ell, \boldsymbol{u}_\ell)$ to calculate the new functions, so it is still a one-step method.*

Exercise C.3 *Approximate a solution of the ODE*

$$\dot{y}(t) = y - y^2 \qquad \& \quad y(0) = 0.5$$

by the Runge-Kutta method of order 4 and with a stepwidth $h = 0.4$.

$$
\begin{aligned}
\boldsymbol{k}_1 &= \boldsymbol{F}(t_0 + 0h, \boldsymbol{u}_0) = 0.25 \\
\boldsymbol{k}_2 &= \boldsymbol{F}(t_0 + 0.5h, \boldsymbol{u}_0 + 0.5h\boldsymbol{k}_1) = 0.24750 \\
\boldsymbol{k}_3 &= \boldsymbol{F}(t_0 + 0.5h, \boldsymbol{u}_0 + 0.5h\boldsymbol{k}_2) = 0.24755 \\
\boldsymbol{k}_4 &= \boldsymbol{F}(t_0 + 1h, \boldsymbol{u}_0 + h\boldsymbol{k}_3) = 0.24020\,.
\end{aligned}
$$

The combination provides the next point of the numerical solution:

$$\boldsymbol{u}_1 = \boldsymbol{u}_0 + h\left(\frac{1}{6}\boldsymbol{k}_1 + \frac{1}{3}\boldsymbol{k}_2 + \frac{1}{3}\boldsymbol{k}_3 + \frac{1}{6}\boldsymbol{k}_4\right) = 0.59869\,.$$

In this particular case, we can also find the exact solution of the ODE:

$$y(t) = \left(1 + \left(\frac{1}{y_0} - 1\right) \mathrm{e}^{-t}\right)^{-1} \tag{C.13}$$

and compare this with the numerical solution. The Euler polygon and the Runge-Kutta method approximate the general behavior quite well, but the the second method performs better with the same stepwidth $h = 0.4$ (cf. fig. C.1 and fig. C.2).

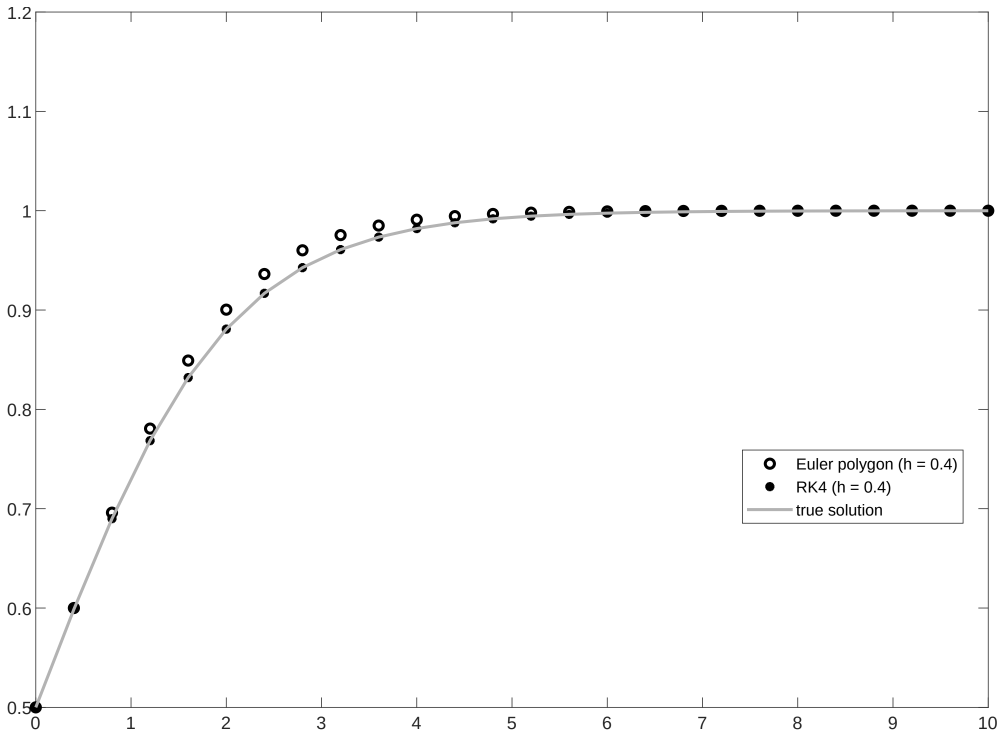

Figure C.1.: Numerical solution and the exact solution for the ODE $y' = y - y^2$.

Exercise C.4 *Implement the Runge-Kutta method of order 4 with a constant stepwidth h in* MATLAB*. The differential equations should be entered via function handles. Test the routine with equation (C.3) and the initial value $\boldsymbol{y}(1) = (4, 1)^{\mathsf{T}}$.*

Outlook: Linear multistep method

As the evaluation of the function $\boldsymbol{F}$ might be time consuming, linear multi-step methods have been derived.

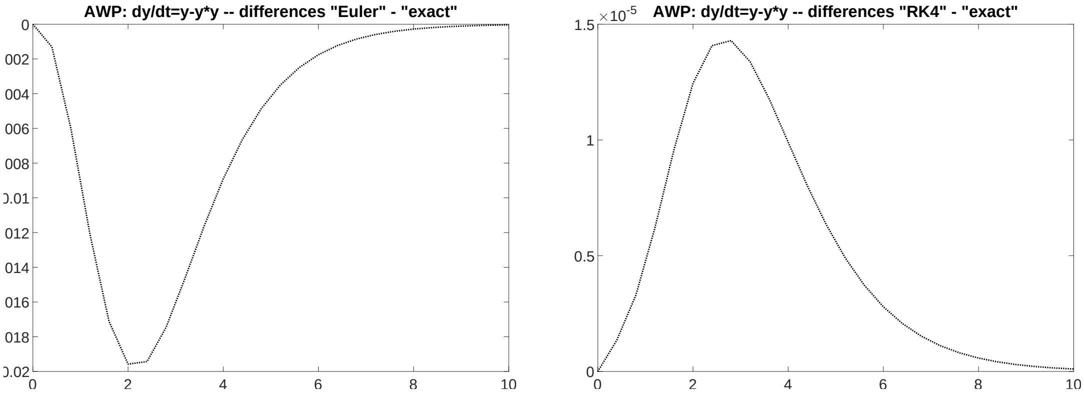

(a) approximation by Euler method **(b)** approximation by RK4 method

Figure C.2.: Differences between the numerical approximation and the exact solution for the ODE $y' = y - y^2$.

In this group of methods a subset of previous N points

$$\Big\{(x_{\ell-1}, \boldsymbol{u}_{\ell-1}), (x_{\ell-2}, \boldsymbol{u}_{\ell-2}), (x_{\ell-3}, \boldsymbol{u}_{\ell-3}), \ldots\Big\}$$

is used for a polynomial approximation and the integral representation is calculated by their linear combination. In the next step, the "oldest" element of the subset is removed and the "latest" is added.

To avoid the solution of a non-linear equation, so-called predictor-corrector methods—a combination of explicit/implicit form—are in use. (In satellite geodesy for example the Adams-Moulton method of order 12 is popular, which keeps always the last 12 points for prediction and correction in orbit simulations.)

D. Clairaut's differential equation

In satellite geodesy, the equation of motion is a differential equation of second order and in three variables. If we restrict ourselves to radial symmetric forces, the equation can be reduced to a non-linear differential equation of first order and in one variable. Hence, the solution is – in theory – possible by the ansatz of separation and an integration.

D.1. Radial symmetric force fields

A radial symmetric force field is described by $\boldsymbol{F} = f(\|\boldsymbol{r}\|)\boldsymbol{r} = f(r)\boldsymbol{r}$ with an arbitrary scalar function $f(r)$. The corresponding potential is determined by integration:

$$\bar{U}(r) = -\int_c^r \bar{r} f(\bar{r})\, \mathrm{d}\bar{r}\,. \tag{D.1}$$

Remark D.1 *Please note, that we use the physical convention $\boldsymbol{r} = -\nabla\bar{U}$ in this Chapter.*

Exercise D.1 *Verify that the potential $\bar{U}(r)$ correspond to the force field $\boldsymbol{F}$.*

Conservation of the angular momentum

The (mass specific) angular momentum is calculated by the cross product $\boldsymbol{L} = \boldsymbol{r} \times \dot{\boldsymbol{r}}$.

Considering the radial symmetric force field leads to

$$\frac{\mathrm{d}\boldsymbol{L}}{\mathrm{d}t} = \dot{\boldsymbol{r}} \times \dot{\boldsymbol{r}} + \boldsymbol{r} \times \ddot{\boldsymbol{r}} = \boldsymbol{0} + \boldsymbol{r} \times f(r)\boldsymbol{r} = \boldsymbol{0}\,. \tag{D.2}$$

Hence, the angular momentum $\boldsymbol{L}$ is preserved, and the motion takes place in a constant orbital plane!

Conservation of the energy

We differentiate the sum of the kinetic energy $E_{\text{kin}} = \frac{1}{2}v^2 = \frac{1}{2}\dot{\boldsymbol{r}}^\top \dot{\boldsymbol{r}}$ and the gravitational potential $\bar{U}(r)$ w.r.t. time

$$\begin{aligned}\frac{\mathrm{d}E}{\mathrm{d}t} &= \frac{\mathrm{d}\{E_{\text{kin}} + E_{\text{pot}}\}}{\mathrm{d}t} \\ &= \frac{1}{2}\ddot{\boldsymbol{r}}^\top \dot{\boldsymbol{r}} + \frac{1}{2}\dot{\boldsymbol{r}}^\top \ddot{\boldsymbol{r}} + \frac{\mathrm{d}\bar{U}}{\mathrm{d}r}\frac{\mathrm{d}r}{\mathrm{d}t} \\ &= f(r)\boldsymbol{r}^\top \dot{\boldsymbol{r}} - rf(r)\frac{\mathrm{d}r}{\mathrm{d}t} = \\ &= f(r)\Big(\boldsymbol{r}^\top \dot{\boldsymbol{r}} - \dot{r}r\Big) = 0\,.\end{aligned}$$

Hence, the total energy E is preserved.

Polar coordinates

If the motion takes place in a plane, we can describe it by polar coordinates. This requires the definition of an origin $\mathbf{0}$, a chosen axis, and an angle. We set the origin into the symmetry center and choose the direction towards the smallest distance between orbit and center as reference axis. The angle is measured w.r.t to the axis, and the later one is related with the angle $\nu = 0$. For compactness, we could call these quantities "true anomaly" and the "distance to perigee", although these names are referring to conic sections per definition.

The orbit in the orbital plane is described by a vector

$$\boldsymbol{r}_f = r\begin{pmatrix}\cos\nu \\ \sin\nu \\ 0\end{pmatrix} = r\boldsymbol{e}_r$$

with a time depending radius r. Differentiation provides us

$$\dot{\boldsymbol{r}}_f = \frac{\mathrm{d}r}{\mathrm{d}t}\begin{pmatrix}\cos\nu \\ \sin\nu \\ 0\end{pmatrix} + r\begin{pmatrix}-\dot{\nu}\sin\nu \\ \dot{\nu}\cos\nu \\ 0\end{pmatrix} = \frac{\mathrm{d}r}{\mathrm{d}t}\boldsymbol{e}_r + r\dot{\nu}\boldsymbol{e}_\nu\,.$$

The kinetic energy is found by a scalar product

$$E_{\text{kin}} = \frac{1}{2}\dot{\boldsymbol{r}}^\top \dot{\boldsymbol{r}} = \frac{1}{2}\left(\frac{\mathrm{d}r}{\mathrm{d}t}\boldsymbol{e}_r + r\dot{\nu}\boldsymbol{e}_\nu\right)^\top\left(\frac{\mathrm{d}r}{\mathrm{d}t}\boldsymbol{e}_r + r\dot{\nu}\boldsymbol{e}_\nu\right) = \frac{1}{2}\left(\frac{\mathrm{d}r}{\mathrm{d}t}\right)^2 + r^2\dot{\nu}^2$$

where we considered the orthogonality $\boldsymbol{e}_r^\top \boldsymbol{e}_\nu = 0$.

We add the gravitational potential to obtain the total energy

$$E = \tfrac{1}{2}\left[\left(\tfrac{\mathrm{d}r}{\mathrm{d}t}\right)^2 + r^2\dot{\nu}^2\right] + \bar{U}(r)\,. \tag{D.3}$$

This equation links the orbit, radius and its derivative in the orbital plane, with energy and potential.

D.2. Clairaut's differential equation

Equation (D.3) contains the derivative $\frac{\mathrm{d}r}{\mathrm{d}t}$ but also the quantity $\dot{\nu}$. We are looking for a differential equation with the radius as a function of the angle ν. Considering the chain rule $\frac{\mathrm{d}r}{\mathrm{d}t} = \frac{\mathrm{d}r}{\mathrm{d}\nu}\frac{\mathrm{d}\nu}{\mathrm{d}t}$, the equation is reformulated:

$$\begin{aligned}
\left(\frac{\mathrm{d}r}{\mathrm{d}t}\right)^2 &= 2(E - \bar{U}(r)) - r^2\dot{\nu}^2 \\
\left(\frac{\mathrm{d}r}{\mathrm{d}\nu}\right)^2 \dot{\nu}^2 &= 2(E - \bar{U}(r)) - r^2\dot{\nu}^2 \\
\left(\frac{\mathrm{d}r}{\mathrm{d}\nu}\right) &= \pm\sqrt{\frac{2(E - \bar{U}(r))}{\dot{\nu}^2} - r^2} = \pm\underbrace{\sqrt{\frac{2(E - \bar{U}(r))}{L^2} r^4 - r^2}}_{=g(r)}
\end{aligned}$$

where the last line uses the angular momentum $L = r^2\dot{\nu}$. In principle, we have found a differential equation for the orbit already, but a small simplification is obtained by introducing the inverse radius $\sigma = r^{-1}$ as a new variable (*Guthmann*, 1994, pp. 70).

The transformation $\frac{\mathrm{d}\sigma}{\mathrm{d}\nu} = \frac{\mathrm{d}r^{-1}}{\mathrm{d}\nu} = -r^{-2}\frac{\mathrm{d}r}{\mathrm{d}\nu}$ leads to *Clairaut's (differential) equation*[1]

Clairaut'sche (Differential-) Gleichung

$$\begin{aligned}
\frac{\mathrm{d}\sigma}{\mathrm{d}\nu} &= -g(\sigma^{-1})\sigma^2 = -\sigma^2\sqrt{\frac{2\Big(E - \bar{U}\left(\frac{1}{\sigma}\right)\Big)}{L^2}\frac{1}{\sigma^4} - \frac{1}{\sigma^2}} \\
\frac{\mathrm{d}\sigma}{\mathrm{d}\nu} &= -\sqrt{\frac{2\Big(E - \bar{U}\left(\frac{1}{\sigma}\right)\Big)}{L^2} - \sigma^2}\,.
\end{aligned} \tag{D.4}$$

(The equation in this form is only valid for orbits with $L \neq 0$.)

[1] Alexis Claude Clairaut (1713–1765), French mathematitcian, astronomer and geophysicist. His name is also related to Clairaut's theorem (hydrostatic equilibrum), Clairaut's relation (geodesic lines) and another Clairaut's equation (planar curves)

D.3. Clairaut's differential equation and the Kepler problem

D.3.1. Derive the orbit from the potential

With the sign convention of this chapter, the potential of the Kepler problem is given by $\bar{U}(r) = -\frac{GM}{r} = -GM\sigma$. We introduce this potential in the differential equation

$$\frac{\mathrm{d}\sigma}{\mathrm{d}\nu} = -\sqrt{\frac{2\Big(E + GM\sigma\Big)}{L^2} - \sigma^2} = -\sqrt{A_0 + A_1\sigma - \sigma^2} \tag{D.5}$$

with $A_0 = \frac{2E}{L^2}$ and $A_1 = \frac{2GM}{L^2}$ (cf. (*Guthmann*, 1994, pp. 78)).

The ansatz of separation leads to

$$\int\limits_0^\nu \mathrm{d}\nu = \int\limits_{\sigma_0}^\sigma \frac{\mathrm{d}\sigma}{-\sqrt{A_0 + A_1\sigma - \sigma^2}} \,. \tag{D.6}$$

The integrand is transformed into a standard form $\sqrt{1-\xi^2}$ by completing the squares

$$\frac{1}{-\sqrt{A_0 + A_1\sigma + \left(\frac{A_1}{2}\right)^2 - \left(\frac{A_1}{2}\right)^2 - \sigma^2}} = \frac{1}{-\sqrt{\Big(\frac{A_1^2}{4} + A_0\Big) - \left(\sigma - \frac{A_1}{2}\right)^2}} =$$

$$\frac{1}{-\sqrt{\frac{A_1^2}{4} + A_0}\sqrt{1 - \left(\frac{\sigma - \frac{A_1}{2}}{\sqrt{\frac{A_1^2}{4} + A_0}}\right)^2}} = \frac{1}{-\sqrt{\frac{A_1^2}{4} + A_0}}\frac{1}{\sqrt{1-\xi^2}}$$

with $\xi := \frac{\sigma - \frac{A_1}{2}}{\sqrt{\frac{A_1^2}{4} + A_0}}$.

This substitution reduces the integration:

$$\begin{aligned}\int\limits_0^\nu \mathrm{d}\nu \ &= \int\limits_{\sigma_0}^\sigma \frac{\mathrm{d}\sigma}{-\sqrt{A_0 + A_1\sigma - \sigma^2}} = \int\limits_{\xi_0}^\xi \frac{\mathrm{d}\xi}{-\sqrt{1-\xi^2}} \\ &\Longrightarrow \nu = \arccos\xi - \arccos\xi_0 \\ &\Longrightarrow \xi = \cos(\nu + \arccos\xi_0)\,.\end{aligned}$$

The angle is rewritten by $\nu_0 := \arccos\xi$

To find the inverse radius σ, we solve

$$\xi = \frac{\sigma - \frac{A_1}{2}}{\sqrt{\frac{A_1^2}{4} + A_0}} = \cos(\nu + \nu_0)$$

$$\sigma = \frac{A_1}{2} + \sqrt{\frac{A_1^2}{4} + A_0} \cos(\nu + \nu_0)$$

and for the radius itself:

$$\begin{aligned} r = \sigma^{-1} &= \frac{1}{\frac{A_1}{2} + \sqrt{\frac{A_1^2}{4} + A_0} \cos(\nu + \nu_0)} \\ &= \frac{\frac{2}{A_1}}{1 + \sqrt{1 + \frac{4A_0}{A_1^2}} \cos(\nu + \nu_0)} \\ &= \frac{\frac{L^2}{GM}}{1 + \sqrt{1 + \frac{4 \cdot 2E}{L^2} \left(\frac{L^2}{2GM}\right)^2} \cos(\nu + \nu_0)} . \end{aligned}$$

A comparison with the radius $r(\nu) = p/(1 + e \cos \nu)$ leads to the known identity $p = L^2/GM$ and a new expression for the eccentricity.

Exercise D.2 *Verify for an elliptic orbit, that the eccentricity could be written via*

$$e = \sqrt{1 + \frac{4 \cdot 2E}{L^2} \left(\frac{L^2}{2GM}\right)^2} . \tag{D.7}$$

In case of an elliptic orbit, we know the energy $E = \frac{GM}{-2a}$ *and the relation* $p = \frac{L^2}{GM}$*:*

$$\begin{aligned} e &\stackrel{!}{=} \sqrt{1 + \frac{4 \cdot 2E}{L^2} \left(\frac{L^2}{2GM}\right)^2} = \sqrt{1 + 2\frac{EL^2}{(GM)^2}} \\ &= \sqrt{1 + \frac{2\left(\frac{GM}{(-2a)}\right)(pGM)}{(GM)^2}} = \sqrt{1 - \frac{p}{a}} \end{aligned}$$

and the last line is correct due to $ae^2 = a - p$*.*

***Remark D.2** As a side effect, we learned another expression for the norm of the Laplace vector:*

$$e = \frac{\|\boldsymbol{B}\|}{GM} = \sqrt{1 + 2\frac{EL^2}{(GM)^2}} = \frac{\sqrt{(GM)^2 + 2EL^2}}{GM}$$
$$\Longrightarrow \|\boldsymbol{B}\| = \sqrt{(GM)^2 + 2EL^2}$$

in terms of energy and angular momentum.

All in all we have shown, that the potential $\bar{U} = -GM\sigma$ leads to an orbit in the form of a conic section.

D.3.2. Derive the potential from the orbit

So far, we have shown, that the conic sections are a consequence of the gravitational potential $U = GM/r$. Are there any other gravitational potentials, which can cause an orbit in the form of a conic section?

Clairaut's differential equation can be solved for the potential:

$$\bar{U}(r)\left(\frac{1}{\sigma}\right) = -\frac{L^2}{2}\left[\left(\frac{\mathrm{d}\sigma}{\mathrm{d}\nu}\right)^2 + \sigma^2\right] + E\,. \tag{D.8}$$

Hence, if the orbit is given, the required potential can be derived. In polar coordinates, a conic section is given by

$$r(\nu) = \frac{p}{1 + e\cos\nu}$$
$$\Longrightarrow \sigma = \frac{1}{p}(1 + e\cos\nu)$$

with one focus in the origin. The differentiation w.r.t. the anomaly provides

$$\frac{\mathrm{d}\sigma}{\mathrm{d}\nu} = \frac{1}{p}(-e\sin\nu)$$

and in the potential formula (D.8):

$$\bar{U}\left(\frac{1}{\sigma}\right) = -\frac{L^2}{2}\left[\left(\frac{1}{p}(-e\sin\nu)\right)^2 + \left(\frac{1}{p}(1 + e\cos\nu)\right)^2\right] + E$$

$$
\begin{aligned}
&= -\frac{L^2}{p}\left(\frac{e^2(\sin^2\nu + \cos^2\nu) + 2e\cos\nu + 1}{2p}\right) + E \\
&= -\frac{L^2}{p}\left(\frac{e^2 + 1 + 2e\cos\nu}{2p}\right) + E \\
&= -\frac{L^2}{p}\left(\frac{e^2 - 1 + 1 + 1 + 2e\cos\nu}{2p}\right) + E \\
&= -\frac{L^2}{p}\left(\frac{e^2 - 1}{2p} + \underbrace{\frac{2 + 2e\cos\nu}{2p}}_{\sigma}\right) + E \\
&= -\frac{L^2}{p}\sigma + \underbrace{\left(E - \frac{L^2}{p}\frac{e^2 - 1}{2p}\right)}_{\text{const.}} .
\end{aligned}
$$

It was shown before, that the relation $\frac{L^2}{p} = GM$ holds for conic sections. Hence, we verified that the potential

$$
\bar{U}\left(\frac{1}{\sigma}\right) = -GM\sigma + \text{const.} \tag{D.9}
$$

is necessary for an orbit in the form of a conic section.

Exercise D.3 *Convince yourself, that the constant* $\left(E - \frac{L^2}{p}\frac{e^2-1}{2p}\right) = 0$ *will vanish for elliptic, parabolic and hyperbolic orbits.*

Exercise D.4 *Investigate the inverse radius* $\sigma(\nu)$ *in a modified gravitational potential*

$$
\bar{U} = -\frac{A}{r} + \frac{B}{r^2} \tag{D.10}
$$

for $A > 0$ *and* $|B| << A$ $(A, B \in \mathbb{R})$.

E. Theory of epicycles und Equant

E.1. Aristotele

Aristotele (384–322 BC) was a Greek scientist and philosopher, who published in many fields including physics, biology, zoology, metaphysics, logic, ethics, poetry, economics. politics and government. He derived his knowledge in different ways, ranging from own observations and deduction, but also theological/logical arguments or secondhand reports. The theorems were well known and popular for centuries, sometimes with surprising twists: Several statements in zoology have obtained blind believe, followed by critical considerations, and finally confirmations in the last 200 years, e.g. the active camouflage of the octopus or the usage of the elephants' trunks as snorkel[1].

Many books of Aristotele – written in Greek – were preserved through Arabic translation and reception. The books were translated into Latin in the 12th century. In both cultures, discussing and commenting the ancient philosophers was the beginning of science. The catholic faculty of the University of Paris tried to ban the books about nature in 1210 and again in 1215, as the work neglected a genesis of Earth or Sun[2]. The ban was not successful and other universities like Toulouse[3] and Oxford made Aristotele to the basis of the curriculum, which quickly spread over Europe. Some more details on conflict of church and Aristotele's theorems could be found in (*Heuser*, 2008, pp. 106–108).

Aristotele postulates in celestial mechanics were on logic and philosophy: *Sun, Moon, the visible planets, and all stars are attached on concentric spheres around the Earth, which is in the center of the universe and move on perfect circles. Each sphere has its own uniform (angular) velocity. The motion is generated in the outermost sphere/circle by a prime mover.*

Remark E.1 *The idea of one sphere covering all fix stars cannot be falsified by ancient observations. The measurement of declination and right ascension seems to indicate a*

[1] `en.wikipedia/wiki/Aristotele` and `en.wikipedia/wiki/Aristotele%27s_biology`

[2] Aristotele discussed and postulated arguments against infinity in dimensions, but accepted an infinite time or lifespan for the cosmos

[3] The university of Toulouse published advertisements, that all students are allowed to read the banned books

constant rotation around the Earth. The relative movements in terms of angles are below the measurement accuracy. (Today, the Doppler shift demonstrates also a movement in radial direction.)

It was recognized already by ancient astronomers, that their observations for planets showed retrograde motion and variable brightness, which contradicted the uniform angular velocities. With today's knowledge, two reasons can be identified (*Grigull*, 1996):

- Planets are not moving on circles, but on ellipses with the Sun in one focus.
- Observations are not measured from a geometrical center, but from a moving Earth which orbits around the Sun as well.

Rettung der Phänomene

Many astronomers were active in so-called *saving the phenomena* (in Greek: "$\sigma\acute{\omega}\zeta\epsilon\iota\nu$ $\tau\grave{\alpha}$ $\phi\alpha\iota\nu\acute{o}\mu\epsilon\nu\alpha$" = "*sōzein ta phainómena*"). This research program should describe the irregular motions of celestial bodies by circular motions with constant velocity to obey Aristotele's rules. Fundamental tricks were the *theory of epicycles*, an eccentric Earth and the introduction of an *equant* as reference point.

Epizykeltheorie

Äquant

Even Copernicus kept the circular motion with constant velocity—and a modified theory of epicycles—, and changed only the center to a location close to the Sun.

E.2. Theory of epicycles

Epicycles[4] were a model to describe the motion of Sun, Moon and planets w.r.t. an observer on Earth. The celestial body was assumed to move in a smaller circle—called an *epicycle*—whose center turned on a larger circle known as *deferent*. If the observations don't fit to the model, smaller circles on the epicyle can be introduced by iteration. The procedure can be considered as a kind of Fourier series.

Epizykel

Deferent

To be precise, we shall allow a three dimensional model with spheres instead of circles, but we want to keep the discussion simple. Epicycles in a plane are represented by the sum

$$\boldsymbol{z} = A \begin{pmatrix} \cos\zeta(t) \\ \sin\zeta(t) \end{pmatrix} + \sum_{\ell=1}^{L} B_\ell \begin{pmatrix} \cos(\beta_\ell + Z_\ell(t)) \\ \sin(\beta_\ell + Z_\ell(t)) \end{pmatrix} \tag{E.1}$$

with $|B_\ell| < A$. In the following, we use only one small epicycle and skip the index $\ell = L = 1$. The formula includes several planar curves depending on the two radius and the function $\zeta(t)$ and $Z_\ell(t)$ (cf. fig. E.1).

[4] Similar curves are produced if a circle rolls on the circumference, which is called an epicylcoid in geometry.

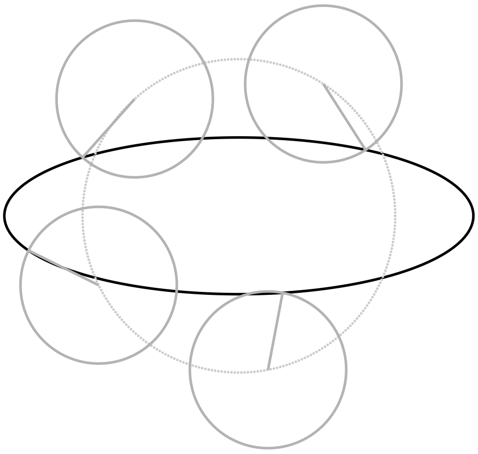

(a) $Z/\zeta = -1$: ellipse

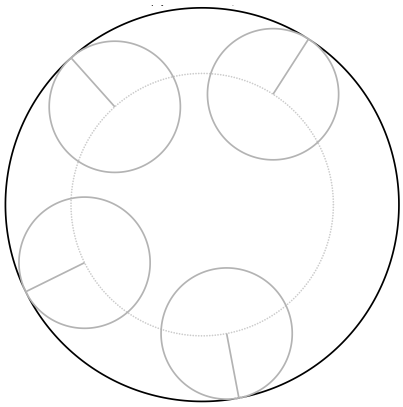

(b) $Z/\zeta = +1$: circle

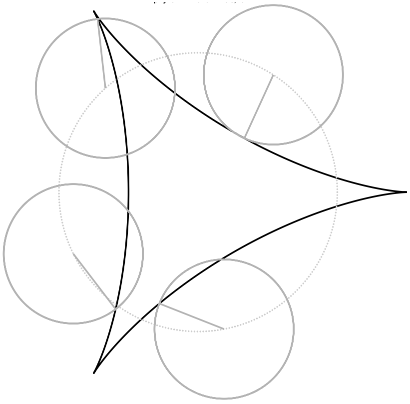

(c) $Z/\zeta = -2$:

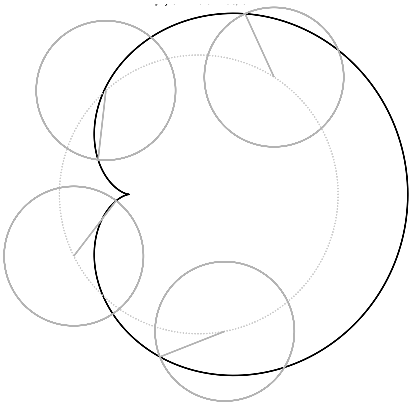

(d) $Z/\zeta = +2$:

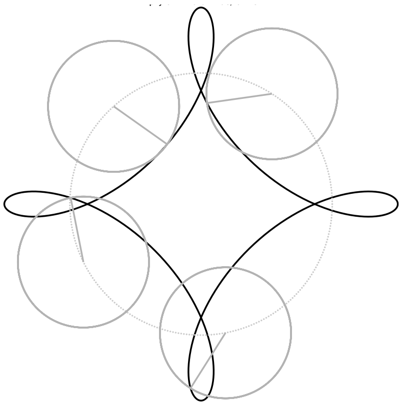

(e) $Z/\zeta = -3$:

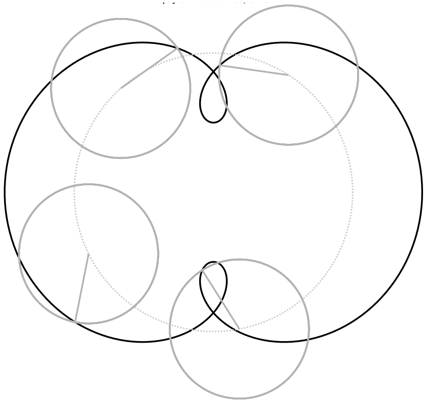

(f) $Z/\zeta = +3$:

Figure E.1.: A set of epicycles with $A = 1$, $B_1 = 0.5$ and a constant ratio Z/ζ

Ellipses are a special case of epicycles with $Z(t) = -\zeta(t)$ at each time point. The angle β causes only a rotation of the figure, and we set $\beta = 0$ in the following. The equation of an ellipse is

$$\frac{x^2}{(A+B)^2} + \frac{y^2}{(A-B)^2} = 1$$
$$\underbrace{(A^2 - 2AB + B^2)x^2 + (A^2 + 2AB + B^2)y^2}_{LHS} = (A+B)^2(A-B)^2$$

where $a = (A + B)$ and $b = (A - B)$ are the semi-axis.

We insert $x = A\cos\zeta + B\cos(-\zeta)$ and $y = B\sin\zeta + B\sin(-\zeta) = y = B\sin\zeta - B\sin\zeta$ from formula (E.1) in the LHS and ignore the argument t:

$$\begin{aligned}
\text{LHS} &= (A^2 - 2AB + B^2)x^2 + y^2(A^2 + 2AB + B^2) = \\
&= (A^2 - 2AB + B^2)(A^2\cos^2\zeta + 2AB\cos^2\zeta + B^2\cos^2\zeta) + \\
&\quad +(A^2 + 2AB + B^2)(A^2\sin^2\zeta - 2AB\sin^2\zeta + B^2\sin^2\zeta) \\
&= \cos^2\zeta(A^2 - 2AB + B^2)(A^2 + 2AB + B^2) + \sin^2\zeta(A^2 + 2AB + B^2)(A^2 - 2AB + B^2) \\
&= (\cos^2\zeta + \sin^2\zeta)(A^2 - 2AB + B^2)(A^2 + 2AB + B^2) \\
&= (A - B)^2(A + B)^2 = \text{RHS}
\end{aligned}$$

Hence, the geometrical model of epicycles describes ellipses for $Z = -\zeta$. The formula (E.1) with $L = 1$ is sufficient for a heliocentric model. From a Earth-related oberservation point more iterative epicycles $L > 1$ might be necessary in the model. The locations of planets, Moon or Sun can be derived with this theory up to accuracy of observations, if non-uniform motions are accepted.

E.3. Equant

An epicycle model explained the retrograd motion, but not the time of the observations. For saving the phenomena, Hipparch suggested to locate the Earth center eccentric w.r.t. the center of the deferent, quasi into a focus. (In Aristotele's original model, this will cause problems as the spheres were considered to be solid objects.)

Äquant

As the motion shall was still not uniform in this model, an hypothetical location—the so called *equant*—was postulated, in which the the angular velocity shall be seen uniform. A reasonable location might be on the axis, which is defined by the center of the deferent and the center of the Earth.

In modern knowledge, the question might occur, whether the second focus of an ellipse might be an approximation of the equant. The linearity of the anomalies is investigated in fig. E.2 by subtracting the mean anomaly M at the same time point. It turned out, that for an eccentricity $e = 0.2$, the eccentric anomaly E shows a maximal misfit of about 25° and the true anomaly ν shows a misfit of 10°. A new defined anomaly μ in the empty focus stays below 0.8°.

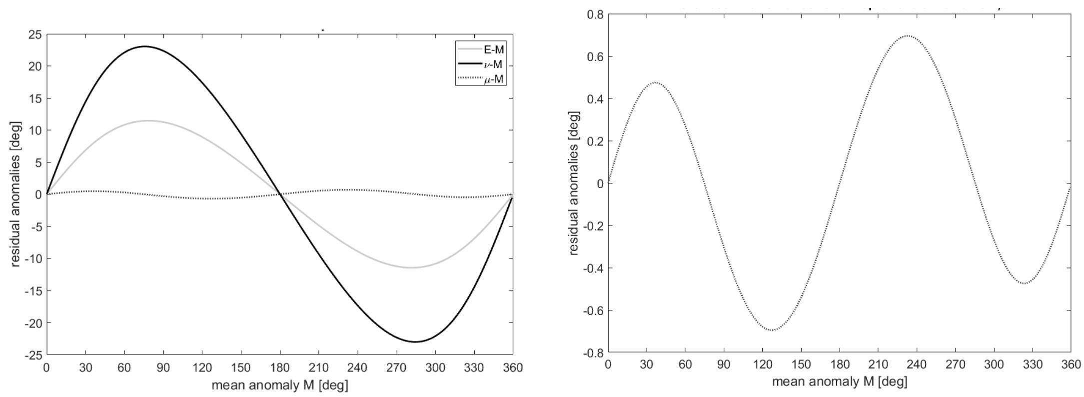

(a) all anomalies **(b)** zoom for $\mu - M$

Figure E.2.: "Linearity" of the residual anomalies $(E - M)$ and $(\nu - M)$ and $(\mu - M)$ for an ellipse with the eccentricity $e = 0.2$

E.3.1. Focus with central mass

If we use the notation and knowledge of today, we can start with the area of an inifintesmal triangle

$$\mathrm{d}A_1 = \frac{1}{2} r \cdot r \,\mathrm{d}\nu \Rightarrow 2\frac{\mathrm{d}A_1}{\mathrm{d}t} = r^2 \frac{\mathrm{d}\nu}{\mathrm{d}t} = r^2 \omega_1 = c$$

- r: current radius depending on location
- $r\,\mathrm{d}\nu$: finite line tangential to the orbit
- $\omega_1 = \frac{\mathrm{d}\nu}{\mathrm{d}t}$: angular velocity
- c: constant due to law of area conservation

After one revolution, the area $A = ab\pi$ is covered within the revolution time T:

$$2\frac{\mathrm{d}A_1}{\mathrm{d}t} = 2\frac{ab\pi}{T} = nab = na^2\sqrt{1 - e^2}$$

with $n = \frac{2\pi}{T}$. Solving for the angular velocity leads to

$$\omega_1 = \frac{c}{r^2} = \frac{na^2\sqrt{1-e^2}}{r^2}$$

The radius $r = a(1 - e\cos E)$ is known, and we obtain

$$\frac{\omega_1}{n} = \frac{c}{nr^2} = \frac{a^2\sqrt{1-e^2}}{a^2(1-e\cos E)^2}$$

Remember the binomial series expansion

$$(1 \pm y)^\alpha = \sum_{k=1}^{\infty} \binom{\alpha}{k} (\pm y)^k$$

will lead to

$$\begin{aligned}
\tfrac{\omega_1}{n} &= \left(1 - \tfrac{e^2}{2} - \tfrac{e^4}{8} - \tfrac{e^6}{16} + ...\right)\left(1 - 2(e\cos E) + 3(e\cos E)^2...\right) = \\
&= 1 - e(2\cos E) + e^2(3\cos^2 E - 0.5) + \mathcal{O}(e^3) \\
\Rightarrow \nu &= \textstyle\int \omega_1 \, \mathrm{d}t = n\Big[1 - e(2\cos E) + e^2(3\cos^2 E - 0.5) + \mathcal{O}(e^3)\Big]t
\end{aligned}$$

The true anomaly is now a function in the eccentric anomaly and the eccentricity.

E.3.2. Focus without mass

An infinitesimal triangle can be derived for the second focus (empty focus, antifocus, ...) as well:

$$\mathrm{d}A_2 = \frac{1}{2}\rho \cdot r\,\mathrm{d}\mu \Rightarrow 2\frac{\mathrm{d}A_2}{\mathrm{d}t} = \rho r\frac{\mathrm{d}\mu}{\mathrm{d}t} = r\rho\omega_2 = c$$

- r: distance between focus with mass and the satellite
- ρ: distance between focus without mass and the satellite
- $r\,\mathrm{d}\mu$: finite line tangential to the orbit
- $\omega_2 = \frac{\mathrm{d}\mu}{\mathrm{d}t}$: angular velocity
- c: constant due to law of area conservation

After one revolution, the relation

$$2\frac{\mathrm{d}A_2}{\mathrm{d}t} = 2\frac{ab\pi}{T} = na^2\sqrt{1-e^2} \Leftrightarrow \omega_2 = \frac{na^2\sqrt{1-e^2}}{r\rho}$$

holds. Considering $\rho = 2a - r = a(1 + e\cos E)$ provides

$$\frac{\omega_2}{n} = \frac{a^2\sqrt{1-e^2}}{a(1-e\cos E)a(1+e\cos E)} = \frac{\sqrt{1-e^2}}{(1-e^2\cos^2 E)}$$

The geometrical series

$$(1-y^2)^{-1} = \sum_{k=1}(y^2)^k$$

leads to

$$\begin{aligned}
\tfrac{\omega_2}{n} &= \left(1 - \tfrac{e^2}{2} - \tfrac{e^4}{8}...\right)\left(1 + (e^2\cos^2 E) + (e^2\cos^2 E)^2...\right) = \\
&= 1 + e^2(\cos^2 E - 0.5) + \mathcal{O}(e^4) \\
\Rightarrow \mu &= \textstyle\int \omega_2 \,\mathrm{d}t = n\Big[1 - e^2(\cos^2 E - 0.5) + \mathcal{O}(e^4)\Big]t
\end{aligned}$$

The new anomaly μ is "more linear" than the true anomaly ν, as the misfit if of order e^2 instead of e.

Bibliography

Balmino, G., E. J. Schrama, and N. Sneeuw, Compatibility of first-order circular orbit perturbations theories; consequences for cross-track inclination functions, *Journal of Geodesy*, *70*(9), 544–561, DOI `https://doi.org/10.1007/BF00867863`, 1996.

Bettadpur, S., Hotine's nonsingular geopotential formulation and its expression in the perifocal frame, *Tech. rep.*, CSR TM 91-04, Center for Space Research, Austin, Texas, 1991.

Bettadpur, S., Hotine's geopotential formulation: revisited, *Bull. Geod.*, *69*, DOI `https://doi.org/10.1007/BF00815482`, 1995.

Betti, B., and F. Sansò, The integrated approach to satellite geodesy, in *Theory of Satellite Geodesy and Gravity Field Determination*, vol. 25, edited by F. Sansò and R. Rummel, pp. 373–416, Springer Berlin Heidelberg, Berlin, Heidelberg, DOI `https://doi.org/10.1007/BFb0010557`, lecture Notes in Earth Sciences, 1989.

Forward, R., Review of artificial satellite gravity gradiometer techniques for geodesy, in *The use of artificial satellites for geodesy and geodynamics*, edited by G. Veids, 1973.

Gooding, R., Lumped Fifteenth order Harmonics in the Geopotential, *Nature phys. Sci.*, *231*, 168–169, DOI `https://doi.org/10.1038/physci231168a0`, 1971.

Grigull, U., Sechzig Jahre Kepler-Kommission, *Tech. rep.*, Verlag der Bayerischen Akademie der Wissenschaften, 1996.

Guthmann, A., *Einführung in die Himmelsmechanik und Ephimeridenrechnung*, BI Wissenschaftsverlag, Mannheim, Leipzig, Wien, Zürich, 1994.

Heiskanen, W., and H. Moritz, *Physical Geodesy*, W. H. Freeman and Company, San Fransisco, 1967.

Heuser, H., *Unendlichkeiten*, B. G. Teubner Verlag / GWV Fachverlage GmbH, Wiesbaden, 2008.

Hotine, M., *Mathematical Geodesy*, ESSA Monograph 2, U.S. Dept. of Commerce, Washington DC, 1969.

Ilk, K., *Ein Beitrag zur Dynamik ausgedehnter Körper: Gravitationswechselwirkung*, C: Heft 288, Dt. Geodät. Komm. bei d. Bayer. Akad. d. Wiss, 1983.

Kaula, W. M., *Theory of Satellite Geodesy: Applications of Satellites to Geodesy*, Blaisdell Publishing Company, Waltham Massachusetts, 1966.

Klokočník, J., J. Kostelecký, and H. Li, Best lumped coefficients from resonances for direct use in Earth gravity field modelling, *Bulletin of the Astronomical Institutes of Czechoslovakia*, *41*(1), 17–26, 1990.

Koop, R., Global gravity modelling using satellite gravity gradiometry, *Tech. rep.*, Netherlands Geodetic Commission, 1993.

Montenbruck, O., and E. Gill, *Satellite Orbits – Models, Methods and Applications*, Springer Verlag Berlin Heidelberg New York, 2001.

Oppenhäuser, G., and A. G. Bird, Artemis Finally Gets to Work!, *esa bulletin*, (114), 2003.

Rummel, R., Satellite gradiometry, in *Die Arbeiten des Sonderforschungsbereiches 78 Satellitengeodäsie der Technischen Universität München 1984 und 1985, Veröffentlichungen der BEK, Astronomisch-Geodätische Arbeiten*, edited by M. Schneider, 48, pp. 123–139, Verlag der Bayerischen Akademie der Wissenschaften, 1986.

Rummel, R., and M. van Gelderen, Meissl scheme - spectral characteristics of physical geodesy, *manuscripta geodaetica*, *20*(5), 379–385, 1995.

Rummel, R., M. van Gelderen, R. Koop, E. Schrama, F. Sansò, M. Brovelli, F. Miggliaccio, and F. Sacerdote, Spherical harmonic analysis of satellite gradiometry, *Tech. Rep. 39*, Netherlands Geodetic Commission, 1993.

Schrama, E., The Role of Orbit Errors in Processing Satellite Altimeter Data, *Tech. rep.*, Netherlands Geodetic Commission, 1989.

Seeber, G., *Satellite Geodesy (2. Edition)*, Walter de Gruyter, Berlin, New York, 2003.

Sneeuw, N., Representation coefficients and their use in satellite geodesy, *manuscr.geod.*, *17*, 1992.